

ยางธรรมชาติสภิมไฮโดรจินตเตรียมโดยไดอิมิดรีตักชันและวัลคาไนเซต



นาย โฆษิต สิมมา

# สถาบันวิทยบริการ จุฬาลงกรณ์มหาวิทยาลัย

วิทยานิพนธ์นี้เป็นส่วนหนึ่งของการศึกษาตามหลักสูตรปริญญาวิทยาศาสตรมหาบัณฑิต

สาขาวิชาปิโตรเคมีและวิทยาศาสตร์พอลิเมอร์

คณะวิทยาศาสตร์ จุฬาลงกรณ์มหาวิทยาลัย

ปีการศึกษา 2551

ลิขสิทธิ์ของจุฬาลงกรณ์มหาวิทยาลัย

HYDROGENATED SKIM NATURAL RUBBER PREPARED BY DIIMIDE  
REDUCTION AND ITS VULCANIZATES



Mr. Khosit Simma

สถาบันวิทยบริการ

จุฬาลงกรณ์มหาวิทยาลัย

A Thesis Submitted in Partial Fulfillment of the Requirements  
for the Degree of Master of Science Program in Petrochemistry and Polymer Science

Faculty of Science

Chulalongkorn University

Academic Year 2008

Copyright of Chulalongkorn University



โมฆิต สิมมา : ยางธรรมชาติสกิมไฮโดรจิเนตเตรียมโดยอิมิครีคักชันและวัลคาไนเซต  
(HYDROGENATED SKIM NATURAL RUBBER PREPARED BY DIIMIDE  
REDUCTION AND ITS VULCANIZATES) อ. ที่ปรึกษาวิทยานิพนธ์หลัก : ศ.ดร.  
ภัทรพรหม ประศาสน์สารกิจ, 98 หน้า

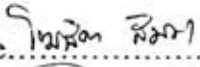

ไฮโดรจิเนชันเป็นกระบวนการปรับปรุงทางเคมีที่สำคัญอย่างหนึ่งโดยสามารถปรับปรุงสมบัติทางกายภาพ เคมี และสมบัติทางความร้อนของพอลิเมอร์ชนิดไม่อิ่มตัว น้ำยางธรรมชาติสกิมเป็นผลพลอยได้จากกระบวนการผลิตน้ำยางธรรมชาติเข้มข้นถูกไฮโดรจิเนตเป็นเอทิลีน-โพรพิลีนโคพอลิเมอร์ด้วยไดอิมิครีคักชันโดยใช้ไฮดราซีนและไฮโดรเจนเปอร์ออกไซด์โดยมีคอปเปอร์ซัลเฟตเป็นตัวเร่งปฏิกิริยา ยางธรรมชาติสกิมไฮโดรจิเนตตรวจสอบด้วยเทคนิคทางฟูเรียร์อินฟราเรดและนิวเคลียร์แมกเนติกเรโซแนนซ์สเปกโตรสโคปี การศึกษาผลของตัวแปรต่อระดับไฮโดรจิเนชัน พบว่าที่อุณหภูมิต่ำ ระยะเวลาการทำปฏิกิริยานาน ไฮดราซีนในปริมาณที่สูง ไฮโดรเจนเปอร์ออกไซด์และคอปเปอร์ซัลเฟตในปริมาณที่ต่ำเป็นสภาวะที่เหมาะสมสำหรับไฮโดรจิเนชันด้วยไดอิมิครีคักชันของน้ำยางธรรมชาติสกิม พบว่าคอปเปอร์อะซิเตตเป็นตัวเร่งปฏิกิริยาที่มีประสิทธิภาพสูงสุด ผลการทดลองทางจุลศาสตร์แสดงว่า ไฮโดรจิเนชันน้ำยางธรรมชาติสกิมเป็นปฏิกิริยาอันดับหนึ่งขึ้นกับความเข้มข้นของพันธะคู่ ค่าพลังงานกระตุ้นของการไฮโดรจิเนชันแบบใช้ตัวเร่งปฏิกิริยาและไม่ใช้ตัวเร่งปฏิกิริยามีค่า 9.5 และ 21.1 กิโลจูลต่อโมลตามลำดับ การศึกษาสมบัติทางความร้อนแสดงว่าเสถียรภาพทางความร้อนของยางธรรมชาติสกิมไฮโดรจิเนตเพิ่มสูงขึ้นกว่าพอลิเมอร์ตั้งต้น การศึกษาสัณฐานวิทยาของน้ำยางธรรมชาติสกิมไฮโดรจิเนตด้วยทรานส์มิสชันอิเล็กตรอนไมโครกราฟแสดงโมเดลแบบชั้นของ ส่วนไฮโดรจิเนตและส่วนไม่ถูกไฮโดรจิเนต ขนาดอนุภาคและการกระจายขนาดอนุภาคของยางธรรมชาติสกิมไฮโดรจิเนตไม่เปลี่ยนแปลงในระหว่างไฮโดรจิเนชัน นอกจากนี้ยังมีการศึกษาสมบัติเชิงกลและความต้านทานต่อโอโซนระหว่างของผสมยางธรรมชาติสกิมไฮโดรจิเนตและยางธรรมชาติอีกด้วย การเพิ่มสัดส่วนของยางธรรมชาติสกิมไฮโดรจิเนตในของผสมมีสมบัติทนทานต่อโอโซนได้ดีขึ้นโดยพื้นผิวมีรอยแตกลดลง

สาขาวิชา..ปิโตรเคมีและวิทยาศาสตร์พอลิเมอร์..ลายมือชื่อนิสิต.....โมฆิต สิมมา  
ปีการศึกษา..2551.....ลายมือชื่อ อ. ที่ปรึกษาวิทยานิพนธ์หลัก.....

## 4972241723 : MAJOR PETROCHEMISTRY AND POLYMER SCIENCE  
KEYWORDS: HYDROGENATION / DIIMIDE REDUCTION / HYDRAZINE /  
HYDROGEN PEROXIDE / SKIM NATURAL RUBBER LATEX

KHOSIT SIMMA : HYDROGENATED SKIM NATURAL RUBBER  
PREPARED BY DIIMIDE REDUCTION AND ITS VULCANIZATES.  
ADVISOR : PROF. PATTARAPAN PRASASSARAKICH, Ph.D., 98 pp.

Hydrogenation is an important method of chemical modification, which improves the physical, chemical and thermal properties of diene based polymers. Skim natural rubber latex (SNRL) produced as a by-product from the production of concentrated natural rubber latex, could be hydrogenated to a strictly alternating ethylene-propylene copolymer (EPDM) by diimide reduction, using hydrazine and hydrogen peroxide with copper sulfate as catalyst. The hydrogenated products were characterized by FTIR and NMR spectroscopy. The effect of various reaction parameters on the hydrogenation level, were investigated. Low temperature, long reaction time, high amount of hydrazine and lesser amount of hydrogen peroxide and copper sulfate were required to optimize the hydrogenation reaction of SNRL. Copper acetate was a highly active catalyst for the reaction. The kinetic result indicated that the diimide hydrogenation of SNRL exhibited a first order behavior with respect to the C=C concentration. The activation energy of catalytic and non-catalytic diimide hydrogenation of SNRL was 9.5 and 21.1 kJ/mol, respectively. The thermogravimetric analysis indicated that the thermal stability of hydrogenated skim natural rubber (HSNR) was higher than their parent polymer. From TEM micrograph of hydrogenated SNRL particles, non-hydrogenated rubber core and hydrogenated rubber layer were observed according to the layer model. The particle size and particle size distribution of hydrogenated SNRL were not changed during hydrogenation. In addition, the mechanical properties and ozone resistance of vulcanized HSNR blends were also investigated. The increase in HSNR content in the blends could retard the ozonolysis resulting in the surface cracking.

Field of Study..Petrochemistry and Polymer Science...Student's Signature   
Academic Year...2008.....Advisor's Signature 

## ACKNOWLEDGEMENTS

The author would like to express his gratitude to his supervisor, Prof. Dr. Pattarapan Prasassarakich for her encouraging guidance, supervision, support and helpful suggestion throughout his research. The author also would like to acknowledge Assoc. Prof. Dr. Supawan Tantayanon, Assist. Prof. Dr. Warinthorn Chavasiri and Dr. Aungsutorn Mahittikul for serving as chairman and members of thesis committee, respectively.

The author wishes to express his thankfulness to all people in the associated institutions for their kind assistance and collaboration: Miss. Sukanya Subkerd and Miss. Suvimon Wonglerdvisavakorn for support the NMR analysis; Dr. Aungsutorn Mahittikul for helpful suggestion throughout his research.

Many thanks are going to technicians of the Department of Chemical Technology, Chulalongkorn University and Rubber Research Institute for assisting in polymer characterization.

The authors also gratefully acknowledged the funding support from Center for Petroleum, Petrochemical and Advanced Materials (NCE-PPAM) and the Graduate School of Chulalongkorn University.

Finally, the author wishes to express his deep gratitude to his family for their love, support and encouragement throughout graduate study.

# CONTENTS

	<b>PAGE</b>
ABSTRACT (THAI).....	iv
ABSTRACT (ENGLISH).....	v
ACKNOWLEDGEMENTS.....	vi
CONTENTS.....	vii
LIST OF TABLES.....	x
LIST OF FIGURES.....	xi
LIST OF ABBREVIATIONS.....	xiv
CHAPTER I : INTRODUCTION.....	1
1.1 The Purpose of The Investigation.....	1
1.2 Objectives.....	2
1.3 Scopes of The Investigation.....	2
CHAPTER II : THEORY AND LITERATURE REVIEWS.....	3
2.1 Natural Rubber Latex.....	3
2.2 Skim Natural Rubber Latex.....	8
2.3 Concentrated Natural Rubber Latex.....	9
2.4 Chemical Modification via Hydrogenation of Diene-Based Polymers.....	12
2.5 Hydrogenation of Latex by Diimide Reduction.....	12
2.6 Literature Reviews.....	14
CHAPTER III : EXPERIMENTAL.....	18
3.1 Chemicals.....	18
3.2 Glasswares.....	19
3.3 Equipments.....	19
3.4 Diimide Hydrogenation Procedure.....	19
3.5 Blending and Vulcanization Process of Rubber.....	20
3.6 Characterization Methods.....	21
3.6.1 Fourier-Transform Infrared Spectroscopic Analysis.....	21
3.6.2 Nuclear Magnetic Resonance Spectroscopic Analysis.....	21

	<b>PAGE</b>
3.6.3 Particle Size and Size Distribution Analysis.....	22
3.6.4 Thermogravimetric Analysis.....	22
3.6.5 Differential Scanning Calorimetry.....	22
3.6.6 Morphological Study.....	22
3.6.7 Rheometric Characteristics of Blends.....	23
3.6.8 Mechanical Properties of HSNR/NR Vulcanizates Before and After Thermal Aging.....	23
3.6.9 Morphology of HSNR/NR Vulcanizates.....	23
3.6.10 Ozone Resistance Test.....	24
3.6.11 Determination of Crosslink Density.....	24
 CHAPTER IV : RESULTS AND DISSCUSION.....	 26
4.1 FTIR and NMR Spectroscopic Characterization.....	26
4.2 Effect of Process Parameters on SNRL Diimide Hydrogenation.....	31
4.2.1 Effect of Copper Sulfate Concentration.....	31
4.2.2 Effect of Hydrazine Concentration.....	33
4.2.3 Effect of Hydrogen Peroxide Concentration.....	35
4.2.4 Effect of Rubber Concentration.....	36
4.2.5 Effect of Hydrogenation Temperature.....	38
4.3 Kinetic Study of SNRL Diimide Hydrogenation.....	39
4.4 Improvement of Redox System.....	45
4.4.1 Effect of Sodium Dodecyl Sulfate Concentration.....	45
4.4.2 Effect of Hydroquinone Concentration.....	46
4.5 Effect of Catalyst Type and Boric Acid Concentration.....	48
4.6 The Distribution of Carbon–Carbon Double Bonds in HSNRL Particles.....	50
4.7 Thermal properties.....	54
4.7.1 Glass Transition Temperature.....	55
4.7.2 Decomposition Temperature.....	58
4.8 Cure Characteristics of HSNR/NR Blends.....	59



	<b>PAGE</b>
4.9 Mechanical Properties of HSNR/NR Vulcanizates.....	62
4.10 Thermal Stability of HSNR/NR Vulcanizates.....	64
4.11 Ozone Resistance of Vulcanized Hydrogenated Skim Natural Rubber.....	66
<b>CHAPTER V : CONCLUSION AND SUGGESTION.....</b>	<b>71</b>
5.1 Conclusions.....	71
5.2 Suggestions for The Future Work.....	72
<b>REFERENCES.....</b>	<b>73</b>
<b>APPENDICES.....</b>	<b>79</b>
APPENDIX A.....	81
APPENDIX B.....	82
APPENDIX C.....	84
APPENDIX D.....	90
APPENDIX E.....	95
APPENDIX F.....	96
<b>VITA.....</b>	<b>98</b>

สถาบันวิทยบริการ  
จุฬาลงกรณ์มหาวิทยาลัย

## LIST OF TABLES

TABLE	PAGE
2.1 Composition of fresh natural rubber latex.....	4
3.1 Formulation of rubber compounds.....	21
3.2 Classification of cracking on rubber surface.....	25
4.1 Rate constant of diimide hydrogenation of SNRL.....	40
4.2 Effect of catalyst types on SNRL hydrogenation.....	48
4.3 Glass transition temperature and decomposition temperature of rubber samples.....	56
4.4 Effect of EPV vulcanization system on cure characteristics of HSNR/NR.....	61
4.5 Effect of blend ratio on the thermal stability of HSNR/NR cured by EPV system with 2 phr of DCP.....	62
4.6 Ozone cracking of vulcanized rubber.....	68
A-1 Properties of skim natural rubber latex.....	80
A-2 Properties of standard thai natural rubber 5L (STR-5L).....	81
A-3 Properties of ethylene-propylene-diene copolymer (EPDM).....	81
C-1 FTIR Assignments for SNR.....	86
C-2 <sup>13</sup> C-NMR assignments for SNR and HSNR.....	89
D-1 Results of SNRL by diimide hydrogenation in presence of copper sulfate as catalyst.....	90
D-2 Effect of SDS concentration on SNRL hydrogenation.....	92
D-3 Effect of hydroquinone concentration on SNRL hydrogenation.....	92
D-4 Effect of boric acid concentration on SNRL hydrogenation.....	93
D-5 Effect of number of treatment on SNRL hydrogenation.....	93
D-6 Results for kinetic study of SNRL by diimide hydrogenation.....	94
E-1 The cure characteristics of various for HSNR/NR blends using moving die rheometer.....	95
F-1 Data of tensile strength of vulcanized rubber samples.....	96
F-2 Data of elongation at break (%) of vulcanized rubber samples.....	96
F-3 Data of hardness of vulcanized rubber samples.....	97

## LIST OF FIGURES

FIGURE	PAGE
2.1 Chemical structure of natural rubber.....	3
2.2 The structure of rubber particles.....	4
2.3 Type of molecular weight distribution curves of natural rubber.....	5
2.4 Schematic representation of gel phase in natural rubber.....	7
2.5 Presumed structure of branching and crosslinking of natural rubber.....	7
2.6 Molecular weight distribution curves of skim natural rubber and ordinary rubber.....	8
2.7 Creaming process of natural rubber latex.....	9
2.8 Commercial production of concentrated latex and skim rubber.....	11
2.9 Proposed mechanism for diimide hydrogenation.....	15
2.10 Model of distribution of double bonds in hydrogenated SBR latex particles: (a) Layer model; (b) Uniform model.....	16
4.1 FT-IR spectra of (a) SNR and (b) HSNR.....	28
4.2 <sup>1</sup> H-NMR spectra of (a) SNR and (b) HSNR.....	29
4.3 <sup>13</sup> C-NMR spectra of (a) SNR and (b) HSNR.....	30
4.4 Effect of copper sulfate concentration on SNRL hydrogenation. [N <sub>2</sub> H <sub>4</sub> ] = 2.21 M; [H <sub>2</sub> O <sub>2</sub> ] = 3.54 M; [C=C] = 0.55 M; T = 60°C; time = 6 h.....	32
4.5 The proposed mechanism of diimide hydrogenation.....	33
4.6 Effect of hydrazine concentration on SNRL hydrogenation. [CuSO <sub>4</sub> ] = 49.38 μM; [H <sub>2</sub> O <sub>2</sub> ] = 3.54M; [C=C] = 0.55M; T = 60°C; time = 6 h.....	34
4.7 Effect of hydrogen peroxide concentration on SNRL hydrogenation. [CuSO <sub>4</sub> ] = 49.38 μM; [N <sub>2</sub> H <sub>4</sub> ] = 2.21M; [C=C] = 0.55M; T = 60°C; time = 6 h.....	36
4.8 Effect of rubber concentration on SNRL hydrogenation.[CuSO <sub>4</sub> ] = 8 μmol; [N <sub>2</sub> H <sub>4</sub> ] = 0.35 mol; [H <sub>2</sub> O <sub>2</sub> ] = 0.57 mol; T = 60°C; time = 6 h (creaming SNRL (●) and SNRL (■)).....	37
4.9 Effect of reaction temperature on SNRL hydrogenation. [CuSO <sub>4</sub> ] = 49.38 μM; [N <sub>2</sub> H <sub>4</sub> ] = 2.21 M; [H <sub>2</sub> O <sub>2</sub> ] = 3.54 M; [C=C] = 0.55 M; time = 6 h.....	39

FIGURE	PAGE
4.10 Non-catalytic hydrogenation profiles of SNRL hydrogenation. (a) Conversion profiles and (b) first-order in ln plot. $[\text{N}_2\text{H}_4] = 2.21 \text{ M}$ ; $[\text{H}_2\text{O}_2] = 3.54 \text{ M}$ ; $[\text{C}=\text{C}] = 0.55 \text{ M}$ ; $T = 60^\circ\text{C}$ (●), $70^\circ\text{C}$ (■) and $80^\circ\text{C}$ (▲),.....	41
4.11 Catalytic hydrogenation profiles of SNRL hydrogenation. (a) Conversion profiles and (b) first-order in ln plot. $[\text{CuSO}_4] = 49.38$ $\mu\text{M}$ ; $[\text{N}_2\text{H}_4] = 2.21 \text{ M}$ ; $[\text{H}_2\text{O}_2] = 3.54 \text{ M}$ ; $[\text{C}=\text{C}] = 0.55 \text{ M}$ ; $T = 60^\circ\text{C}$ (●), $70^\circ\text{C}$ (■) and $80^\circ\text{C}$ (▲).....	42
4.12 (a) Arrhenius plots and (b) Eyring plots of SNRL hydrogenation. $[\text{N}_2\text{H}_4] = 2.21 \text{ M}$ ; $[\text{H}_2\text{O}_2] = 3.54 \text{ M}$ ; $[\text{C}=\text{C}] = 0.55 \text{ M}$ ; $T = 60\text{-}80^\circ\text{C}$ ; time = 6 h (catalytic (□) and non-catalytic hydrogenation (■)).....	44
4.13 Effect of SDS concentration on SNRL hydrogenation. $[\text{CuSO}_4] = 49.38$ $\mu\text{M}$ ; $[\text{N}_2\text{H}_4] = 2.21 \text{ M}$ ; $[\text{H}_2\text{O}_2] = 3.54 \text{ M}$ ; $[\text{C}=\text{C}] = 0.55 \text{ M}$ ; $T = 60^\circ\text{C}$ ; time = 6 h.....	46
4.14 Effect of hydroquinone concentration on SNRL hydrogenation. $[\text{CuSO}_4] = 49.38 \mu\text{M}$ ; $[\text{N}_2\text{H}_4] = 2.21 \text{ M}$ ; $[\text{H}_2\text{O}_2] = 3.54 \text{ M}$ ; $[\text{C}=\text{C}] = 0.55 \text{ M}$ ; $T = 60^\circ\text{C}$ ; time = 6 h (%hydrogenation (●) and %gel content (■))......	47
4.15 Effect of boric acid concentration on SNRL hydrogenation. $[\text{N}_2\text{H}_4] = 2.21 \text{ M}$ ; $[\text{H}_2\text{O}_2] = 3.54 \text{ M}$ ; $[\text{C}=\text{C}] = 0.55 \text{ M}$ ; $T = 60^\circ\text{C}$ ; time = 6 h.....	50
4.16 Effect of number of treatment on SNRL hydrogenation: The first hydrogenation treatment $[\text{CuSO}_4] = 49.38 \mu\text{M}$ ; $[\text{N}_2\text{H}_4] = 2.21 \text{ M}$ ; $[\text{H}_2\text{O}_2] = 3.54 \text{ M}$ ; $[\text{C}=\text{C}] = 0.55 \text{ M}$ ; $T = 60^\circ\text{C}$ ; time = 6 h; the second, third and fourth hydrogenation treatments $[\text{CuSO}_4] = 8 \mu\text{mol}$ ; $[\text{N}_2\text{H}_4] = 0.35 \text{ mol}$ ; $[\text{H}_2\text{O}_2] = 0.57 \text{ mol}$ ; $T = 60^\circ\text{C}$ ; time = 6 h.....	52
4.17 TEM micrograph of (a) SNRL (b) HSNRL 64.5% (1 <sup>st</sup> treatment) (c) HSNRL 83.5% (4 <sup>th</sup> treatments) (magnification: 3,000x).....	53
4.18 Particle size distribution of HSNRL 0% (●), 64.5% (▲) and 83.5% (■).....	54
4.19 DSC thermograms of (a) SNR, (b) HSNR 64.5% and (c) EPDM.....	57
4.20 TGA thermograms of (a) SNR, (b) HSNR 32.9%, (c) HSNR 64.5%, (d) HSNR 83.5% and (d) EPDM.....	59

<b>FIGURE</b>	<b>PAGE</b>
4.21 Cure characteristics of vulcanized at various rubber blend ratios of HSNR/NR cured by EPV system with 2 phr of DCP; HSNR/NR = 0/100 (■), HSNR/NR = 25/75 (○), HSNR/NR = 50/50 (▲), HSNR/NR = 75/25 (◇) and HSNR/NR = 100/0 (●).....	61
4.22 Scanning electron micrograph of tensile fracture surface of vulcanized at various rubber blend ratios of HSNR/NR cured by EPV system: (a) HSNR/NR = 0/100; (b) HSNR/NR = 25/75; (c) HSNR/NR = 50/50; (d) HSNR/NR = 75/25; (e) HSNR/NR = 100/0 (magnification: 2000×).....	65
4.23 Possible reactions following ozonolysis of a diene-containing polymer.....	67
4.24 Surface of HSNR/NR vulcanizates at various blend ratios after exposure to ozonised air of 50 pphm ozone concentration at 40°C for 24 h: (a) 0/100, (b) 25/75, (c) 50/50, (d) 75/25, (e) 100/0.....	69
4.25 Surface of HSNR/NR vulcanizates at various blend ratios after exposure to ozonised air of 50 pphm ozone concentration at 40°C for 48 h: (a) 0/100, (b) 25/75, (c) 50/50, (d) 75/25, (e) 100/0.....	70
C-1 <sup>1</sup> H-NMR spectra of (a) HSNR, (b) EPDM.....	87
C-2 <sup>13</sup> C-NMR spectra of (a) HSNR, (b) EPDM.....	88

## LIST OF ABBREVIATIONS

ASTM	: American Standard Testing Method
CBS	: <i>N</i> -Cyclohexylbenzothiazole-2-Sulfenamide
CCD Camera	: Charge Coupled Devices Camera
DCP	: Dicumyl Peroxide
DRC	: Dry Rubber Content
DSC	: Differential Scanning Calorimetry
EPDM	: Ethylene-Propylene Copolymer
EPV	: Efficient-Peroxide Vulcanization
FT-IR	: Fourier-Transform Infrared Spectrometer
GPC	: Gel Permeation ChromatoGraphy Analyzer
HD	: Hydrogenation Degree
HSNR	: Hydrogenated Skim Natural Rubber
ISO	: International Standardization for Organization
k'	: Rate Constant
NBR	: Acylonitrile-Butadiene Rubber
MDR	: Moving Die Rheometer
MW	: Molecular Weight
MWD	: Molecular Weight Distribution
NMR	: Nuclear Magnetic Resonance Spectrometer
NR	: Natural Rubber
OsO <sub>4</sub>	: Osmium Tratroxide
phr	: Part Per Hundred
ppm	: Part Per Million
pphm	: Part Per Hundred Million
SBR	: Styrene-Butadiene Rubber
SEM	: Scanning Electron Microscope
SNRL	: Skim Natural Rubber Latex
STR 5L	: Standard Thai Rubber 5L
TEM	: Transmission Electron Microscope
T <sub>f</sub>	: Final Decomposition Temperature
T <sub>g</sub>	: Glass Transition Temperature

$T_{id}$	: Initial Decomposition Temperature
$T_{max}$	: Maximum Decomposition Temperature
TGA	: Thermogravimetric Analysis
TMTD	: Tetramethylthiuram Disulfide
x	: Extent of Hydrogenation
ZnO	: Zinc Oxide



สถาบันวิทยบริการ  
จุฬาลงกรณ์มหาวิทยาลัย

# CHAPTER I

## INTRODUCTION

### 1.1 The Purpose of The Investigation

The chemical modification of polymer has been an interesting method to improve or produce novel polymeric materials, which are inaccessible or difficult to prepare by conventional polymerization processes. Hydrogenation, one type of chemical modification of unsaturated polymer, is an importance method to reduce the amount of unsaturation; consequently, the structure of the hydrogenated polymer has better resistance to thermal and oxidative degradation. Significant examples of hydrogenated polymer products in the commercial synthetic rubber industry include hydrogenated styrene-butadiene rubber (HSBR) produced by Shell and hydrogenated acrylonitrile-butadiene rubber (HNBR) manufactured by Zeon Chemicals and Lanxess Inc. Both hydrogenated rubbers have excellent high temperature stability and resistance to oxygen, ozone and ultraviolet radiation, which are far superior to those of the parent rubber [1]. Diene based polymers e.g., polyisoprene (PI), polybutadiene (PBD), nitrile butadiene rubber (NBR) as well as natural rubber (NR) have carbon-carbon double bonds unsaturation in the backbone structure. The residual carbon-carbon double bonds in the polymer structure are susceptible to thermal and oxidative degradation when exposed to harsh environments, resulting in a decline of the structure properties of the polymers.

The production of concentrated natural rubber latex in Thailand has been estimated 220 thousand tons per annual. Most of the concentrate latex is produced by the centrifugation technique. Large volumes of skim natural rubber latex are also produced as a by-product from this process. The approximately 10-12 percent of latex, which enters the centrifuge, effluxes as skim rubber latex. Therefore, it is estimated that about 13 thousand tons of skim natural rubber latex were produced each year. Skim rubber is evaluated to be a low grade of natural rubber due to presence of number of impurities in it, which has the decrease in the physical and mechanical properties [2]. Skim natural rubber latex (SNRL) contains high amount of *cis*-1,4-



polyisoprene, which is an unsaturated structure and is therefore susceptible to thermal and oxidative degradation.

Thus, skim natural rubber latex required improvement of some of its properties in order to be used for a wider range of applications in the rubber product. Chemical modification of diene-based polymers is an alternative method to modify polymers to obtain the desired property. In the research work, the hydrogenation of skim natural rubber latex is required to produce more valuable hydrogenated skim natural rubber latex.

## **1.2 Objectives**

The objectives of this research can be summarized as follows;

1. Study the diimide hydrogenation of skim natural rubber latex and the effect of reaction parameters on the hydrogenation degree.
2. Study the thermal properties of hydrogenated skim natural rubber.
3. Study the mechanical properties and physical properties of the hydrogenated skim natural rubber/natural rubber (HSNR/NR) blends.

## **1.3 Scopes of The Investigation**

1. Literature survey and in-dept study for this research work.
2. Prepare the hydrogenated skim natural rubber latex by diimide reduction technique. The effect of reaction parameters on the hydrogenation degree were investigated and the kinetic study of hydrogenation rate in the presence of catalyst and non-catalytic hydrogenation were also studied.
3. Characterize the hydrogenated skim natural rubber.
4. Prepare the hydrogenated skim natural rubber/natural rubber (HSNR/NR) blends with efficient-peroxide vulcanization (EPV) system.
5. Investigate the mechanical properties and physical properties of the HSNR/NR blends.
6. Summarize the results and suggest future work.

## CHAPTER II

### THEORY AND LITERATURE REVIEWS

#### 2.1 Natural Rubber Latex

Natural rubber latex, collected by tapping from *hevea brasiliensis* trees, is a colloidal suspension of rubber particles in an aqueous serum phase. The latex that exuded from the cutting is called the fresh natural rubber latex or fresh latex. The major polymer structure component of natural rubber determined by using fourier transform infrared (FTIR), nuclear magnetic resonance (NMR) and X-ray is isoprene unit ( $C_5H_8$ ), which is in the *cis*-1,4-configuration more than 94%. Tanaka [3] reported that rubber chain is composed of unidentified initiating terminal groups, two *trans*-isoprene units and a long chain of *cis*-isoprene units terminated with unidentified chain end groups. The unidentified initiating and chain end groups are possibly oligopeptides ( $\omega'$ ) and a fatty acid esters ( $\alpha'$ ), respectively. The chemical structure of natural rubber is shown in Figure 2.1.

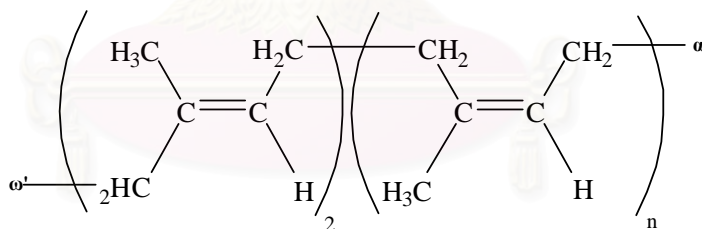


**Figure 2.1** Chemical structure of natural rubber [3].

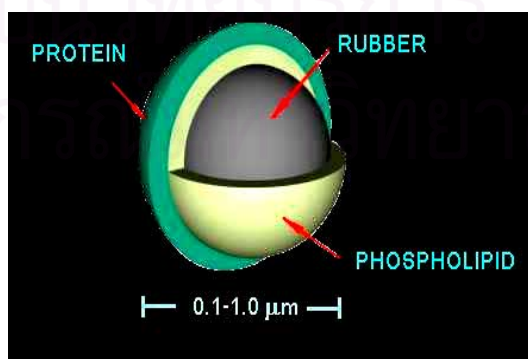
Fresh latex consists of approximately 30–40% dry rubber content (DRC) and 5–10% non-rubber substances. The non-rubber components include proteins, carbohydrates, lipids and inorganic salts. Its composition varies according to the clones of rubber, age of rubber tree and tapping method. The composition of typical fresh latex is present in Table 2.1.

**Table 2.1** Composition of fresh natural rubber latex [4]

Constituent	Composition* (% w/v)
Rubber hydrocarbon	36.0
Proteins	1.4
Carbohydrates	1.6
Neutral lipids	1.0
Glycolipids + phospholipids	0.6
Inorganic constituents	0.5
Water	58.5

\*The %composition of fresh natural rubber latex varies according to clonal variations of rubber clones.

Rubber particles in natural rubber latex are spherical droplets of hydrocarbon, which are stabilized by the negative charge of surface-absorbed proteins and phospholipids [5] as shown in Figure 2.2. After exuding from the hevea trees, latex will be coagulated within a few hours. This process occurs as a result of biochemical reactions with microorganisms and non-rubber component, e.g., sucrose and fructose. Consequently, the preservation is necessary; ammonium was added as a preservative against bacterial attack and to provide long-term stability through hydrolysis of phospholipids to fatty acid soaps.

**Figure 2.2** The structure of rubber particles [5].

Hevea rubber is a polymer of very high molecular weight with broad molecular weight distribution (MWD). The broad MWD of hevea rubber is presumed to be derived from the branching and crosslinking reaction by certain special functional groups in rubber molecules. Osmometry, light scattering, solution viscometry and gel permeation chromatography have been commonly used to determine the molecular weight (MW) of rubber. MWD can be obtained by the analysis of fraction samples, which are usually obtained by solvent fractionation techniques. Among these techniques gel permeation chromatography (GPC) is the most popular method for the determination of the MWD as well as MW of natural rubber. By using GPC, it was found that the MWD of natural rubber in freshly tapped latex is bimodal [6]. MWD of various clonal rubbers was classified three types as shown in Figure 2.3:

Type A distinctly bimodal distribution with nearly equal peak height.

Type B bimodal distribution with small low molecular weight peak.

Type C skewed unimodal distribution with a shoulder in the low MW region.

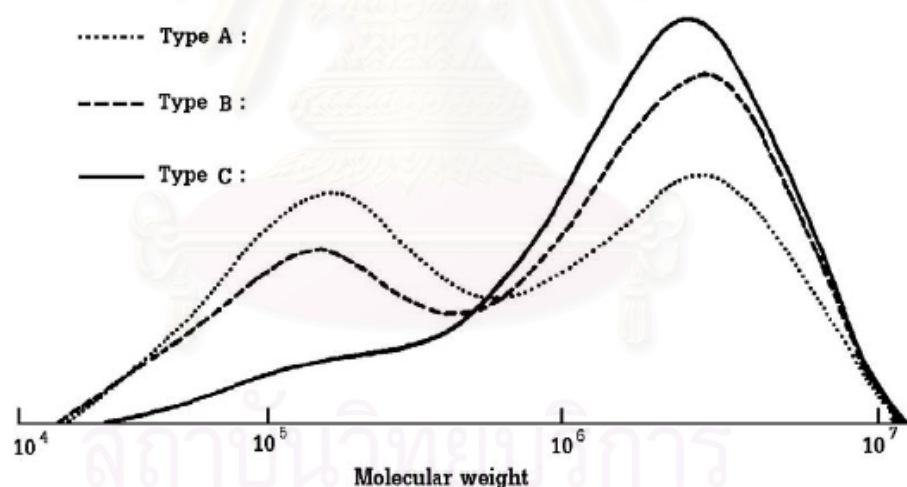


**Figure 2.3** Type of molecular weight distribution curves of natural rubber [7].

The high molecular weight peak in MWD is centered at around  $1 \times 10^6$  and  $2.5 \times 10^6$ , while it is around  $1 \times 10^5$ - $2 \times 10^5$  for the low molecular weight peak. The average molecular weight is  $M_w = 1.6$ - $2.3 \times 10^6$  and  $M_n = 2.0$ - $5.2 \times 10^5$ . The polydispersity index ( $M_w/M_n$ ) is extremely wide ranging from 2.5 to 10. The molecular weight of natural rubber can be reduced by various factors such as

mechanical or chemical mastication, exposure to sunlight and heat treatment. This is due to the degradation of rubber chain.

There are two components called “sol” and “gel” in natural rubber. The sol phase is a rubber part that dissolves easily in good solvents such as cyclohexane, toluene, tetrahydrofuran (THF), *etc.*, while the gel phase swells without dissolving. Commercially available dry hevea rubber contains 5-50% gel phase, depending on the clonal origin of the rubber, processing conditions, time and the storage temperature. The true gel phase in natural rubber was presumed to consist of small crosslink latex particles or “microgels” [8] as shown in Figure 2.4. The microgels are combined into a matrix with the sol fractions and form an apparent gel phase. The gel phase in natural rubber contains nitrogenous and mineral components higher than the sol phase. This can be postulated that the gel phase is linked up with the network of proteins via hydrogen bonding. The gel contents of rubber can be decreased by deproteinization and transesterification [9]. These treatments decompose the branching and crosslink composed of protein and fatty acid ester group, respectively. This can be attributed to the fact that the branching and crosslink are composed of two type branch-points. One is presumed to be formed by the intermolecular interaction of proteins and another by phosphoric ester group and long chain fatty acid ester group as shown in Figure 2.5.

In addition, the gel phase in hevea rubber is sometimes classified to “loose gel” or “soft gel” and “tight gel” or “hard gel”. The soft is derived from various non-rubber components, which can be decomposed by chemical reaction such as enzymatic deproteinization, transesterification and saponification [9]. On the other hand, the hard is formed by crosslinking of unsaturated rubber chain, which can not be decomposed by chemical reaction.

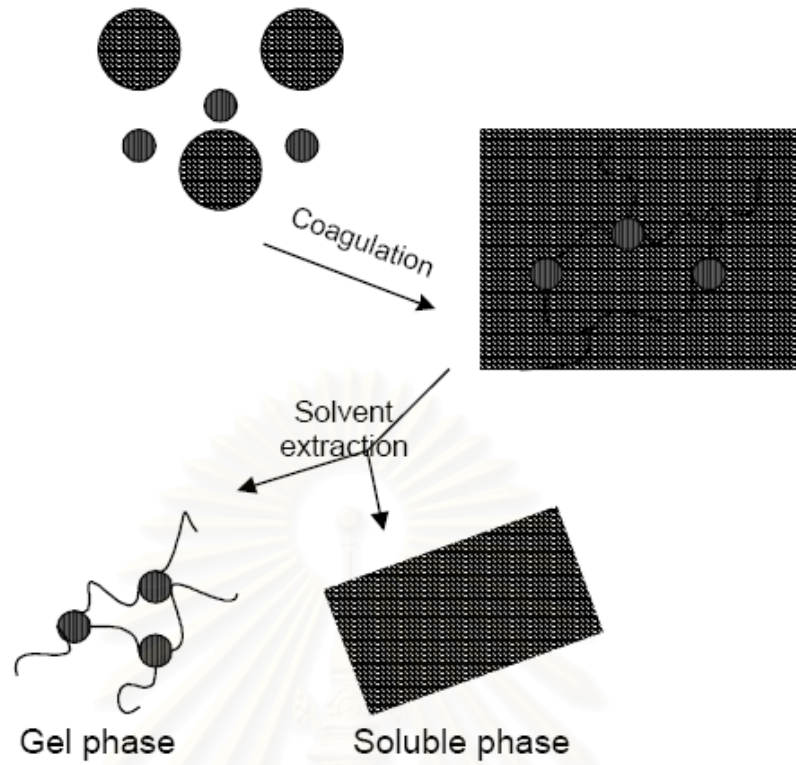


**Figure 2.4** Schematic representation of gel phase in natural rubber [8].

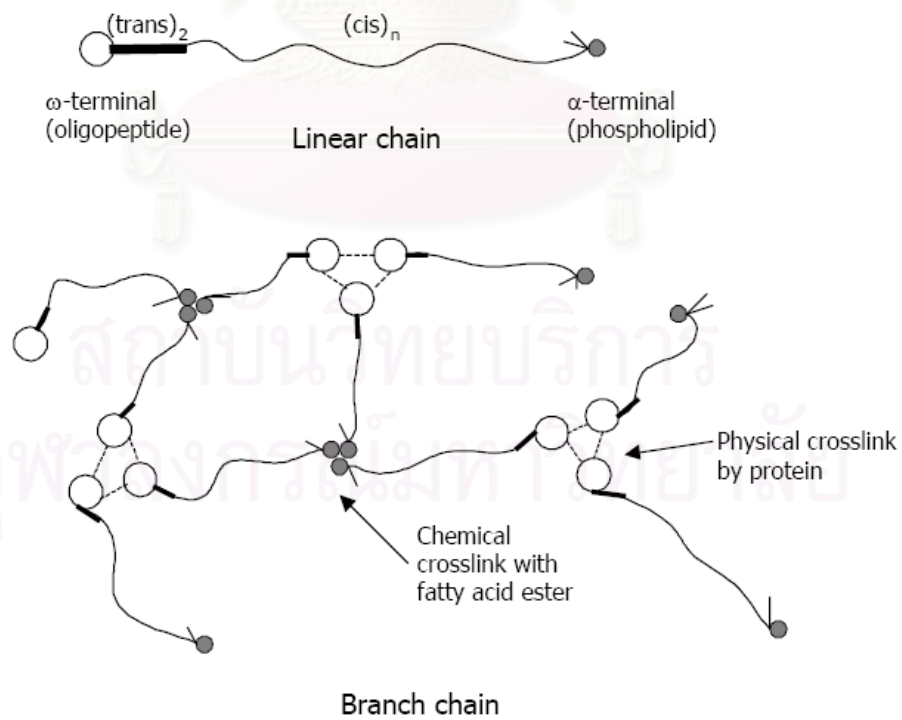


**Figure 2.5** Presumed structure of branching and crosslinking of natural rubber [9].

## 2.2 Skim Natural Rubber

Skim natural rubber obtained from skim latex contains 75-85% rubber hydrocarbon with 9-18% proteins and 5-10 % acetone-soluble material. Skim rubber, which has not been purified, contains a much higher proportion of natural non-rubber substances than normal rubber. This due to the fact that skim natural rubber is mostly derived from small rubber particles with a high specific surface. Impurities such as protein have a higher specific gravity than rubber and migrate to the serum fraction during centrifuging.

Actually, skim natural rubber composed of linear rubber molecule with non-phospholipid groups at the terminal end. Thus, it contains non-branching and gel. Rubber molecules in skim natural rubber also show the lower nitrogenous compounds and attached to rubber molecules. In addition, skim natural rubber shows a unimodal molecular weight distribution, which differ from the ordinary rubber (Figure 2.6). It also shows low green strength compared to the ordinary natural rubber due to the low fatty acid ester content. Furthermore, the natural antioxidant in skim natural rubber was assumed to be absent.

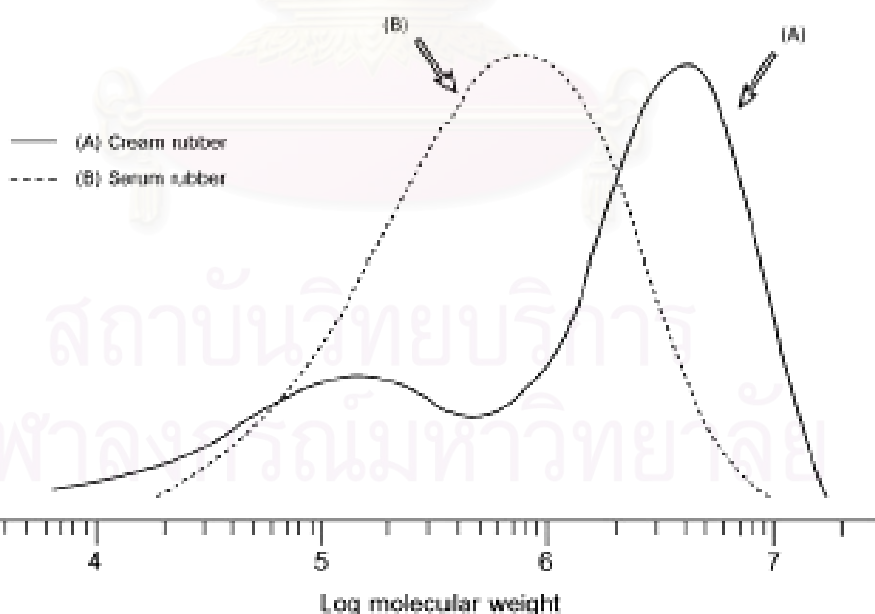


**Figure 2.6** Molecular weight distribution curves of skim natural rubber and ordinary rubber [10].

### 2.3 Concentration of Natural Rubber Latex

Fresh field latex from *hevea brasiliensis* tree has a rubber content of ca. 30-40% DRC, dispersed in water or dispersion medium. The concentration of latex is necessary not only to reduce the volume of latex for transportation, but also to reduce the ratio of non-aqueous substances to dry rubber content. In addition, several of the industrial processes use the latex which has concentration higher than 33%.

Various methods, which have been proposed for concentrated natural rubber latex, four have received serious attention as practicable process. These are evaporation, creaming, centrifugation, electrodecantation.

Concentration by creaming is sedimentation process using creaming agent e.g. ammonium alginate. In NRL, the density of rubber particles is less than that of dispersion medium. After creaming, therefore the rubber particles tend to rise to the surface of the dispersion medium. The concentrated latex is known as cream, while the dilute latex forming the lower layer is known as skim as shown in Figure 2.7. The serum layer is drained off after incubation for about 40 hours.

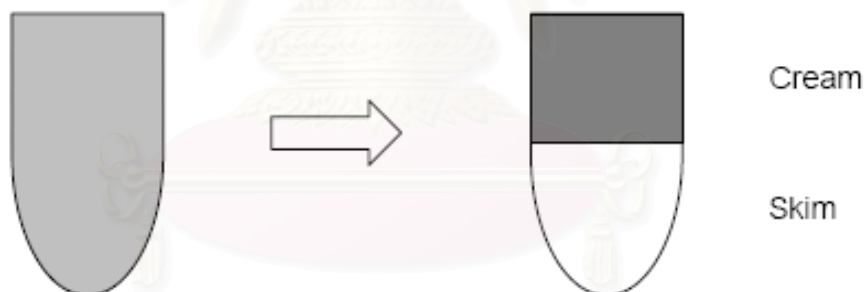


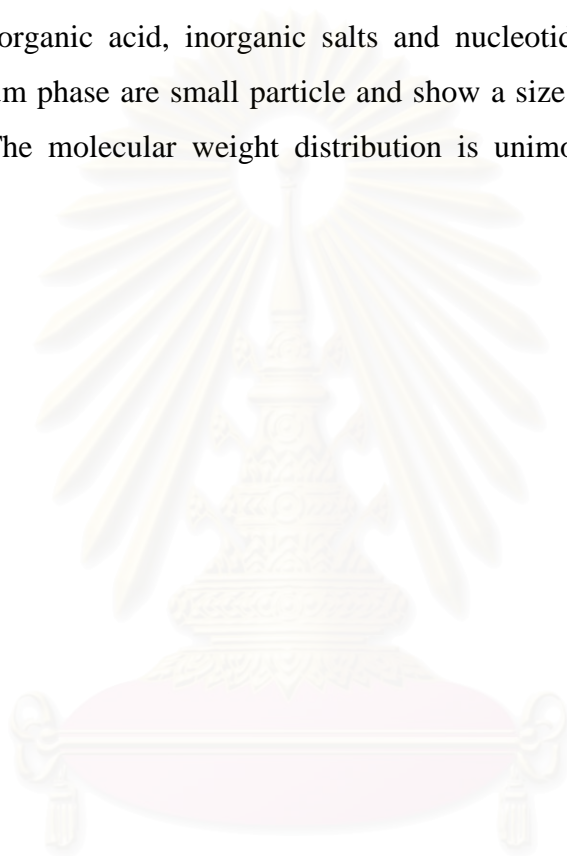
**Figure 2.7** Creaming process of natural rubber latex.

Among the methods currently used for the concentration of natural rubber latex, centrifuge is the most important; about 90% of concentrated latex used in industrial is produced by centrifugation. Centrifugation is a type of accelerated creaming process, which successful concentration can be obtained with significant difference between with the density of the rubber particles that of the aqueous phase. The centrifuge concentrate is known as cream, and dilute latex obtained as a by-product is known as skim. The production process of concentrated latex by centrifugation is shown in Figure 2.8.



Concentrated latex consists of approximately 60% DRC with a lesser amount of non-rubber substances. The most of rubber particles in this cream phase are large particles, which show a size distribution ranging from 0.1-0.3  $\mu\text{m}$ . The molecular weight of the rubber from cream phase is a typical bimodal molecular weight distribution, which peak at MW of  $2 \times 10^6$  g/mol and  $1.2 \times 10^5$  g/mol.

The serum of skim latex are contain amount of rubber particle 4-10 %DRC, with high amount of non-rubber component, including amino acid, proteins, carbohydrates, organic acid, inorganic salts and nucleotidic materials. The rubber particles in serum phase are small particle and show a size distribution in a range of 0.05-0.3  $\mu\text{m}$ . The molecular weight distribution is unimodal, with peak at  $1 \times 10^6$  g/mol.



สถาบันวิทยบริการ  
จุฬาลงกรณ์มหาวิทยาลัย

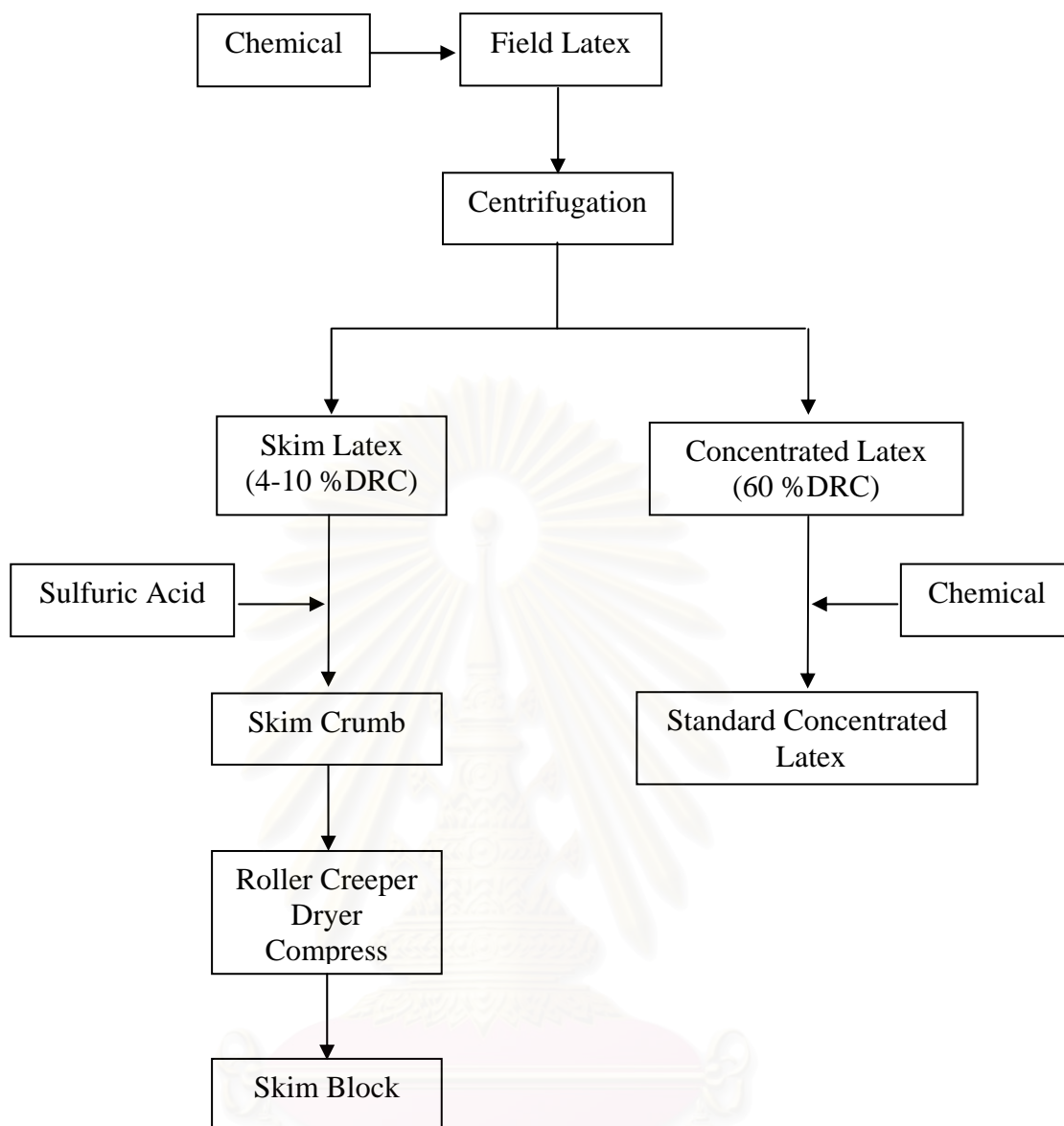


**Figure 2.8** Commercial production of concentrated latex and skim rubber [11].

## 2.4 Chemical Modification via Hydrogenation of Diene-Based Polymers

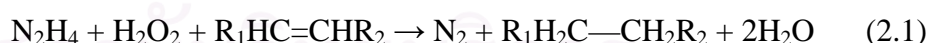
The chemical modification of polymer has been an interesting method to improve or produce novel polymeric materials, which are inaccessible or difficult to prepare by conventional polymerization processes. Chemical modifications such as crosslinking, grafting, degradation, oxidation, isomerization and cyclization have been studied for altering and optimizing the physical and mechanical properties of polymers [12]. Diene based polymers e.g., polyisoprene (PI), polybutadiene (PBD),

nitrile butadiene rubber (NBR) as well as natural rubber (SNR) have carbon-carbon double bonds unsaturation in the backbone structure. The residual carbon-carbon double bonds in the polymer structure are susceptible to thermal and oxidative degradation when exposed to harsh environments, resulting in a decline of the structure properties of the polymers.

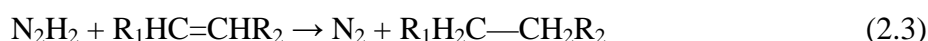
Hydrogenation, one type of chemical modification of unsaturated polymer, is an importance method to reduce the amount of unsaturation; consequently, the structure of the hydrogenated polymer has better resistance to thermal and oxidative degradation. Significant examples of hydrogenated polymer products in the commercial synthetic rubber industry include hydrogenated styrene-butadiene rubber (HSBR) produced by Shell and hydrogenated acrylonitrile-butadiene rubber (HNBR) manufactured by Zeon Chemicals and Lanxess Inc. Both of there hydrogenated rubber have excellent high temperature stability and resistance to oxygen, ozone and ultraviolet radiation, which are far superior to those of the parent rubber. Hydrogenation can be carried out by both catalytic (homogeneous, heterogeneous) and non-catalytic (diimide) process [13]. Homogeneous catalysts are favored for catalytic hydrogenation of unsaturation polymers in solution because they have higher selectivity and do not involve a macroscopic diffusion problem.

## 2.5 Hydrogenation of Latex by Diimide Reduction

The overall diimide hydrogenation reaction of polymer is presented in eq. 2.1.



Diimide hydrogenation is achieved by two steps: (1) the reaction between hydrazine and hydrogen peroxide to produce the diimide and (2) the reaction between diimide and carbon-carbon double bonds to form hydrogenated polymer, as given by the following equations:



However, according to the reactivity of diimide, two side reactions possibly accompany the hydrogenation reaction. One is the further reaction of diimide with hydrogen peroxide to generate nitrogen gas, which most likely occurs on the interface as the nitrogen peroxide resides in the water phase. The other side reaction is the reaction between two diimide molecules to produce one molecule of hydrazine and to release one nitrogen gas molecule, which most likely occurs in the rubber phase.



The four reactions represented by eq. 2.2, 2.3, 2.4, 2.5 comprise the framework of the diimide hydrogenation of latex. Equation 2.2 may occur at the interface of the rubber particles and also the bulk aqueous phase. Diimide may get consumed by way of eq. 2.4 either at the interface or in the aqueous phase before it actually diffuses into the rubber particles. Equation 2.5 is the radical source for crosslinking. There are three competing parallel processes in the reaction mechanism

1. The reaction of eq. 2.2 may occur at the interface and also in the bulk aqueous phase. Diimide generated in the aqueous phase would not be available for the hydrogenation reaction in the organic phase. Thus, this competition influences the efficiency of the diimide utilization in the aqueous phase.
2. The reaction of eq. 2.4 is competes with the diimide diffusion process for diimide before it diffuse into the rubber particles. This competition influences the efficiency of diimide utilization at the interface.
3. The reaction eq. 2.5 is competes with eq. 2.2 for diimide. This competition influences the diimide utilization efficiency in the rubber phase, and also set up the platform for radical generation and crosslinking.

## 2.6 Literature Reviews

Diimide hydrogenation of acrylonitrile-butadiene rubber (NBR) in latex form was discovered by Wideman [14], which involved a system containing hydrazine hydrate, an oxidant and metal-ion catalyst (i.e., called the diimide reduction technique) without using any pressure vessel, organic solvent or hydrogen gas.

Parker *et al.* [15] proposed a mechanism of diimide hydrogenation for nitrile-butadiene rubber (NBR) latex. The diimide hydrogenating agent was generated from the hydrazine/hydrogen peroxide system at the surface of the polymer particles. Carboxylated surfactants adsorbed at the latex particle surface play an important role by forming hydrazinium carboxylates with hydrazine and copper ions. The mechanisms for diimide hydrogenation are shown in Figure 2.9.

He *et al.* [16] compared the diimide hydrogenation of styrene-butadiene rubber (SBR) latex with respect to different particle sizes. It was found that the hydrogenation of carbon-carbon double bonds depends on the latex particle size. Hydrogenation of SBR latex with a diameter of 50 nm could be hydrogenated to 91% hydrogenation, using 1 mol of hydrazine and 1 mole of hydrogen peroxide per mole of carbon-carbon double bond. For the latex with a diameter of 230 nm, the hydrogenation degree was only 42%. A Layer model was proposed to explain the effect of particle size, as shown in Figure 2.10. They pointed out that the surface density of copper ion catalyst in the particle surface was an important parameter in controlling the degree of hydrogenation of hydrogenated styrene-butadiene rubber (HSBR).

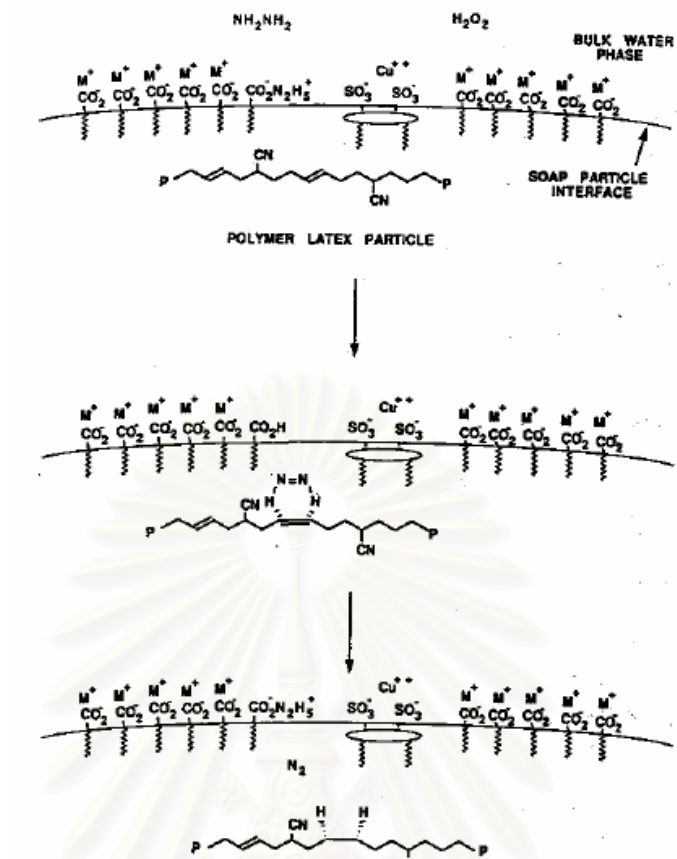


Figure 2.9 Proposed mechanism for diimide hydrogenation [15].

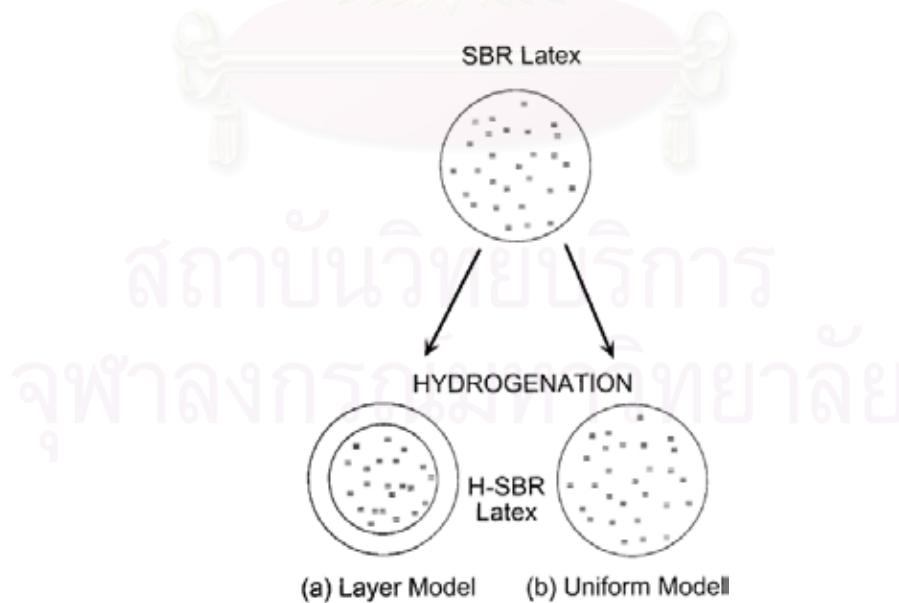


Figure 2.10 Model of distribution of double bonds in hydrogenated SBR latex particles: (a) Layer model; (b) Uniform model [16].

Belt *et al.* [17, 18] reported several patents on diimide hydrogenation, in which, boric acid was used as a catalyst. It was claimed that a compound was added before, during or after the hydrogenation to break crosslinks formed during the hydrogenation. The compound can be chosen from primary or secondary amines, hydroxylamine, imines, azines, hydrazones, and oximes. The emulsion form of *N*-1,4-dimethylphenyl (*N*-phenyl)-*p*-phenylenediamine was also suggested to reduce gel formation.

Xie *et al.* [19] studied the diimide reaction conditions on both hydrogenation and crosslinking. Ferrous sulfate is better than cupric sulfate as a catalyst for catalyzing the diimide hydrogenation of carboxylic styrene-butadiene rubber (XSBR) latex. The hydrogenation degree can reach over 90%. By using sodium *N,N*-dimethyldithiocarbamate and *p*-tert-butyl-pyrocatechol as the inhibitors, the gel content in the final rubber product could be reduced.

Xie *et al.* [20] studied the effect of hydrogenation of nitrile-butadiene rubber latex (HNBR). A hydrogenation degree of 87% was achieved after 6 h at 40°C for a mole ratio of hydrazine to carbon-carbon double bond of 2.5:1. It is important to use an inhibitor, *p*-tert-butyl-pyrocatechol, during hydrogenation to prevent the formation of a large amount of gel and it reduced the gel content from 94.3% to 21.7%.

Zhou *et al.* [21] also studied hydrogenation of acrylonitrile-butadiene rubber (NBR) latex by hydrogen peroxide and hydrazine with boric acid as catalyst. It was found that drop-wise addition of hydrogen peroxide with post reaction at ambient temperature was the most effective way of conducting diimide hydrogenation. The hydrogenated NBR with a hydrogenation degree of 81.3% within 6 h at 60°C and a gel mass fraction of 3.1% was obtained when hydroquinone was used as an inhibitor.

Lin *et al.* [22] investigated hydrogenation of nitrile-butadiene rubber (NBR) latex via diimide reduction by examining hydrogenation efficiency (HE) and hydrogenation degree (HD). It has been found that the hydrogenation efficiency, which is defined as the ratio of amount of hydrogen peroxide consumed for the hydrogenation to total amount of hydrogen peroxide reacts, varies with both the type

of catalyst and degree of hydrogenation. Boric acid used as a promoter, can bring the hydrogenation efficiency to a level of nearly 100% when the degree of hydrogenation is below 60%. The hydrogenation efficiency decreased in the range of low hydrogenation degree caused from side reactions at the inter-phase of the latex particles, which modulated by the catalyst and the addition rate of hydrogen peroxide; whereas the decrease in the hydrogenation efficiency in the range of high hydrogenation degree, which caused by side reactions within the polymer phase was also reported.

Lin *et al.* [23] also investigated the gel formation in the hydrogenated polymer via diimide hydrogenation. The results indicated that hydrogen peroxide decomposition, some reactions related to oxygen, and the redox reaction between hydrogen peroxide and hydrazine are capable to generating radicals. However, radicals generated in the aqueous phase do not appear to initiate the crosslinking of diene-based polymers in the latex form. It was proposed that the primary radicals giving rise to crosslinking are generated in the polymer phase *in situ*, and the step responsible for generating these organic radicals is possibly the diimide disproportionation reaction. At the higher degree of hydrogenation, the hydrogenation efficiency decreased, and the gel content of polymer increased sharply.

Lin *et al.* [24] studied the simulation of the diimide hydrogenation process carried out by taking into account the diimide generation reaction, the hydrogenation reaction, the side reaction between hydrogen peroxide and diimide, the disproportionation of diimide and the diimide diffusion process. It was found that the diimide diffusion interfered with the diimide hydrogenation of nitrile-butadiene rubber (NBR) latex, even though the particle diameter was as small as 72 nm.

Mahittikul *et al.* [25] studied diimide hydrogenation of natural rubber latex (NRL) using copper sulfate as catalyst. It was found that 67.8% hydrogenation was achieved within 6 h at 55°C and low rubber concentration and high hydrazine concentration provided the optimum condition. Moreover, the diimide hydrogenation of NRL provided a method to improve the thermal stability of natural rubber.



## CHAPTER III

### EXPERIMENTAL AND DATA CHARACTERIZATION

#### 3.1 Chemicals

1. Skim natural rubber latex (SNRL) : Pan Asia Biotechnology Ltd.
2. Natural rubber (STR-5L) : Pan Asia Biotechnology Ltd.
3. Ethylene-propylene copolymer (EPDM) : Pan Asia Biotechnology Ltd.
4. Hydrazine hydrate (100%) : Merck
5. Hydrogen peroxide  
(30% aqueous solution) : Merck
6. Copper (II) sulfate : Merck
7. Copper (II) acetate : Merck
8. Copper (II) chloride : Merck
9. Ferric (II) sulfate : Merck
10. Zinc (II) sulfate : Merck
11. Boric acid : Fisher
12. Sodium *n*-dodecyl sulfate : Fisher
13. Hydroquinone : BDH
14. Silicone oil : Ajax Finechem
15. Hydroxy propyl methyl cellulose : Apex
16. Ethanol 95% : SR Lap
17. D-chloroform : Merck
18. Toluene : Fisher
19. Stearic acid : Imperial Industrial  
Chemicals Co. Ltd.
20. Zinc oxide : Pan Innovation Ltd.
21. *N*-cyclohexylbenzothiazole  
-2-sulfenamide : Flexsys (Monsanto)
22. Tetramethylthiuram disulfide : Flexsys (Monsanto)
23. Dicumyl peroxide : Petch Thai Chemical Co. Ltd.

### 3.2 Glasswares

1. 4-Neck round bottom reactor, 500 cm<sup>3</sup> capacity
2. Condenser
3. Round bottom flask
4. Other general laboratory glassware

### 3.3 Equipments

1. Fourier transform infrared spectrometer : Thermo 470 FT-IR spectrometer
2. Nuclear magnetic resonance spectrometer : Bruker 400 MHz spectrometer
3. Nano-sizer : Malvern zetasizer nano series
4. Thermogravimetric analyzer : Perkin-Elmer Pyris Diamond TG/DTA
5. Differential scanning calorimeter : Mettler Toledo DSC 822
6. Transmission electron microscope : JEOL JEM 2010
7. Moving die rheometer : TECHPRO
8. Universal Testing Machine : LLOYD model LR5K
9. Hardness Testing Machine : Rockwell Hardness Tester 4150AR
10. Scanning electron microscope : JEOL model JSM – 6480 LV
11. Ozone resistance tester : HAMPDEN, Northampton, England

### 3.4 Diimide Hydrogenation Procedure

The skim natural rubber latex was added into a 500 mL four-necked flask. After stirred for 30 min, a catalyst copper sulfate and hydrazine hydrate were added respectively, and stirred for 60 min. Then, the mixture was heated to reaction temperature. At particular temperature, hydrogen peroxide was added drop-wise at a rate so that the temperature of the mixture did not increase. During addition of hydrogen peroxide, if too many bubbles were formed, small antiform agent (Dow

Corning silicone oil) was added as necessary to minimize forming. The mixture was post-reacted for 30 min while cooling to room temperature. The hydrogenated skim natural rubber latex was coagulated into ethanol, washed several times, filtered and dried under vacuum at room temperature.

### 3.5 Blending and Vulcanization Process of Rubber

The preparation of hydrogenated skim natural rubber/natural rubber (HSNR/NR) blends was performed using a two-roll mill at room temperature in order to avoid the overcure of NR in the rubber blends. NR was masticated for 2 min before mixing with HSNR. When the rubber blend was homogenized (ca. 5 min), the chemicals for vulcanization were added. Zinc oxide and stearic acid were both used as the activator. Dicumyl peroxide (DCP) as peroxide and tetramethylthiuram disulfide (TMTD) and *N*-cyclohexylbenzothiazole-2-sulfenamide (CBS) as sulfur donor accelerator were used as the vulcanizing agent. The processing time after the addition of each component was ca. 2 min. The sheet of rubber compounds was kept at room temperature for 24 h and vulcanized in compression mold at 150°C. The vulcanization system, efficient-peroxide vulcanization (EPV) was employed and the compound recipes for blends are given in Table 3.1. The blends of HSNR (>60% hydrogenation) and NR at 0/100, 25/75, 50/50, 75/25 and 100/0 wt ratio were prepared.

**Table 3.1** Formulation of rubber compounds.

Ingredients	EPV Vulcanization systems
%Hydrogenation	>60 (HSNR)
HSNR/NR (wt. ratio)	0/100, 25/75, 50/50, 75/25, 100/0
Zinc oxide (phr)	3
Stearic acid (phr)	1.5
CBS (phr)	0.7
DCP (phr)	2
TMTD (phr)	1.5

phr = parts per hundred of rubber by weight.

### 3.6 Characterization Methods

#### 3.6.1 Fourier Transform Infrared Spectroscopy Analysis (FTIR)

The characteristics of skim natural rubber latex and hydrogenated skim natural rubber latex were determined by FTIR. The rubber samples were dissolved in toluene and casted on a potassium bromide disk at atmospheric pressure and dried at room temperature for an FTIR scan obtained with a Thermo 470 FT-IR spectrometer. For each spectrum, 32 scans at a resolution of  $4\text{ cm}^{-1}$  in the range of wave number from  $4000\text{ cm}^{-1}$  to  $400\text{ cm}^{-1}$  were performed.

#### 3.6.2 Nuclear Magnetic Resonance Spectroscopy Analysis (NMR)

The final degree of olefin conversion of hydrogenated skim natural rubber latex was quantified by NMR spectroscopic analysis.  $^1\text{H}$  and  $^{13}\text{C}$ -NMR spectra were recorded on 1% w/v solutions of the in d-chloroform at atmospheric pressure and room temperature. NMR spectra were obtained on a Bruker 400 MHz spectrometer using tetramethyl silane (TMS) as the internal standard. The number of scans of  $^1\text{H}$  and  $^{13}\text{C}$ -NMR spectra were 32 and 96 scans, respectively. The chemical shift ( $\delta$ ) reported was given in part per million (ppm) down field from TMS.

The final degree of hydrogenation of HSNR was evaluated by  $^1\text{H}$ -NMR spectroscopy. Integration of spectra was used to determine the amount of characteristic protons of each structure in the polymer. The integration peak area for the saturated protons ( $-\text{CH}_2-$  and  $-\text{CH}_3$ ) in the range of 0.8-2.3 ppm and the unsaturated protons peak area at 5.2 ppm were measured in order to calculate the degree of hydrogenation using Eq. 2.1:

$$\% \text{Hydrogenation} = \frac{A - 7B}{A + 3B} \times 100 \quad (2.1)$$

where A is the integration peak area of saturated protons and B is the integration peak area of unsaturated protons. The calculation of hydrogenation degree is presented in Appendix C.

### 3.6.3 Particle Size and Size Distribution Analysis

All particle size measurements were conducted in diluted aqueous solution with a solid content of about 0.1% using Nano-sizer (Malvern zetasizer nano series, German). Measurement conditions were wavelength of 633 nm, detector angle of 90° and temperature of 25°C.

### 3.6.4 Thermogravimetric Analysis (TGA)

Thermogravimetric analysis (TGA) of the sample was performed on a Perkin-Elmer Pyris Diamond TG/DTA. The temperature was raised under a nitrogen atmosphere from room temperature to 800°C at a constant heating rate of 10°C/min. The flow rate of nitrogen gas was 50 ml/min. The initial decomposition temperature ( $T_{id}$ ) and the final decomposition temperature ( $T_f$ ) were obtained from the intersection of two tangents at the initial final stages of decomposition, respectively. The maximum decomposition temperature at maximum of mass loss rate ( $T_{max}$ ) was also evaluated.

### 3.6.5 Differential Scanning Calorimetry (DSC)

Differential scanning calorimetry (DSC) of the samples was carried out on a Mettler Toledo DSC 822. The instrument signal is derived from the temperature difference. The sample in a crimped aluminium pan was cooled down to -100°C with liquid nitrogen and then heated up to 25°C with constant heating rate of 10°C/min under nitrogen atmosphere with constant rate of 20°C/min. The glass transition temperature ( $T_g$ ) was calculated from the midpoint of the base-line shift of DSC thermogram.

### 3.6.6 Morphological Study

The morphology of the sample was observed on a JEOL JEM 2010 transmission electron microscope (TEM). A small amount of sample was dispersed in water and dropped on the grid. The sample was then stained with OsO<sub>4</sub> vapor for 24 h before observation. Attachment of osmium atoms to unsaturated hydrocarbon

repeating unit resulted in a dark image for those portions. The TEM micrograph was taken by using a 15 kV electron beam with a magnification of 3000x.

### **3.6.7 Rheometric Characteristics of Blends**

The rheometric characteristics of blends such as minimum torque (ML), maximum torque (MH), scorch time ( $T_{s2}$ ) and optimum cure time ( $T_{c90}$ ) were measured by using a moving die rheometer (TECHPRO, rheotech MD+) at 150°C with frequency 1.7 Hz and amplitude 0.5°, according to ASTM D5289. The test temperature was 150°C in compression mold for the blending of natural rubber and hydrogenated skim natural rubber at optimum cure time.

### **3.6.8 Mechanical Properties of HSNR/NR Vulcanizates**

The mechanical properties in terms of tensile strength, ultimate elongation and hardness of vulcanizates were evaluated. The tensile properties before and after thermal aging at 100°C for  $22 \pm 2$  h of HSNR/NR vulcanizates were investigated. The specimens were cut as a dumbbell shape using a die C according to the standard method ASTM D412. The tensile properties of all vulcanized rubber samples were carried out on a Universal Testing Machine (LLOYD model LR5K) at 500 mm/min of cross-head speed. The elongation of specimens was detected from the extensometer. The average of three specimens was considered as the representative value. The shore hardness of the specimens was also measured according to ASTM D2240 using a type A Durometer.

### **3.6.9 Morphology of HSNR/NR Vulcanizates**

The tensile fracture surfaces of rubber blends were characterized using scanning electron microscopy (SEM). The fracture surfaces after tensile testing were cut and stitched on a SEM stub using double-sided tape. The samples were then sputter – coated with gold and examined using an electron microscope, JEOL model JSM – 6480 LV operated at 15 kV with a magnification of 2000x.

### 3.6.10 Ozone Resistance Test

The test of ozone resistance followed the standard method ISO 1431/1 – 2004 and physical testing standards of rubbers developed by Nishi and Nagano. The specimens were cut to a size of 2.5 cm × 8.0 cm × 2.7 mm. The rubber samples were exposed in an ozone cabinet (HAMPDEN, Northampton, England) at 40°C to an ozone atmosphere of 50 pphm (part per hundred million). Before exposure to ozone, the specimens were stretched by 20% using a specimen holder for 48 h in the absence of light and ozone. The results of ozone cracking were observed at 3, 6, 24, 27 and 48 h. The cracking on rubber surface was examined by using an optical microscope and a CCD camera.

**Table 3.2** Classification of cracking on rubber surface [26].

Number of Cracking	Size and Depth of Cracking
A: a small number of cracking	1. That which cannot be seen with eyes but can be confirmed with 10 times magnifying glass. 2. That which can be confirmed with naked eyes.
B: a large of number cracking	3. That which the deep and comparatively long (below 1 mm). 4. That which the deep and long (above 1 mm and below 3 mm).
C: numberless cracking	5. That which about to crack more than 3 mm or about to severe.

### 3.6.11 Determination of Crosslink Density

The cross-linking efficiency of the specimens was evaluated in terms of crosslink density using an equilibrium solvent swelling test method. The specimens (10 x 10 x 2 mm) accurately weighed were immersed in toluene and allowed to swell in closed vessels for 7 days. Then, the surface of the swollen samples was quickly wiped and weighed ( $w_1$ ). After drying at 40°C for 48 h, the dried rubber samples were weighed again ( $w_2$ ) to determine the amount of adsorbed toluene inside the samples.

The volume fraction of polymer in the swollen specimens ( $v$ ) was calculated using Equation. 2.2:

$$v = \frac{w_2 (\delta_r)^{-1}}{w_2 (\delta_r)^{-1} + (w_1 - w_2)(\delta_s)^{-1}} \quad (2.2)$$

where  $\delta_r$  and  $\delta_s$  are the rubber and solvent densities, respectively [27]. The crosslink density of the specimens was calculated based on the Flory-Rhener equation (Equation. 2.3):

$$-\ln(1-v) + v + \chi v^2 = V_0 n [v^{1/3} - \frac{v}{2}] \quad (2.3)$$

where  $n$  is the number of elastically active chains per unit volume ( $\text{mol}/\text{cm}^3$ ),  $V_0$  is the molar volume of the solvent ( $106.3 \text{ cm}^3/\text{mol}$  for toluene) and  $\chi$  is the Flory-Huggins polymer-solvent interaction term ( $0.393$  for NR-toluene) [28].

สถาบันวิทยบริการ  
จุฬาลงกรณ์มหาวิทยาลัย



## CHAPTER IV

### RESULTS AND DISCUSSION

Skim natural rubber latex (SNRL) is produced as a by-product from the production of concentrated natural rubber latex (NRL). The major component of SNR identified from FTIR and NMR spectroscopy is polyisoprene in *cis*-1,4-configuration. SNR degraded when exposed to sunlight, ozone, oxygen and long term heating due to the unsaturation of carbon-carbon double bonds of the isoprene backbone. Hydrogenation is one type of chemical modification, which reduces the amount of unsaturation and thus changes the properties of diene polymer toward greater stability against thermal and oxidative degradation. The high amount of *cis*-1,4-polyisoprene could be hydrogenated to a strictly alternating ethylene-propylene copolymer by diimide reduction, using hydrazine and hydrogen peroxide with copper sulfate as catalyst. For this technique, gaseous hydrogen, organic solvent and expensive transition metal catalyst are not required. This is especially advantageous when hydrogenated rubber in latex form is demanded.

#### 4.1 FTIR and NMR Spectroscopic Characterization

The structure of non-hydrogenated skim natural rubber (SNR) and hydrogenated skim natural rubber (HSNR) were characterized by Fourier transform infrared (FTIR) spectroscopy as shown in Figure 4.1. FTIR assignments for SNR are presented in Table C-1, Appendix C-1. From FTIR spectra of the HSNR sample, the C=O stretching ( $1732\text{ cm}^{-1}$ ) and C–O stretching ( $1140\text{ cm}^{-1}$ ) appeared. The weak transmittance bands at  $3280$  and  $1530\text{ cm}^{-1}$  remained after the hydrogenation corresponding to the protein impurities in the SNR are >N–H and >N–C=O [29]. The characteristic signal of non-hydrogenated SNR spectrum showed distinct peaks for the C=C unsaturation, *i.e.*, at  $1664\text{ cm}^{-1}$  (C=C stretching) and  $836\text{ cm}^{-1}$  (olefinic C–H bending). It can be noted that the absorbance peaks for the C=C unsaturation decrease after the hydrogenation. The augmentation in the band at  $737\text{ cm}^{-1}$  attributed to the  $-(\text{CH}_2)-$  species increased, as the extent of hydrogenation of C=C increased.

$^1\text{H}$ -NMR spectra for the non-hydrogenated skim natural rubber (SNR) and hydrogenated skim natural rubber (HSNR) are provided in Figure 4.2. Major peaks are obtained in the aliphatic (1.7 and 2.2 ppm) regions. The signals of *cis*-olefinic protons are centered at 5.1 ppm. When the hydrogenation progresses, the olefinic peak area considerably decreases and new peaks appear at 0.8 – 1.2 ppm attributed to  $-\text{CH}_3$  and saturated  $-\text{CH}_2-$  units. This confirms that the carbon-carbon double bonds in SNR are hydrogenated. The extent of hydrogenation was calculated from the change in the integral of peaks representing protons for HSNR, as presented in Appendix C.

Confirmation of the molecular structure of HSNR obtained from  $^{13}\text{C}$ -NMR spectra is shown in Figure 4.3.  $^{13}\text{C}$ -NMR assignments of SNR and HSNR are presented in Table C-2 (Appendix C). The peak area at 135.1 and 124.9 ppm decreases with an increase in the reduction of olefinic carbon-carbon double bonds. On the other hand, four new peaks appear at 37.2, 32.6, 23.5 and 19.6 ppm which are attributed to  $\text{C}_\alpha$ ,  $-\text{CH}$ ,  $\text{C}_\beta$  and  $-\text{CH}_3$ , respectively. This result suggested that HSNR has a formal structure which is similar to EPDM as shown in Figure C-1, C-2 and Table C-3 (Appendix C). Inoue and Nishio [30] also investigated  $^{13}\text{C}$ -NMR spectra of HNR and ethylene-propylene copolymer (EPDM). Four new peaks for carbon in the side chain methyl groups and carbon in the normal chain methylene groups in the 100% HNR can be identified and it is very simple to compare with EPDM, which has ethylene-ethylene bonds and propylene-propylene bonds.

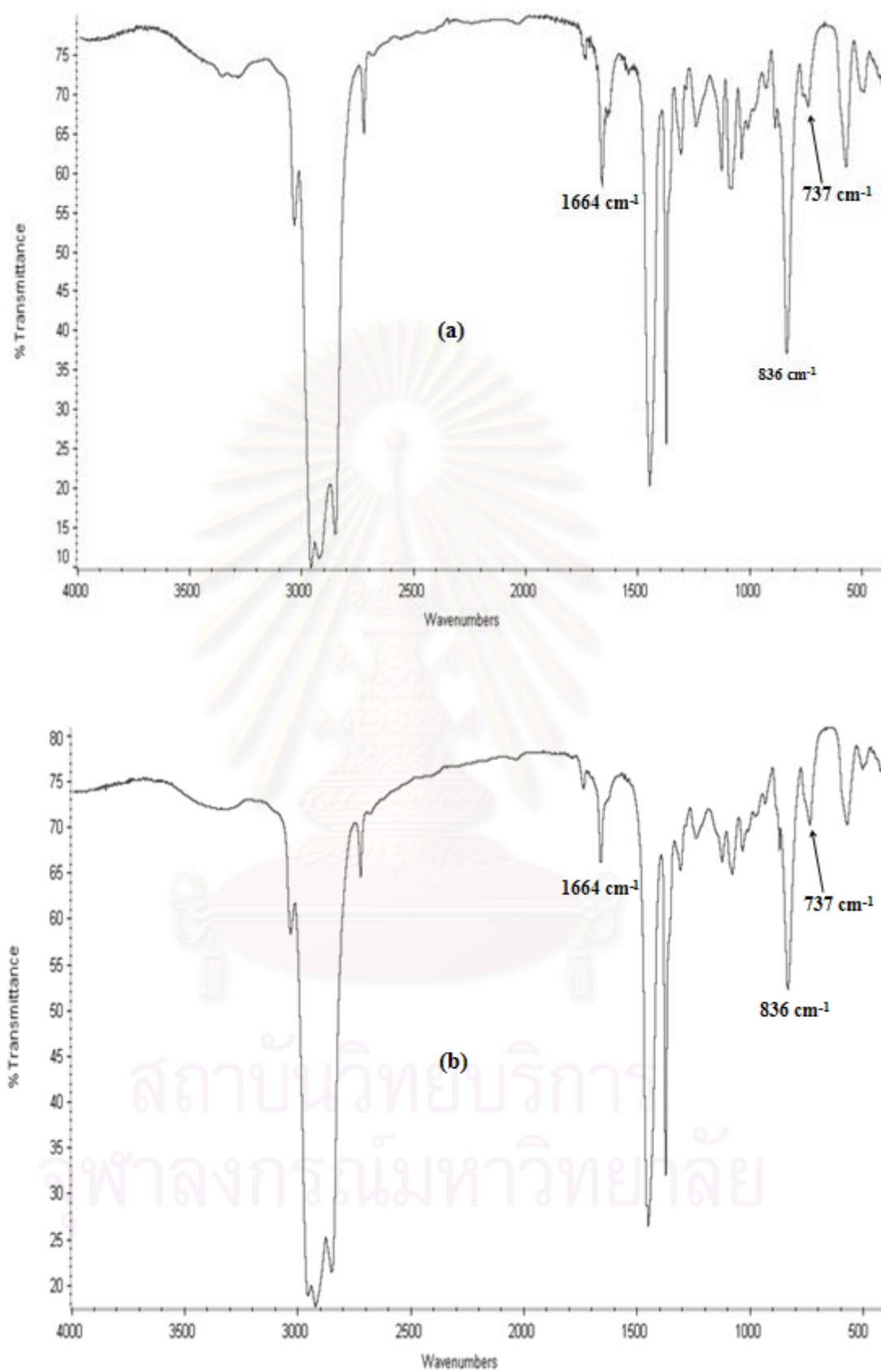


**Figure 4.1** FTIR spectra of (a) SNR and (b) HSNR.

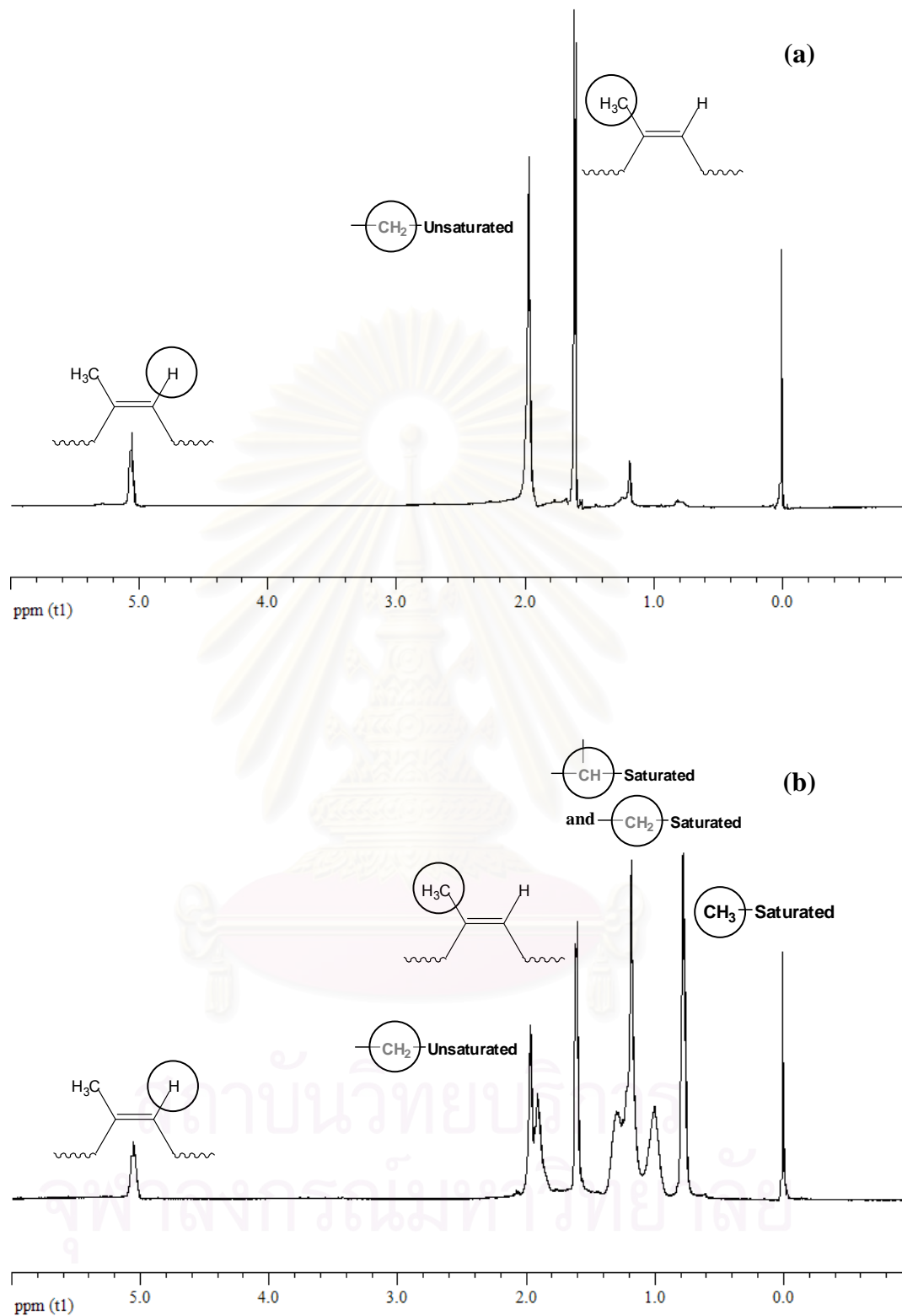


**Figure 4.2**  $^1\text{H}$ -NMR spectra of (a) SNR and (b) HSNR.

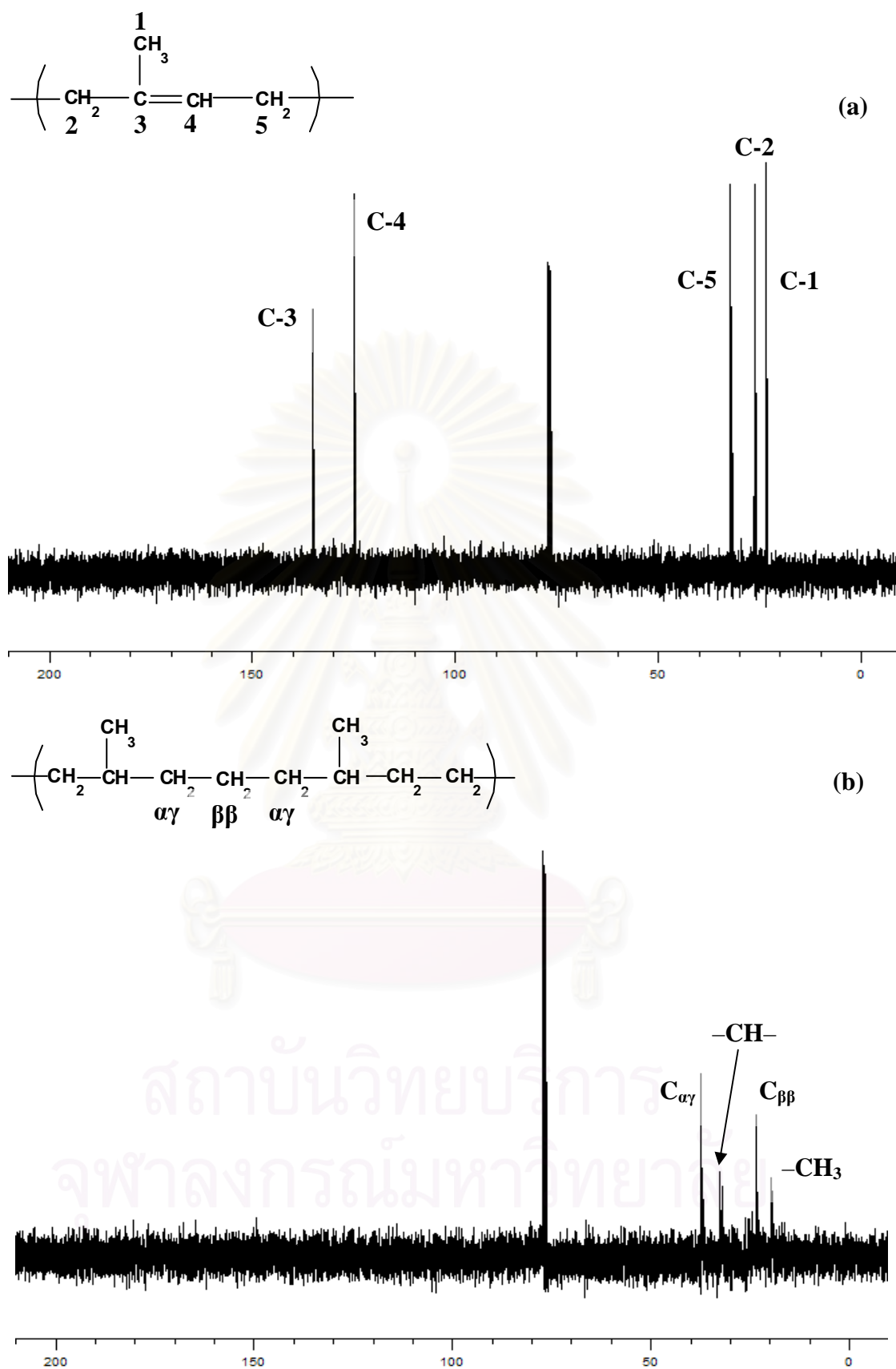


**Figure 4.3**  $^{13}\text{C}$ -NMR spectra of (a) SNR and (b) HSNR.

## 4.2 Effect of Process Parameters on SNRL Diimide Hydrogenation

For hydrogenation of SNR in latex form with diimide in presence of a metal, the diimide species in this system was produced with a redox mechanism between hydrogen peroxide and hydrazine. The effect of various process parameters on SNRL hydrogenation was studied by varying the catalyst concentration, hydrazine concentration, hydrogen peroxide concentration, rubber concentration, reaction time and temperature. The kinetic of SNRL hydrogenation reaction in the presence of catalytic and non-catalytic hydrogenation was also investigated. All details are described below.

### 4.2.1 Effect of Copper Sulfate Concentration

The influence of the copper sulfate concentration on diimide hydrogenation was studied over the range from 0 to 247  $\mu\text{M}$ . The hydrogenation reaction was carried out at  $60^\circ\text{C}$ ,  $[\text{N}_2\text{H}_4] = 2.21 \text{ M}$ ,  $[\text{H}_2\text{O}_2] = 3.54 \text{ M}$ ,  $[\text{C}=\text{C}] = 0.55 \text{ M}$  for 6 h (total volume = 162 mL). The effect of copper sulfate concentration on SNRL hydrogenation is shown in Figure 4.4. It was found that the copper sulfate catalyst played important role on the extent of hydrogenation. In the reduction process, copper ion was able to accelerate the formation of diimide from the  $\text{N}_2\text{H}_4/\text{H}_2\text{O}_2$  redox system. The copper ion in this system can be present in three locations depending on rubber concentration: (a) in water medium; (b) at the polymer surface and (c) inside the latex particle [16]. At high copper sulfate concentration, copper ion may be present in all three locations. On the other hand, copper ion at low copper sulfate concentration may be present only at the polymer surface or in the water media. Localizing copper ion in the water phase will lead only to decomposition reactions of diimide as shown in eq. 4.1 and 4.2 [19]. The disproportionation/decomposition reactions can be represented as:



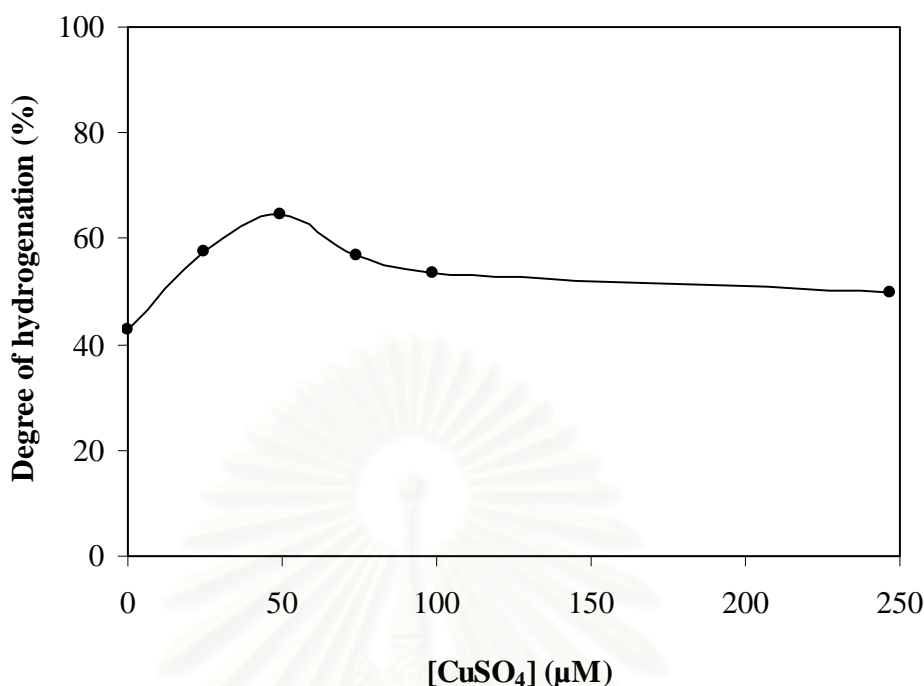
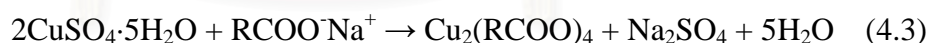


**Figure 4.4** Effect of copper sulfate concentration on SNRL hydrogenation. [N<sub>2</sub>H<sub>4</sub>] = 2.21 M; [H<sub>2</sub>O<sub>2</sub>] = 3.54 M; [C=C] = 0.55 M; T = 60°C; time = 6 h.

Copper ion when added to the system can be distributed over the surface of latex particles by means of a strong complex with the carboxylate soap anions (RCOO<sup>-</sup>Na<sup>+</sup>) of the surfactant [31]. The reaction 4.3 can be presented as follows:



From eq. 4.3, it is seen that the active site is actually bimetallic copper and resides within the surface layer of polymer particle as the bridge species [15]. As the copper ion resides at the surface of polymer latex, where it comes across a large excess of hydrazine in aqueous phase, it is likely that the hydrazine bond between the copper centers through lone electron pairs on nitrogen. Subsequent oxidation of bound hydrazine with hydrogen peroxide then directly produces diimide and water, while the active copper site is regenerated. Diimide is an actual hydrogenating species which reduces the double bonds. The overall diimide hydrogenation reaction of polymer is presented in Figure 4.5.

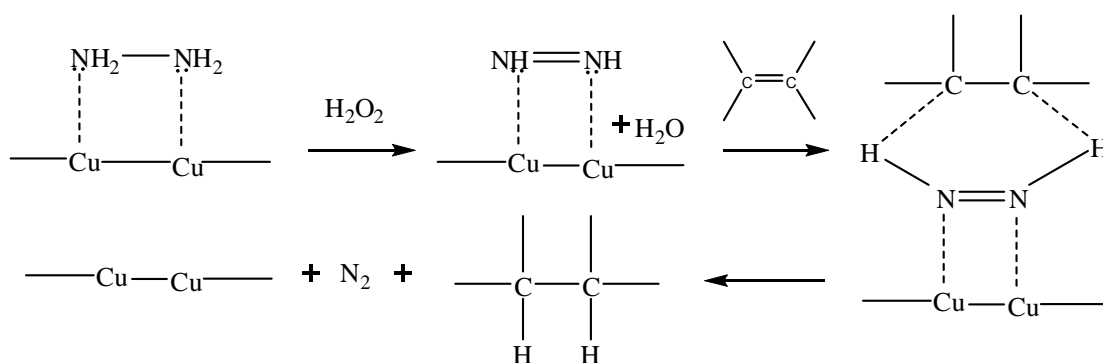


**Figure 4.5** The proposed mechanism of diimide hydrogenation [32].

Thus, the concentration of copper ion at the surface of particle is a key factor which needed to be controlled. Therefore, to reach a high degree of hydrogenation, the copper ion should reside only at the surface of the latex particle. From Figure 4.4, the degree of hydrogenation increased with increasing copper sulfate concentration up until 49.4  $\mu\text{M}$ , thereafter the degree of hydrogenation decreased. The rate of diimide formation would be faster at higher concentration of the catalyst, which in turn may result in an increase in diimide disproportionation as compared to its consumption in the hydrogenation process. At higher copper ion concentration, some free copper ions may also be presented in water medium. This also caused the  $\text{N}_2\text{H}_4/\text{H}_2\text{O}_2$  reaction (decomposition) to mostly occur in the aqueous phase resulting in reduction of the diimide molecules and the decreases in the hydrogenation level.

#### 4.2.2 Effect of Hydrazine Concentration

The effect of hydrazine concentration on diimide hydrogenation was studied over the range of 0.60 to 3.57 M as shown in Figure 4.6. The hydrogenation reaction was carried out at 60°C for 6 h,  $[\text{CuSO}_4] = 49.4 \mu\text{M}$ ;  $[\text{H}_2\text{O}_2] = 3.54 \text{ M}$ ;  $[\text{C}=\text{C}] = 0.55 \text{ M}$ . The results showed that the hydrogenation degree increased with increasing hydrazine concentration. The amount of diimide as the active species for hydrogenation was increased when the hydrazine was in excess. Three possible reactions between hydrazine and hydrogen peroxide are shown in eq. 4.3 - 4.5 may confirm this explanation.



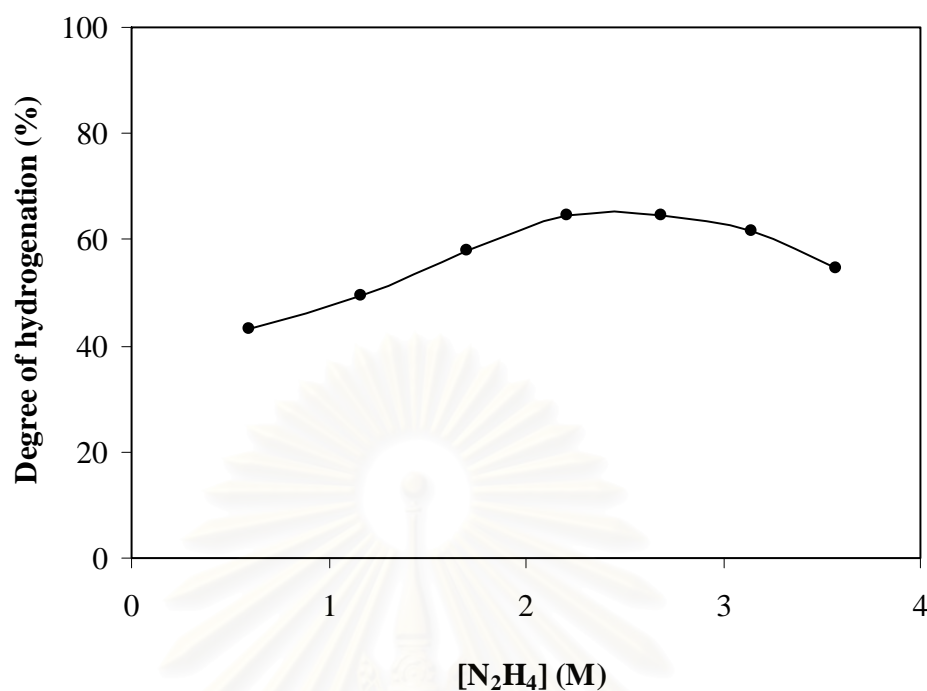
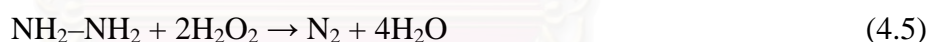
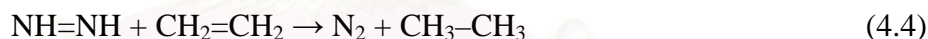
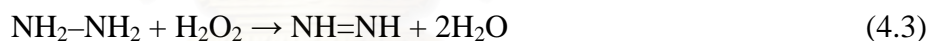


**Figure 4.6** Effect of hydrazine concentration on SNRL hydrogenation. [CuSO<sub>4</sub>] = 49.4 μM; [H<sub>2</sub>O<sub>2</sub>] = 3.54 M; [C=C] = 0.55 M; T = 60°C; time = 6 h.



The reaction between hydrazine and hydrogen peroxide (eq. 4.3) could produce the diimide molecules. In the presence of carbon-carbon double bonds of unsaturated unit in SNRL with copper ion as a catalyst, the diimide species reacted with carbon-carbon double bonds to increase the degree of hydrogenation (eq. 4.4). When the amount of carbon-carbon double bonds of unsaturated unit was decreased and the amount of hydrogen peroxide was increased or in excess then N<sub>2</sub> was produced due to the predomination of eq. 4.5. The higher amount of N<sub>2</sub>H<sub>4</sub>, the more diimide was produced and enhanced the N<sub>2</sub>H<sub>2</sub>/C=C reduction, caused an increase in the hydrogenation degree. On the other hand, the hydrogenation degree decreased when the hydrazine concentration was higher than 2.68 M. This phenomenon can be explained that the diimide species can self-react at high concentration of diimide to

cause a decrease in hydrogenation efficiency (HE). Another possible reason to explain the lower hydrogenation efficiency is that the excess content of diimide in this system may also disperse into the aqueous phase [19]. Similar observation was reported by Mahittikul *et al.* [25].

#### 4.2.3 Effect of Hydrogen Peroxide Concentration

The effect of hydrogen peroxide concentration on diimide hydrogenation was studied over the range of 1.23 to 5.08 M. The hydrogenation reaction was carried out at 60°C for 6 h,  $[\text{CuSO}_4] = 49.4 \mu\text{M}$ ;  $[\text{N}_2\text{H}_4] = 2.21 \text{ M}$ ;  $[\text{C}=\text{C}] = 0.55 \text{ M}$ . The effect of hydrogen peroxide concentration was shown in Figure 4.7. The results showed that the hydrogenation conversion increased with an increase in hydrogen peroxide concentration up until 3.53 M and tend to decrease. This phenomenon may be explained from the two competitive reactions between  $\text{N}_2\text{H}_4$  and  $\text{H}_2\text{O}_2$  (eq. 4.4 and 4.5). Sakar *et al.* [32] claimed that at high hydrogen peroxide concentration, the degree of hydrogenation decreased due to a possible crosslink reaction, which caused a reduction in the number of free carbon-carbon double bonds in latex. At low hydrogen peroxide concentration, the diimide had more chance to diffuse into the rubber phase and the higher hydrogenation efficiency (HE) was achieved [33]. Based on the reaction stoichiometry to produce diimide molecule (eq. 4.3), the suitable ratio for generation of the diimide species was 1:1 of  $[\text{N}_2\text{H}_4]:[\text{H}_2\text{O}_2]$ . But in this experiment, the optimum ratio of  $[\text{N}_2\text{H}_4]:[\text{H}_2\text{O}_2]$  was 1:1.6. It was possible that the hydrogen peroxide was easily decomposed, so it was necessary to have an excess of hydrogen peroxide for effective production of diimide under the present reaction conditions used.

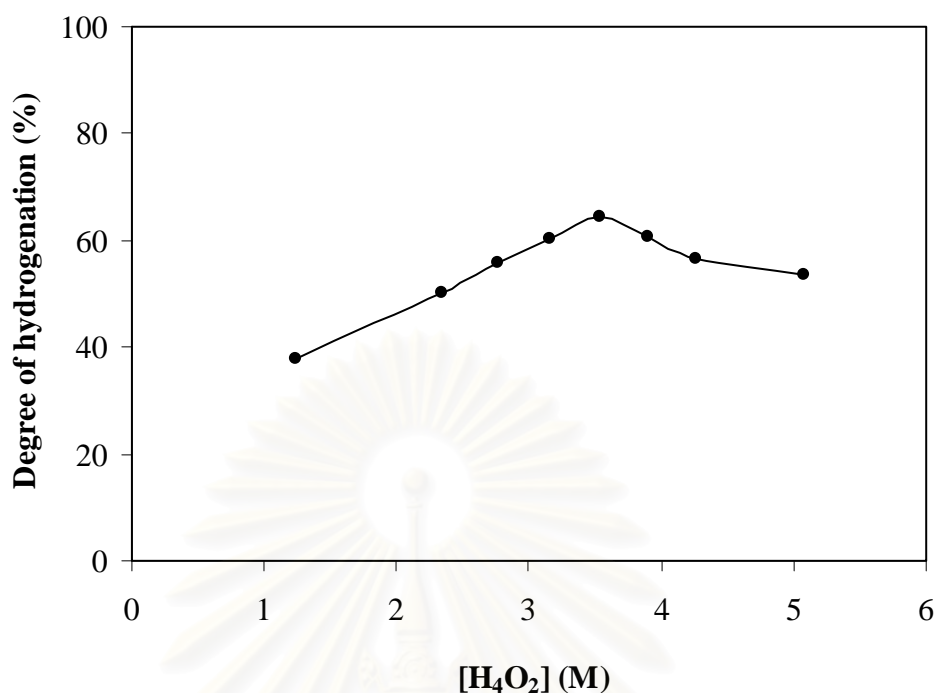


**Figure 4.7** Effect of hydrogen peroxide concentration on SNRL hydrogenation. [CuSO<sub>4</sub>] = 49.4 μM; [N<sub>2</sub>H<sub>4</sub>] = 2.21 M; [C=C] = 0.55 M; T = 60°C; time = 6 h.

#### 4.2.4 Effect of Rubber Concentration

The effect of skim natural rubber concentration on diimide hydrogenation as presented in terms of carbon-carbon double bonds concentration was studied over the range of 0.49 to 0.63 M. The hydrogenation reaction was carried out at 60°C for 6 h, [CuSO<sub>4</sub>] = 8 μmol; [N<sub>2</sub>H<sub>4</sub>] = 0.35 mol; [H<sub>2</sub>O<sub>2</sub>] = 0.57 mol (total volume = 122-282 mL). The influence of skim natural rubber concentration on diimide hydrogenation is shown in Figure 4.8. The extent of hydrogenation increased with increasing rubber concentration up to ~89 mmol and then decreased. At high rubber concentration, the diimide species may self-decompose during the hydrogenation process resulting in a low degree of hydrogenation. On the other hand, at low rubber concentration, it is possible that diimide hydrogenation reaction occurred in a rubber phase rather than in the aqueous phase. The diimide species was in excess when compared to the rubber species in the system. Therefore, the degree of hydrogenation increased at a low volume of rubber. Moreover, the latex viscosity at high rubber concentration was

higher than that at low rubber concentration. At higher rubber concentration, it was difficult for the diimide to diffuse and react with C=C in the rubber structure. Mahittikul *et al.* [25] studied the  $2^3$  factorial experimental designs, the results indicated that C=C showed a negative effect on the degree of hydrogenation. This implied that the degree of hydrogenation decreased with increase in C=C, whereas the interaction of  $N_2H_4$ ,  $H_2O_2$  and C=C, did not have a significant factor affecting hydrogenation degree.

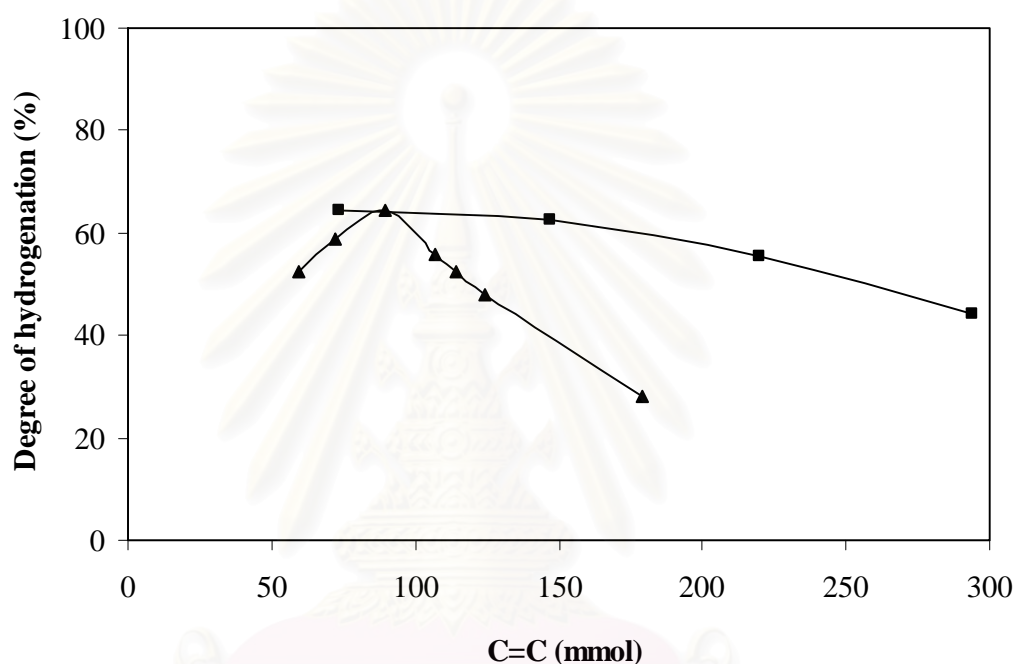


**Figure 4.8** Effect of rubber concentration on SNRL hydrogenation.  $[CuSO_4] = 8 \mu mol$ ;  $[N_2H_4] = 0.35 mol$ ;  $[H_2O_2] = 0.57 mol$ ;  $T = 60^\circ C$ ; time = 6 h (creaming SNRL (■) and SNRL (▲)). (For creaming: rubber 73.5 mmol = 5 %DRC)

Concentration by creaming agent e.g. ammonium alginate [34], *N*-(2-hydroxy)propyl-3-trimethylammonium chitosan chloride (HTACH) [35], hydroxyl propyl-methyl cellulose (HPMC) was applied to recover the residual rubber in the form of concentrated latex and reduce water pollution. In this work, the creaming using HPMC was applied to recover of skim natural rubber (SNR). HPMC was dissolved in deionized water (50 mL) to prepare HPMC solution. The clear solution or transparent light yellow hydrogel was obtained depending on concentration of HPMC. SNR latex (200 g) was mixed with various concentrations of HPMC solution and the

mixture was constantly stirred for 1 h to ensure thorough mixing of the system. The mixture was then allowed to stand at room temperature for 1 day in separating funnel and then concentrated skim natural rubber latex was achieved. The calculation of rubber content is presented in Appendix B.

The effects of concentrated skim natural rubber on diimide hydrogenation at 60°C for 6 h were studied over the range of 5 to 20% dry rubber content (DRC) in the presence of  $[\text{N}_2\text{H}_4] = 0.35 \text{ mol}$ ;  $[\text{H}_2\text{O}_2] = 0.57 \text{ mol}$  and  $[\text{CuSO}_4] = 8 \text{ }\mu\text{mol}$ . Figure 4.10 shows the effect of concentrated skim natural rubber latex. The degree of hydrogenation was significantly decreased with increasing %DRC. It is likely that the active diimide species was not adequate at carbon-carbon double bonds in polymer latex. The concentrated SNR latex at high dry rubber content was more viscous than at low rubber content, it was difficult for the diimide to diffuse and react with carbon-carbon double bonds in rubber structure at high rubber content system.

#### 4.2.5 Effect of Hydrogenation Temperature

The effect of hydrogenation temperature on diimide hydrogenation was studied over the range of 40 to 90°C. The hydrogenation reaction was carried out for 6 h at  $[\text{CuSO}_4] = 49.4 \text{ }\mu\text{M}$ ;  $[\text{N}_2\text{H}_4] = 2.21 \text{ M}$ ;  $[\text{H}_2\text{O}_2] = 3.54 \text{ M}$ ;  $[\text{C}=\text{C}] = 0.55 \text{ M}$ . The results of temperature dependence on diimide hydrogenation are shown in Figure 4.9. The hydrogenation level increased with increasing temperature. These results can be explained that the  $[\text{N}_2\text{H}_2]$  and  $[\text{H}_2\text{O}_2]$  were not effective at low reaction temperature (40-55°C) due to collisions of particles. At the lower temperature, the activity of the reactant molecules is lower. As the reaction temperature increased to 60-80°C, both the probability of collision and activity of the reactant molecules increased. As a result, the degree of hydrogenation increased. On the other hand, hydrogen peroxide tended to decompose more readily and produce free radicals at higher reaction temperature [31, 20]. The free radicals also induce the crosslinking between carbon-carbon double bonds of different rubber segments, thus increased the gel content of the product [19]. This behavior was observed at 90°C and the degree of hydrogenation was dramatically decreased. The optimum reaction temperature for this experiment was 60-80°C, which 64.5-72.2% hydrogenation was achieved in 6 h.

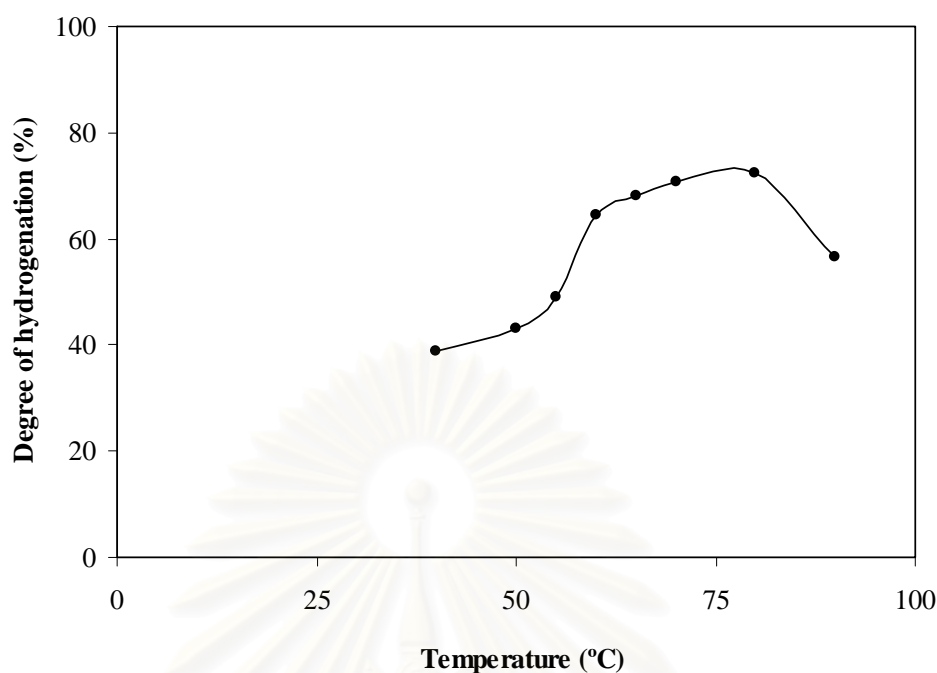


**Figure 4.9** Effect of reaction temperature on SNRL hydrogenation.  $[\text{CuSO}_4] = 49.4 \mu\text{M}$ ;  $[\text{N}_2\text{H}_4] = 2.21 \text{ M}$ ;  $[\text{H}_2\text{O}_2] = 3.54 \text{ M}$ ;  $[\text{C}=\text{C}] = 0.55 \text{ M}$ ; time = 6 h.

### 4.3. Kinetic Study of SNRL Diimide Hydrogenation

Two sets of experiments were performed to study the kinetics of catalytic and non-catalytic SNRL hydrogenation over an interval time from 0 to 12 h,  $[\text{N}_2\text{H}_4] = 2.21 \text{ M}$ ;  $[\text{H}_2\text{O}_2] = 3.54 \text{ M}$ ;  $[\text{C}=\text{C}] = 0.55 \text{ M}$ . Figure 4.11a and 4.12a showed the degree of hydrogenation increased with increasing time reached maximum conversion at 6 h. During an interval of time from 0 to 6 h, the degree of hydrogenation was increased and then leveled off. The reason for the leveling off of the hydrogenation degree after the first 6 h was possible that diimide was formed as an active species at the surface and then diffused into the outer layer of the rubber particles. After 7 h, the conversion was quite stable due to the long reaction time that caused the mass transfer limitation of diimide into C=C inside the rubber particle. In addition, the decomposition of diimide species during the long reaction time may be occurred.

The kinetic result indicated that the diimide hydrogenation rate of SNRL exhibited a first order behavior with respect to carbon-carbon double bonds

concentration in the first 6 h according to eq. 4.6. Equation 4.7 is further expressed in terms of the conversion of unsaturated double bonds (the extent of hydrogenation, x).

$$-\frac{d[C=C]}{dt} = k'[C=C] \quad (4.6)$$

$$-\ln(1-x) = -k' t \quad (4.7)$$

where  $k'$  is the pseudo first order rate constant, calculated from the slope of the linear plot of  $\ln(1-x)$  versus time. Figure 4.10b and 4.11b show the linear plot of  $\ln(1-x)$  versus time for the SNRL hydrogenation. The rate constant ( $k'$ ) of diimide hydrogenation of SNRL in the presence and absence of catalyst are presented in Table 4.1. Mahittikul *et al.* [25] also reported the first order kinetic for hydrogenation of NRL in the presence of  $\text{CuSO}_4$  as catalyst with rate constant of  $\sim 5.4 \times 10^{-5} \text{ s}^{-1}$  at  $55^\circ\text{C}$ .

**Table 4.1** Rate constant of diimide hydrogenation of SNRL

Hydrogenation	$k' \times 10^5 \text{ (s}^{-1}\text{)}$		
	333(K)	343(K)	353(K)
Non-Catalytic <sup>a</sup>	2.61	3.37	4.02
Catalytic <sup>b</sup>	4.91	5.59	5.96

<sup>a</sup>Condition:  $[\text{N}_2\text{H}_4] = 2.21 \text{ M}$ ;  $[\text{H}_2\text{O}_2] = 3.54 \text{ M}$ ;  $[\text{C}=\text{C}] = 0.55 \text{ M}$ .

<sup>b</sup>Condition:  $[\text{CuSO}_4] = 49.4 \text{ }\mu\text{M}$ ;  $[\text{N}_2\text{H}_4] = 2.21 \text{ M}$ ;  $[\text{H}_2\text{O}_2] = 3.54 \text{ M}$ ;  $[\text{C}=\text{C}] = 0.55 \text{ M}$ .

สถาบันวิทยบริการ  
จุฬาลงกรณ์มหาวิทยาลัย

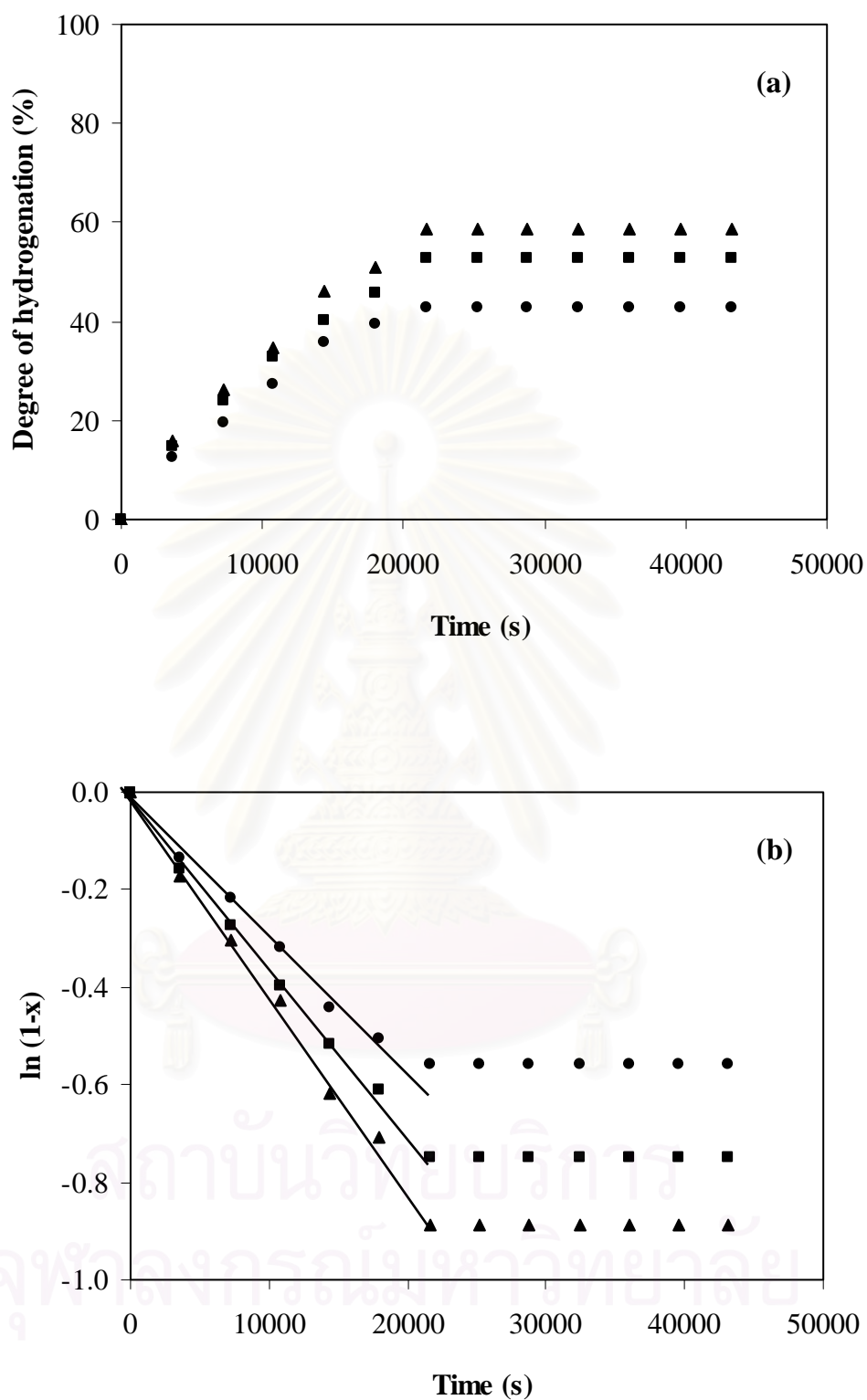


**Figure 4.10** Non-catalytic hydrogenation profiles of SNRL hydrogenation. (a) Conversion profiles and (b) first-order in  $\ln$  plot.  $[\text{N}_2\text{H}_4] = 2.21 \text{ M}$ ;  $[\text{H}_2\text{O}_2] = 3.54 \text{ M}$ ;  $[\text{C}=\text{C}] = 0.55 \text{ M}$ ;  $T = 60^\circ\text{C}$  (●),  $70^\circ\text{C}$  (■) and  $80^\circ\text{C}$  (▲).



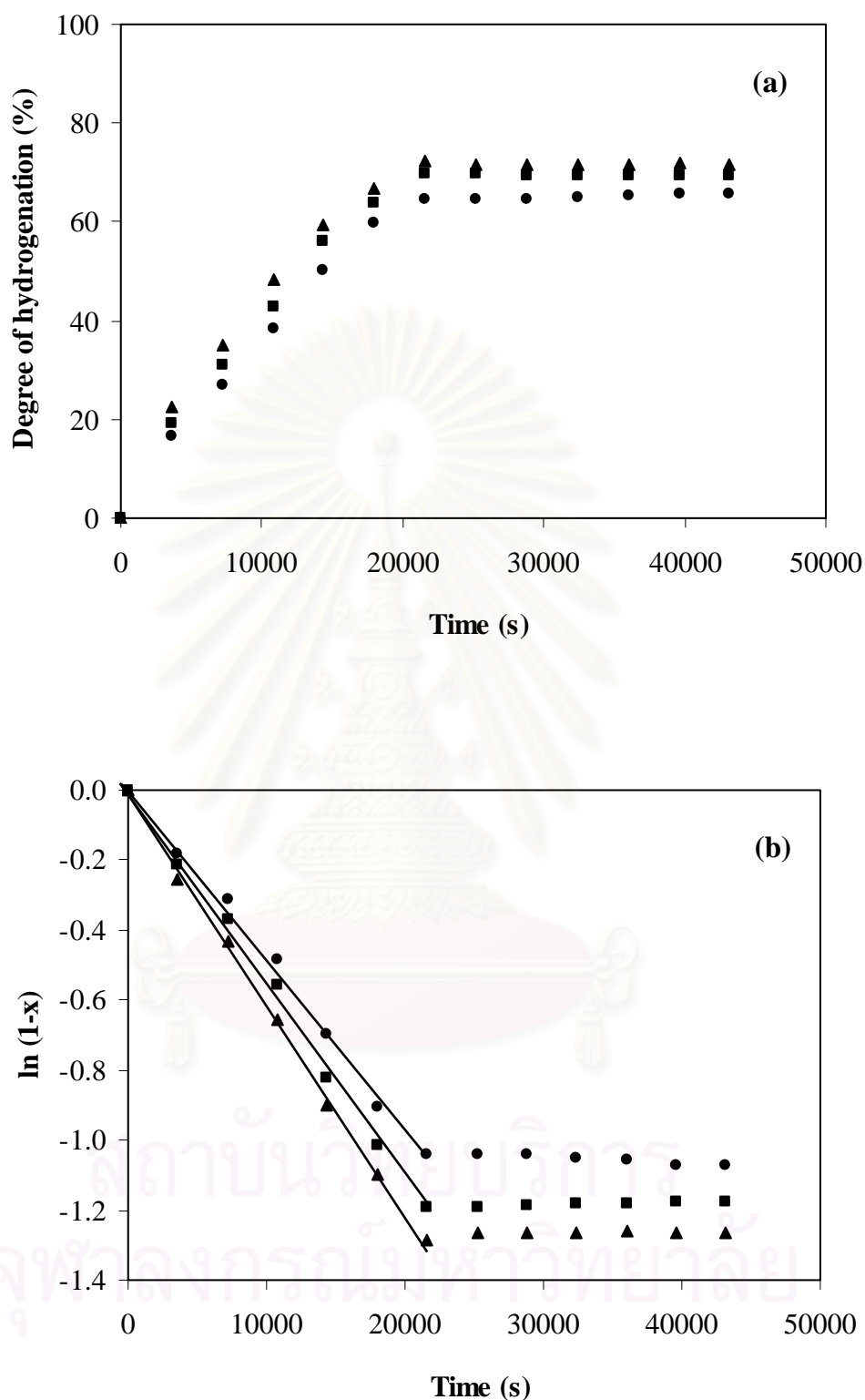


**Figure 4.11** Catalytic hydrogenation profiles of SNRL hydrogenation. (a) Conversion profiles and (b) first-order in  $\ln$  plot.  $[\text{CuSO}_4] = 49.4 \mu\text{M}$ ;  $[\text{N}_2\text{H}_4] = 2.21 \text{ M}$ ;  $[\text{H}_2\text{O}_2] = 3.54 \text{ M}$ ;  $[\text{C}=\text{C}] = 0.55 \text{ M}$ ;  $T = 60^\circ\text{C}$  (●),  $70^\circ\text{C}$  (■) and  $80^\circ\text{C}$  (▲).

The effect of hydrogenation temperature on the conversion profile shows that the degree of hydrogenation increased with increasing reaction temperature. The Arrhenius plot illustrated the temperature influence on the hydrogenation rate (rate constant) as shown in Figure 4.12a. The apparent activation energy ( $E_a$ ) calculated from a least squares regression analysis of plot  $\ln(k')$  versus  $1/T$  of catalytic and non-catalytic hydrogenation was 9.5 and 21.14 kJ/mol, respectively. The activation energy for the diimide hydrogenation of SBR [32] and NRL [25] were earlier reported as 9.5 and 7.1 kJ/mol, respectively. Low activation energy provided the evidence that the diimide hydrogenation were performed with mass-transfer limitation. It can be suggested that catalytic diimide reduction with low activation energy is relatively less sensitive to temperature.

The Eyring equation was used to estimate the apparent activation enthalpy ( $\Delta H$ ) and entropy ( $\Delta S$ ) for the reaction. Figure 4.12b is the Eyring plot from the temperature dependence data. For comparison, the enthalpy and entropy of activation were 18.29 kJ/mol and -116.52 J/mol K for non-catalytic hydrogenation and 6.65 kJ/mol and -86.8 J/mol K for catalytic hydrogenation.

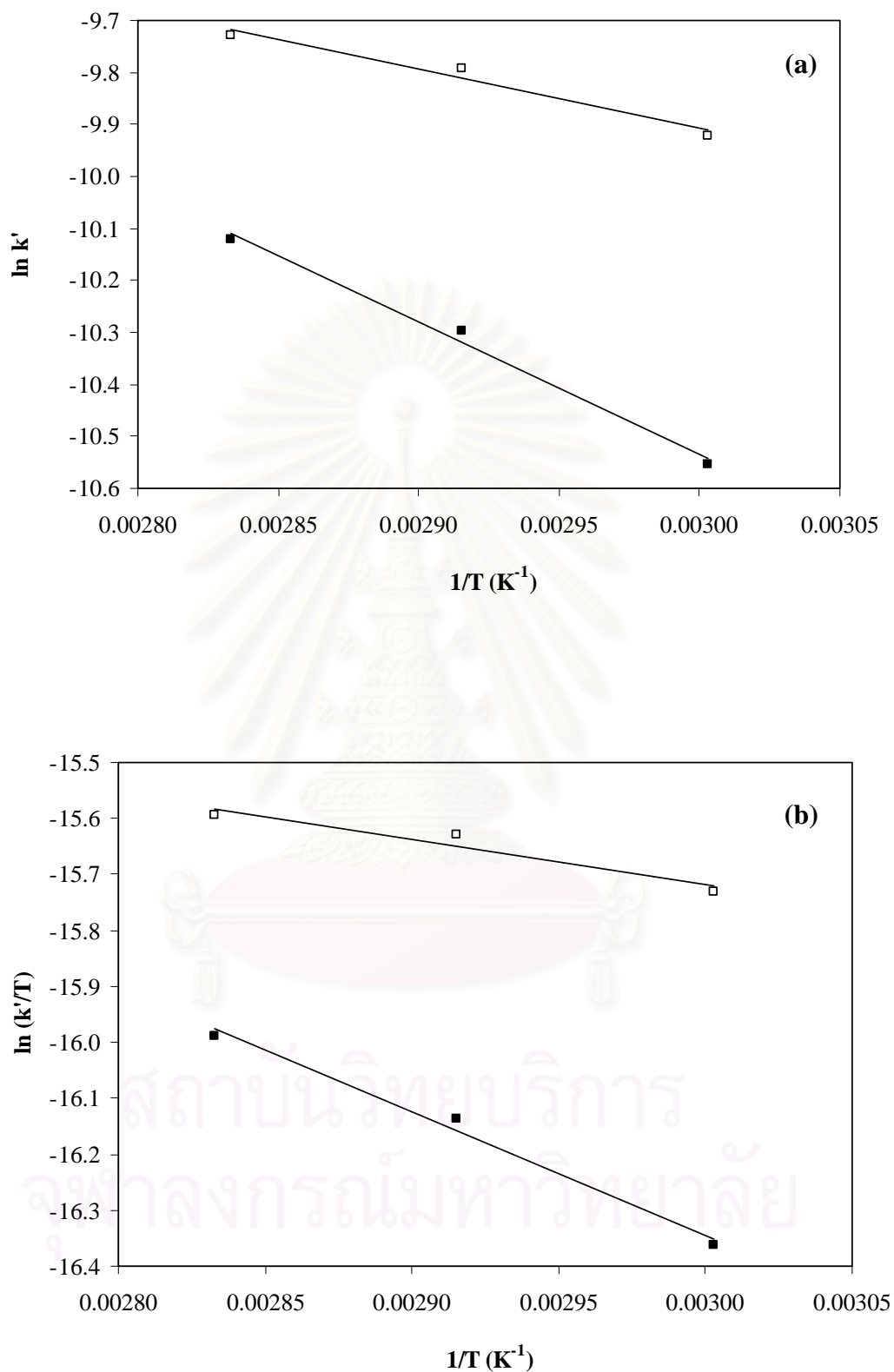


**Figure 4.12** (a) Arrhenius plots and (b) Eyring plots of SNRL hydrogenation.  $[\text{N}_2\text{H}_4] = 2.21 \text{ M}$ ;  $[\text{H}_2\text{O}_2] = 3.54 \text{ M}$ ;  $[\text{C}=\text{C}] = 0.55 \text{ M}$ ;  $T = 60\text{-}80^\circ\text{C}$ ; time = 6 h (catalytic ( $\square$ ) and non-catalytic hydrogenation ( $\blacksquare$ )).

#### 4.4 Improvement of Redox System

To improve the degree of hydrogenation, the addition of sodium dodecyl sulfate, boric acid and hydroquinone was investigated. It was believed that the limitation of diimide hydrogenation of SNRL was caused by the low efficiency of diimide which reacted with the carbon-carbon double bonds.

##### 4.4.1 Effect of Sodium Dodecyl Sulfate Concentration

The effect of sodium dodecyl sulfate (SDS) concentration on diimide hydrogenation has been studied from 0 to 493.8  $\mu\text{M}$  in the presence of  $[\text{CuSO}_4] = 49.4\mu\text{M}$ ;  $[\text{N}_2\text{H}_4] = 2.21 \text{ M}$ ;  $[\text{H}_2\text{O}_2] = 3.54 \text{ M}$ ;  $[\text{C}=\text{C}] = 0.55 \text{ M}$  at  $T = 60^\circ\text{C}$  for 6 h. Parker *et al.* [36] studied the role of surfactant in the diimide hydrogenation process and found that the surfactant had a function in stabilizing the cupric ion on the rubber particle. From Figure 4.13, the degree of hydrogenation decreased with increasing SDS concentration. It is possible that the surfactant formed a micelle trap for the copper sulfate which led to a reduction of the amount of diimide species produced resulting in the decrease in the hydrogenation degree. Moreover, the rubber latex particle covered with phospholipids as outer layer and surfactant also formed a micelle trap for the copper ion.

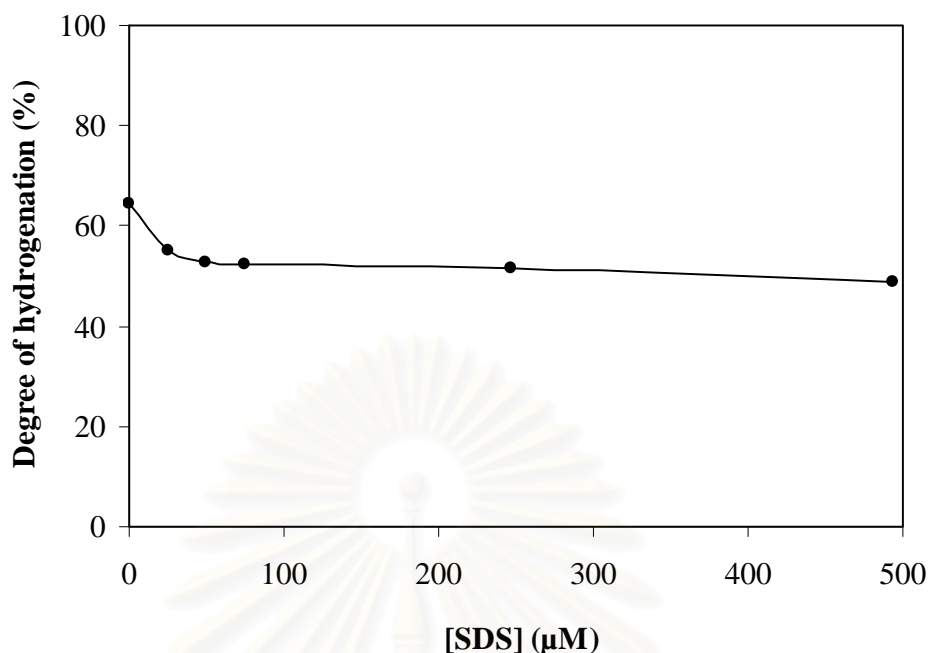


**Figure 4.13** Effect of SDS concentration on SNRL hydrogenation. [CuSO<sub>4</sub>] = 49.4 μM; [N<sub>2</sub>H<sub>4</sub>] = 2.21 M; [H<sub>2</sub>O<sub>2</sub>] = 3.54 M; [C=C] = 0.55 M; T = 60°C; time = 6 h.

#### 4.4.2 Effect of Hydroquinone Concentration

Gel formation is generally observed both for the diimide generated in situ and for the diimide hydrogenation. The mechanism for crosslink bond formation has not been clearly identified. The disproportionation of diimide may cause the crosslinking of rubber backbones according to eq. 4.8 [37].



Inhibitor was added to the diimide NBR latex hydrogenation system in an attempt to capture the free radicals, then reduce gel content and increase degree of hydrogenation [19]. Xie *et al.* [20] used *p*-tert-butyl-procathecol as an inhibitor for gel formation. The results indicated that the presence of this inhibitor reduced the gel content from 94% to 21% for hydrogenation of NBR latex. Hydroquinone is a water-soluble chemical mixed well with the reaction system, radicals generated in the

system will be effectively eliminated and the formation of the potential cross-linking group on the polymer will be avoided. Radical may be generated from the redox reaction between hydrazine and hydrogen peroxide. These radicals were generated in the aqueous phase [23]. Hydroquinone was also applied in this experiment to improve the hydrogenation of SNRL system. The effect of the hydroquinone concentration on diimide hydrogenation was studied over the range from 0 to 3.09 mM in the presence of  $[C=C] = 0.55$  M,  $[N_2H_4] = 2.20$  M,  $[H_2O_2] = 3.53$  M and  $[CuSO_4] = 49.4$   $\mu$ M at  $60^\circ C$  for 6 h and the results are shown in Figure 4.14. It was found that the hydrogenation degree decreased and the gel content decreased with increasing hydroquinone concentration. It can be noted that hydroquinone captured the diimide species in this system, resulting in the decrease in hydrogenation degree. Zhou *et al.* [21] also found that hydroquinone could reduce the gel content from 80% to 3% and provide 80% hydrogenation of NBR in latex form.

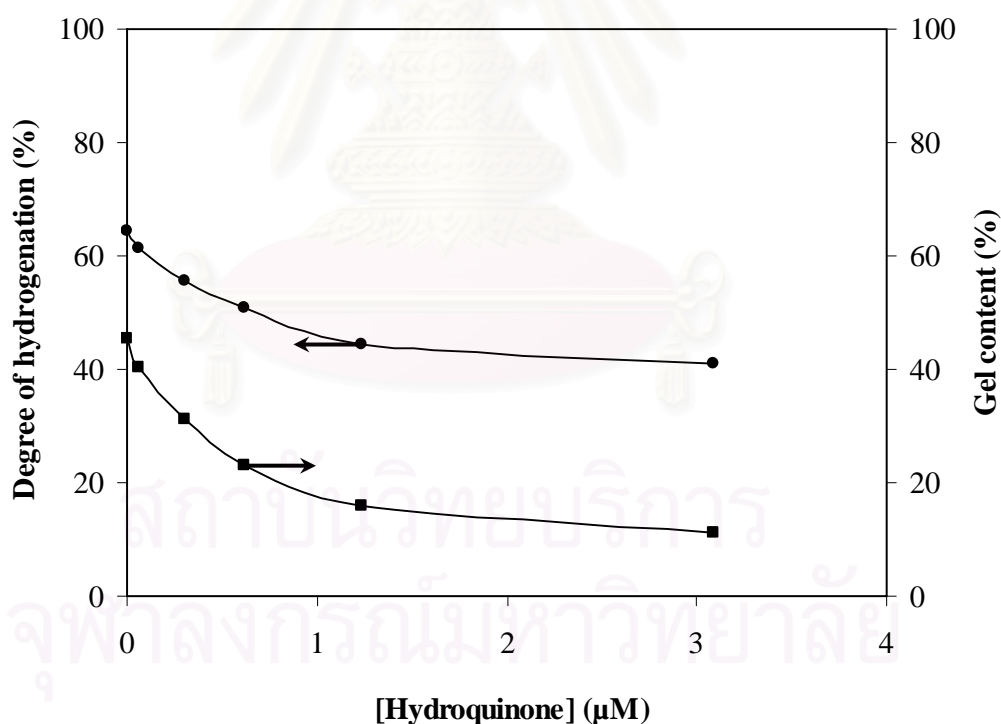


**Figure 4.14** Effect of hydroquinone concentration on SNRL hydrogenation.  $[CuSO_4] = 49.4$   $\mu$ M;  $[N_2H_4] = 2.21$  M;  $[H_2O_2] = 3.54$  M;  $[C=C] = 0.55$  M;  $T = 60^\circ C$ ; time = 6 h (% hydrogenation (●) and % gel content (■)).

#### 4.5 Effect of Catalyst Type and Boric Acid Concentration

The effect of catalyst type on the degree of hydrogenation was also investigated. Various types of catalysts were examined in the presence of  $[C=C] = 0.55$  M,  $[N_2H_4] = 2.21$  M,  $[H_2O_2] = 3.54$  M,  $[Catalyst] = 49.38$   $\mu$ M at  $60^\circ\text{C}$  for 6 h and the results are present in Table 4.2. For the effect of cation, *i.e.*, ferric sulfate, copper sulfate and zinc sulfate, were considered. Copper ion and zinc ion were the most suitable metallic ions for catalyzing the diimide hydrogenation of SNRL. The degree of hydrogenation increased with the following order of cations:  $Fe^{2+} < Cu^{2+}, Zn^{2+}$ . On the other hand, Xie *et al.* [19] reported that  $Fe^{2+}$  was the best catalyst for diimide hydrogenation of carboxylic styrene-butadiene rubber (XSBR) latex, which not only the highest hydrogenation degree but also the lowest gel content was obtained. For comparison, the effect of anion, *i.e.*, copper sulfate, copper chloride and copper acetate were investigated. Acetate group was found to be the most effective anion for the diimide hydrogenation of SNRL. The catalyst activity of the copper complexes was dependent on two properties of catalyst: the basicity of the ligand and the strength of the metal ligand interaction. The catalyst activity of these complexes increased in the same order as the basicity of the ligand;  $Cl^- < SO_4^{2-} < CH_3COO^-$ . The similar results were found for diimide hydrogenation of SBR [32] and NRL [25].

**Table 4.2** Effect of catalyst types on SNRL hydrogenation.

Catalyst*	Hydrogenation (%)
Without catalyst	42.7
FeSO <sub>4</sub>	45.9
ZnSO <sub>4</sub>	60.0
CuSO <sub>4</sub>	64.5
CuCl <sub>2</sub>	47.6
Cu(OAC) <sub>2</sub>	68.4

\*Condition :  $[Catalyst] = 49.38$   $\mu$ M;  $[N_2H_4] = 2.21$  M;  $[H_2O_2] = 3.54$  M;  $[C=C] = 0.55$  M; T =  $60^\circ\text{C}$ ; time = 6 h.

Boric acid is an alternative material to help in promote diimide hydrogenation [23]. Lin *et al.* [22] also reported that the promoting ability of boric acid is unique and is not shared with other weak acids. Boric provides a higher and more stable rate for the reaction, which makes boric acid the most suitable choice in the latex system for promoting diimide formation. It was suggested that boric acid served to lower and mediate the concentration of hydrogen peroxide. The mechanism was proposed in eq. 4.9.



Boric acid was capable to form hydrogen-bonds with hydrogen peroxide. This formation of hydrogen-bonds stabilized hydrogen peroxide and reduced the activity of hydrogen peroxide. As a result, the side reaction of diimide with hydrogen peroxide to produce nitrogen and water (eq. 4.9) was suppressed.

The effect of the boric acid concentration on diimide hydrogenation was studied over the range from 0 to 185 mM in the presence of  $[\text{C}=\text{C}] = 0.55 \text{ M}$ ,  $[\text{N}_2\text{H}_4] = 2.20 \text{ M}$ ,  $[\text{H}_2\text{O}_2] = 3.53 \text{ M}$  at  $60^\circ\text{C}$  for 6 h and the results are shown in Figure 4.15. It was found that the degree of hydrogenation increased with increasing boric acid concentration and reached maximum hydrogenation degree at 62 mM. It is possible that high boric acid concentration suppressed the side reactions [39]. Another possible reason was that when boric acid concentration was increased, the rate of diimide formation was faster and enhanced the extent of the diimide/double bonds reduction [21]. Belt *et al.* [17, 18] reported that a higher degree of hydrogenation and less cross-linking of polymer was achieved for NBR latex when boric acid was used as the catalyst. On the other hand, when the boric acid concentration was above 62 mM, the degree of hydrogenation decreased. It may be possible that the higher boric acid concentration resulted in a side reaction. Moreover, the stability of SNRL might be reduced when a high level of boric acid was added.



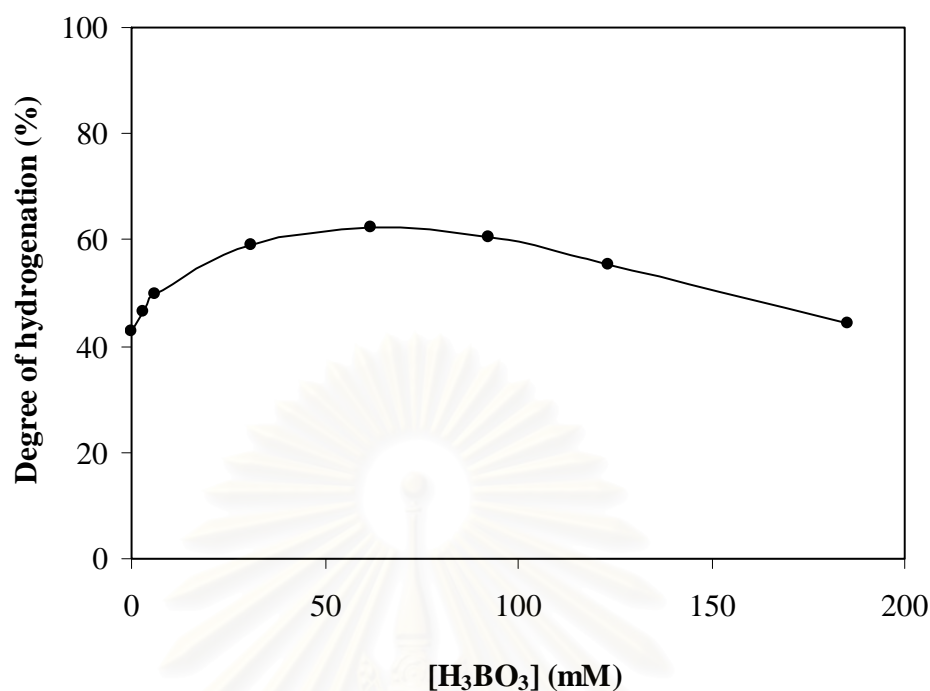


**Figure 4.15** Effect of boric acid concentration on SNRL hydrogenation.  $[\text{N}_2\text{H}_4] = 2.21 \text{ M}$ ;  $[\text{H}_2\text{O}_2] = 3.54 \text{ M}$ ;  $[\text{C}=\text{C}] = 0.55 \text{ M}$ ;  $T = 60^\circ\text{C}$ ; time = 6 h.

#### 4.6 The Distribution of Carbon–Carbon Double Bonds in HSNRL Particles

The distribution of carbon–carbon double bonds of skim natural rubber latex particles during diimide hydrogenation was studied. The condition in the first treatment was  $[\text{CuSO}_4] = 49.4 \mu\text{M}$ ;  $[\text{N}_2\text{H}_4] = 2.21 \text{ M}$ ;  $[\text{H}_2\text{O}_2] = 3.54 \text{ M}$ ;  $[\text{C}=\text{C}] = 0.55 \text{ M}$  at  $60^\circ\text{C}$  for 6 h (Total volume = 162 mL). The product from the previous hydrogenation treatment was used as the starting material for the next hydrogenation treatment at the same reaction condition. Figure 4.16 shows the treatment effect on the degree of hydrogenation after each treatment. It was found that the degree of hydrogenation slightly increased after each hydrogenation. The percentage increase in hydrogenation degree between treatments was 11.2% (for the 1<sup>st</sup> and 2<sup>nd</sup> hydrogenation), 5.73% (2<sup>nd</sup> and 3<sup>rd</sup> hydrogenation) and 2.06% (for 3<sup>rd</sup> and 4<sup>th</sup> hydrogenation). The differences in the hydrogenation level between the hydrogenation treatments reduced with successive treatment.

Two models used to explain the distribution of carbon–carbon double bonds in the polymer latex during diimide hydrogenation are uniform model and layer model

[16]. For the uniform model, the increase in the hydrogenation level between the first and the second treatment, the second and the third, and the third and the fourth hydrogenation treatments are very close to the same value. For the layer model, the increase in hydrogenation level between the first and second hydrogenation treatment, the second and the third, and the third and the fourth hydrogenation treatments are very different and decrease.

Thus, the layer model can be used to explain the distribution of carbon-carbon double bonds of rubber particles in latex during diimide hydrogenation. Moreover, this result suggests that the layer model represents the surface of the particle and resulted in a relatively higher degree of hydrogenation because a lower mobility of highly crosslinked polymer may exist. After the first hydrogenation treatment, the amount of carbon-carbon double bonds in polymer layer was lower than that of the inner portion of the particle. As a result, the disproportionation reaction among diimide molecules became more competitive in this layer and consequently, resulted in a small increase in hydrogenation level after the second and third treatments. Lin *et al.* [24] also suggested that specially designed core-shell latex with an inert core and an NBR shell was observed for the diimide hydrogenation.

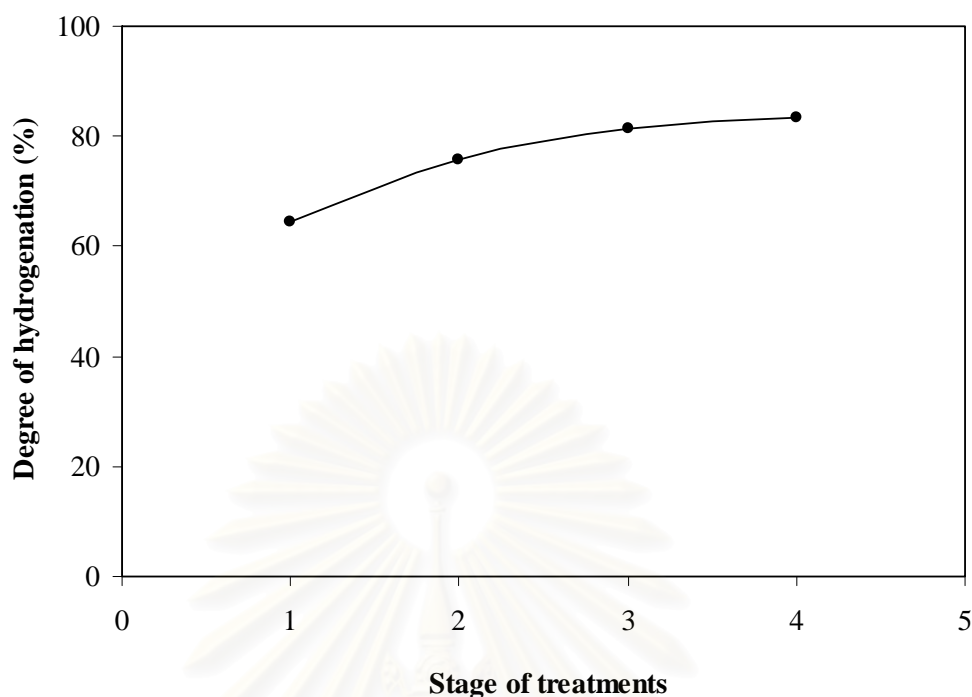


**Figure 4.16** Effect of number of treatment on SNRL hydrogenation: The first hydrogenation treatment  $[\text{CuSO}_4] = 49.38 \mu\text{M}$ ;  $[\text{N}_2\text{H}_4] = 2.21 \text{ M}$ ;  $[\text{H}_2\text{O}_2] = 3.54 \text{ M}$ ;  $[\text{C}=\text{C}] = 0.55 \text{ M}$ ;  $T = 60^\circ\text{C}$ ; time = 6 h; the second, third and fourth hydrogenation treatments  $[\text{CuSO}_4] = 8 \mu\text{mol}$ ;  $[\text{N}_2\text{H}_4] = 0.35 \text{ mol}$ ;  $[\text{H}_2\text{O}_2] = 0.57 \text{ mol}$ ;  $T = 60^\circ\text{C}$ ; time = 6 h.

TEM micrograph was used to explain the morphology of the SNRL particles before and after hydrogenation.  $\text{OsO}_4$  staining agent can only stain at the carbon-carbon double bonds, the lightly colored domain indicates the region of lower carbon-carbon double bonds concentration. For comparison, SNRL and HSNRL at hydrogenation degree of 64.5% (the first treatment) and 83.5% hydrogenation degree (the fourth treatments) are shown in Figure 4.17. SNRL showed relatively sharp particle edges because the concentration of  $\text{OsO}_4$  inside the particle was high. For 64.5% hydrogenated rubber, the contrast between the center and the surface of hydrogenated rubber particle was quite different. For 84.5% hydrogenated rubber latex, much lighter color was observed due to the small amount of carbon-carbon double bonds for  $\text{OsO}_4$  staining. The rubber particle seemed to be hydrogenated from the outer surface layer to the center of rubber particle according to the layer model.

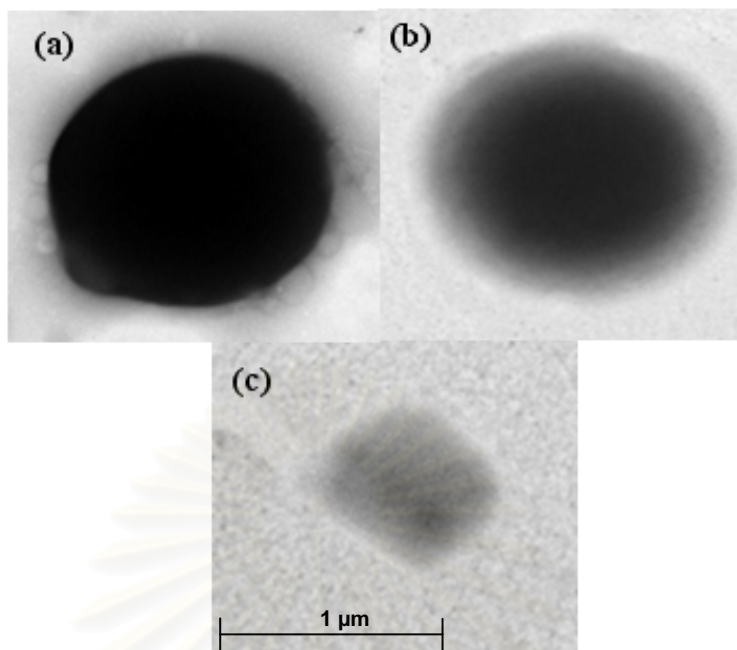


**Figure 4.17** TEM micrograph of (a) SNRL (b) HSNRL 64.5% (1<sup>st</sup> treatment) (c) HSNRL 83.5% (4<sup>th</sup> treatments) (magnification: 3,000x).

To investigate the effect of diimide reduction on particle size distribution of hydrogenated skim natural rubber in latex form, the particle size of non-hydrogenated and hydrogenated products were determined using a particle size analyzer.. Figure 4.18 shows that the particle size distribution of HSNR 0%, 64.5% and 83.5% hydrogenation was not of a narrow size. The particle size of non-hydrogenated and hydrogenated skim natural rubber latex was between 0.1 and 1 micron. The particle size before and after hydrogenation did not significantly changed. The average particle size of HSNRL 0%, 64.5% and 83.5% hydrogenation are 137, 164 and 167 nm, respectively. This implies that the degradation of polymer did not occur during or after diimide hydrogenation.

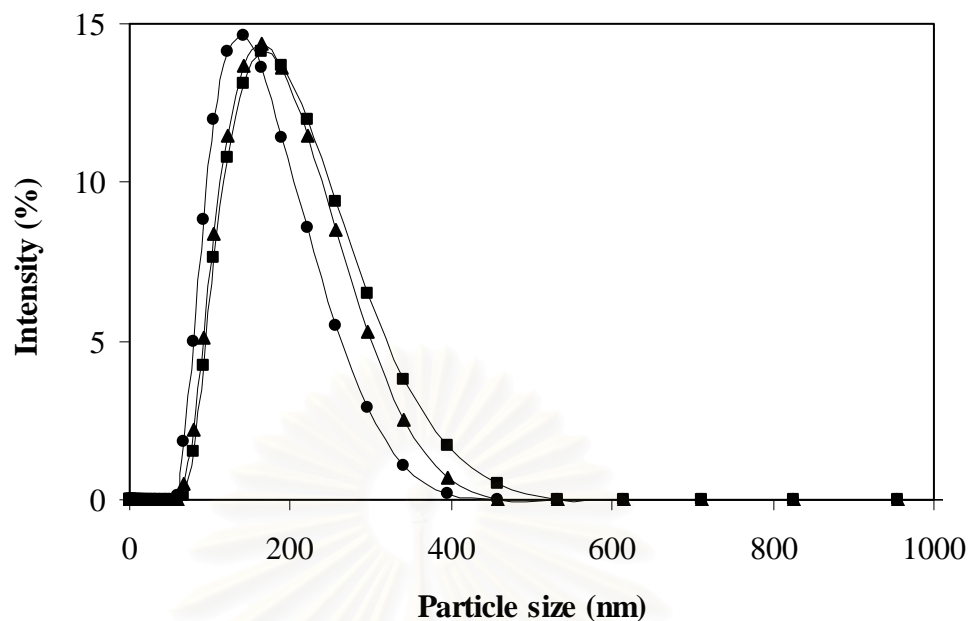


**Figure 4.18** Particle size distribution of HSNRL 0% (●), 64.5% (▲) and 83.5% (■).

#### 4.7 Thermal properties

The physical properties of polymer were determined the performance of polymers in its applications. Thermal analysis, the most important method, could be broadly defined as methods of analysis in which the effect of thermal to provide qualitative or quantitative analytical information. The temperatures of physical transitions are important to determine the level of polymer states are related to the temperature.

There have been some research studies on the thermal properties of hydrogenated rubbers. Hydrogenated nitrile-butadiene rubbers (HNBR) have improved low temperature resistance and improved tensile stress properties [38]. Cassano *et al.* [39] studied the thermal stability of hydrogenated polybutadiene rubber (HBR) and the heat fusion. It was found that both properties increased as the degree of hydrogenation increased from 0 to 89% conversion. Singha *et al.* [40], Parker *et al.* [41] and Kubo *et al.* [42] investigated the thermal properties of hydrogenated natural rubber, styrene-butadiene rubber and nitrile rubber, respectively. The thermal properties of hydrogenated natural rubber (HNR) increased with an increasing in the degree of hydrogenation. Charmondusit [43], Tangthongkul [44], Hinchiranan [45]

and Mahittikul [46] studied the thermal properties of HNR compared with NR. The results showed that high temperature properties of HNR were much better than NR.

#### 4.7.1 Glass Transition Temperature

Differential scanning calorimetry (DSC) is a technique for determining the glass transition temperature ( $T_g$ ) of polymer samples. The glass transition is a phenomenon observed in amorphous polymers [47]. The state of polymer whether it is glassy or rubbery depends on whether its application temperature is above or below its glass transition temperature. It determined from the midpoint of the base-line shift of the thermogram. Generally, polymer may be amorphous, crystalline or a combination of both. The  $T_g$  is a transition related to the motion in the amorphous region of the polymer. Below  $T_g$  an amorphous polymer can be said to have characteristics of a glass, while it becomes more rubbery above  $T_g$  [48].

In this work, the glass transition temperature of SNR and HSNR were determined and compared with ethylene-propylene copolymer (EPDM) as presented in Table 4.3. From Fig. 4.19a and 4.19c, the DSC thermogram of SNR and EPDM samples exhibited one step of base-line shift. The  $T_g$  value of SNR ( $-64^\circ\text{C}$ ) demonstrated the rubber properties at room temperature and the glass properties below  $T_g$ . The standard EPDM has the higher  $T_g$  value of  $-46^\circ\text{C}$ , show a higher degree of crystallization in the polymer structure than SNR. From Fig. 4.19b, HSNR samples showed two step of base-line shift. The first step and second step were at  $-63^\circ\text{C}$  and  $-50^\circ\text{C}$ , respectively. It is possible that after hydrogenation, two different structures of rubber occurred were non-hydrogenated ( $-63^\circ\text{C}$ ) and hydrogenated ( $-50^\circ\text{C}$ ) parts. From TEM micrograph, the hydrogenation of skim natural rubber was found to fit the layer model, non-hydrogenated core and hydrogenated shell layer. The glass transition temperature ( $T_g$ ) of HSNR did not change when hydrogenation degree was increased. A similar observation was also made by Mahittikul *et al.* [25] for diimide hydrogenation of NRL.

**Table 4.3** Glass transition temperature and decomposition temperature of rubber samples.

Rubber	Hydrogenation (%)	T <sub>g</sub> (°C)	T <sub>id</sub> (°C)	T <sub>max</sub> (°C)
SNR	-	-64.3	348.1	377.5
HSNR	32.9	-63.4, -50.7	364.8	400.9
	44.8	-63.2, -50.2	368.9	404.4
	52.7	-63.1, -49.5	376.6	416.2
	64.5	-63.0, -49.5	394.8	429.1
	72.3	-62.3, -49.5	401.7	432.0
	83.5	-61.7, -49.4	406.6	436.5
EPDM <sup>a</sup>	-	-46.4	448.0	462.9

<sup>a</sup>EPDM had an ethylene / propylene ratio of 50 /50 and a diene concentration of 9.5%.

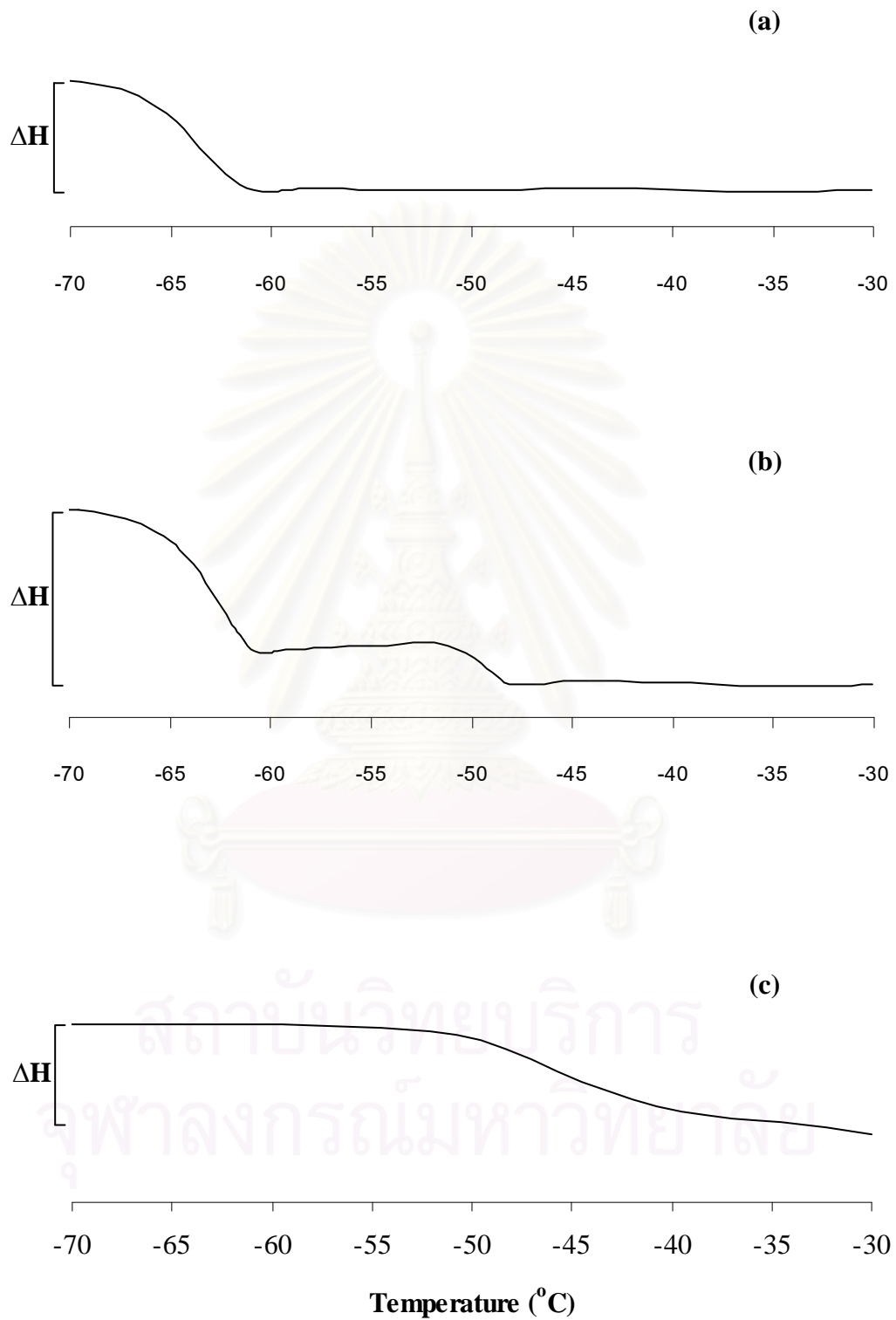


**Figure 4.19** DSC thermograms of (a) SNR, (b) HSNR 64.5% and (c) EPDM.



#### 4.7.2 Decomposition Temperature

Thermogravimetric analysis (TGA) is based on the simple principle of monitoring the change in weight of a sample as the temperature is varied. In this study, the experiments were carried out under nitrogen atmosphere to observe the weight change due to the degradation and to prevent other reaction caused by oxidation. The obtained characteristic curves were used for quantitative analysis. The initial decomposition temperature ( $T_{id}$ ) was determined from the intersection of two tangents at the onset of the decomposition temperature. The maximum decomposition temperature ( $T_{max}$ ) was obtained from the peak maximum of the derivative of the TGA curve.

The degradation behavior of SNR after hydrogenation was studied. The TGA thermogram of the HSNR sample obtained from diimide hydrogenation in the presence of  $CuSO_4$  as shown in Figure 4.20 indicated that polymer degradation is an overall one-step reaction because the TGA curve of the sample is one-step and provides a smooth weight loss curve. The  $T_{id}$  and  $T_{max}$  results are also summarized in Table 4.3, both of  $T_{id}$  and  $T_{max}$  of HSNR samples increase with increase in the reduction of carbon-carbon double bonds in the SNR. Therefore, the hydrogenation could improve the thermal stability of SNR by converting the weak  $\pi$  bond with in SNR to stronger C-H  $\sigma$  bond, which leads to higher thermal stability [43]. Hinchiranan *et al.* [49] also suggested that the degradation temperature increased with increasing reduction of carbon-carbon double bonds in synthetic *cis*-1,4-polyisoprene (CPIP) and NR. Compared with standard EPDM, both  $T_{id}$  and  $T_{max}$  of the completely hydrogenated natural rubber were close to those of EPDM [49, 50]. It can be concluded that the structure of HNR provides a facile entry and alternative method to alternating ethylene-propylene copolymers. Although HSNR has the thermal stability higher than SNR, the decomposition temperature of HSNR is less than that of EPDM. It is possible that the position of carbon-carbon double bonds in HSNR is in the backbone, whereas the unsaturation unit in EPDM is a pendant group and its main structure is still saturated. Thus, EPDM had more resistance to thermal degradation than HSNR.

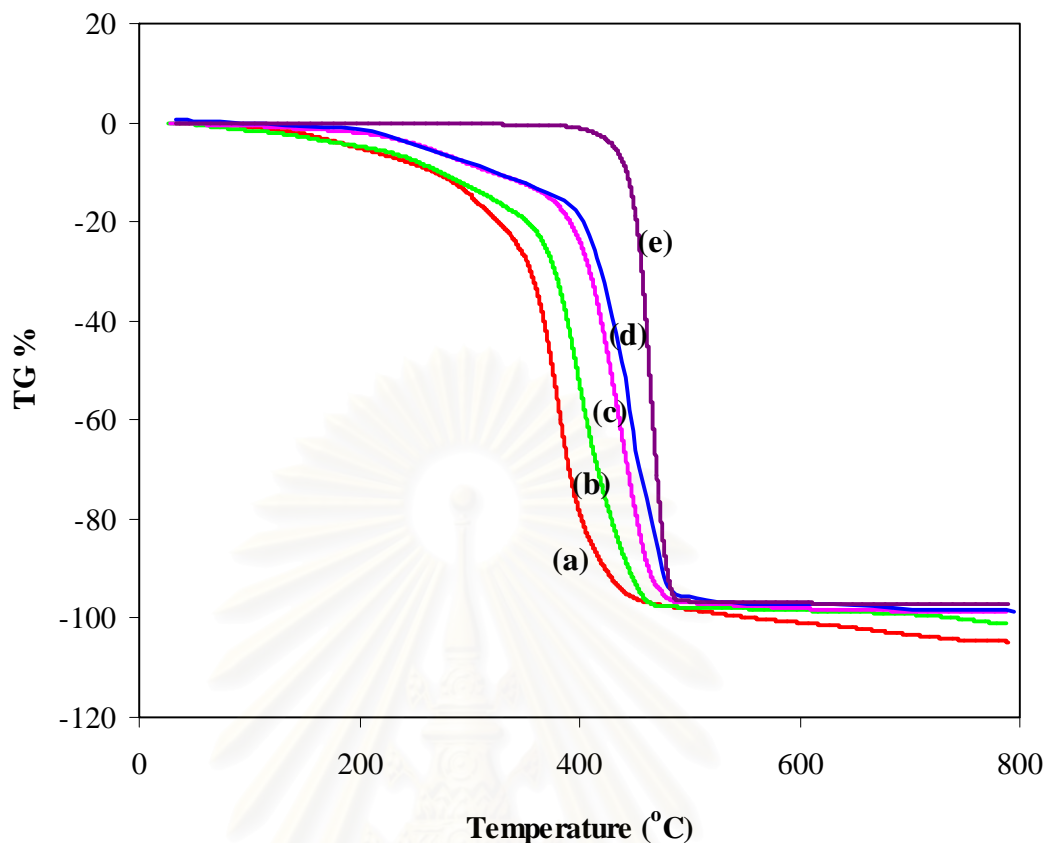
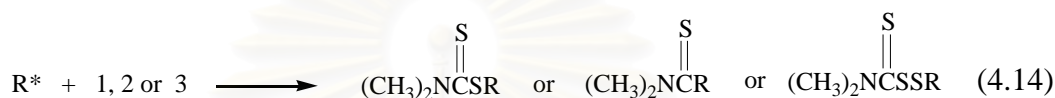
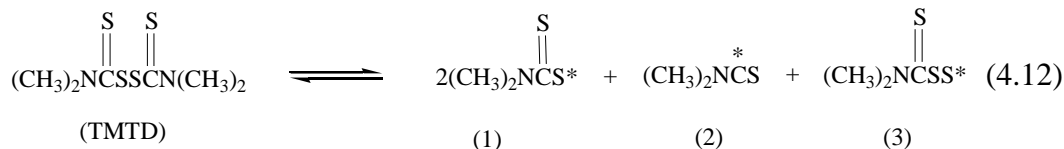
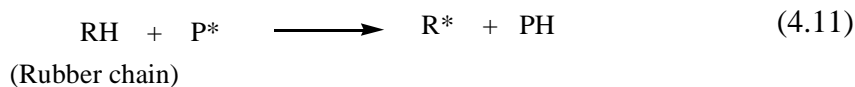
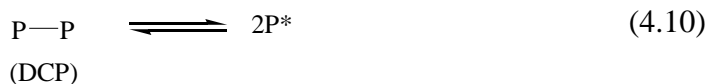


**Figure 4.20** TGA thermograms of (a) SNR, (b) HSNR 32.9%, (c) HSNR 64.5%, (d) HSNR 83.5% and (e) EPDM.

#### 4.8 Cure Characteristics of HSNR/NR Blends

The cure characteristics of various HSNR/NR blends are presented in Table 4.4 and Figure 4.21. The optimum cure time ( $t_{c90}$ ) decreased with increasing HSNR content. It is possible that the remaining unsaturation carbon-carbon double bonds concentration in the backbone structure of HSNR has a higher reactivity for vulcanization [51]. Thus the HSNR/NR blends required shorter  $t_{c90}$  to complete the vulcanization. The possible reaction for vulcanization by the efficient peroxide cure (EPV) system has been postulated by Das *et al.* [52]. The cumyloxy radicals ( $P^*$ ) generated by the thermal dissociation of DCP react with the rubber chain to produce the effective crosslinking site ( $R^*$ ) as shown in eq. 4.10 and 4.11. Some portion of DCP and  $R^*$  was sacrificed by directly combining with thiuram radicals dissociated from TMTD as shown in eq. 4.12-4.14.



The combination of peroxide and a sulfur donor vulcanization system resulted in the improved mechanical properties of the HSNR/NR blends. It was believed that the peroxide possibly retarded the reactivity of the sulfur donor for curing NR in the blend to reduce the cure-rate mismatch due to the imbalance in unsaturation levels of the HSNR and NR. The minimum torques tended to increase with increasing HSNR content. It can be explained that the small portion of NR in the blend was prematurely cured by both TMTD and DCP; whereas the predominant HSNR phase was subsequently cured by only DCP. Therefore, this blend with high HSNR content had higher minimum torque than NR and this similar result was earlier reported by Hinchiranan *et al.* [53] for the HNR/NR blends.

**Table 4.4** Effect of EPV vulcanization system on cure characteristic of HSNR/NR.

HSNR/NR	Minimum Torque (ML, dN·m)	Maximum Torque (MH, dN·m)	Scorch time (ts <sub>2</sub> , min)	Optimum cure time (tc <sub>90</sub> , min)
0/100	0.26 ± 0.01	3.65 ± 0.06	10.3 ± 0.08	25.5 ± 0.47
25/75	0.61 ± 0.05	3.39 ± 0.01	11.0 ± 0.87	24.5 ± 0.45
50/50	0.71 ± 0.13	3.83 ± 0.01	10.5 ± 0.91	22.3 ± 0.15
75/25	0.69 ± 0.10	3.85 ± 0.04	9.98 ± 0.19	21.4 ± 0.14
100/0	0.89 ± 0.10	3.55 ± 0.02	17.5 ± 1.66	21.6 ± 0.40

Test method: The optimum cure time of samples were measured using Moving Die Rheometer (MDR) at 150°C with frequency 1.7 Hz and amplitude 0.5°.

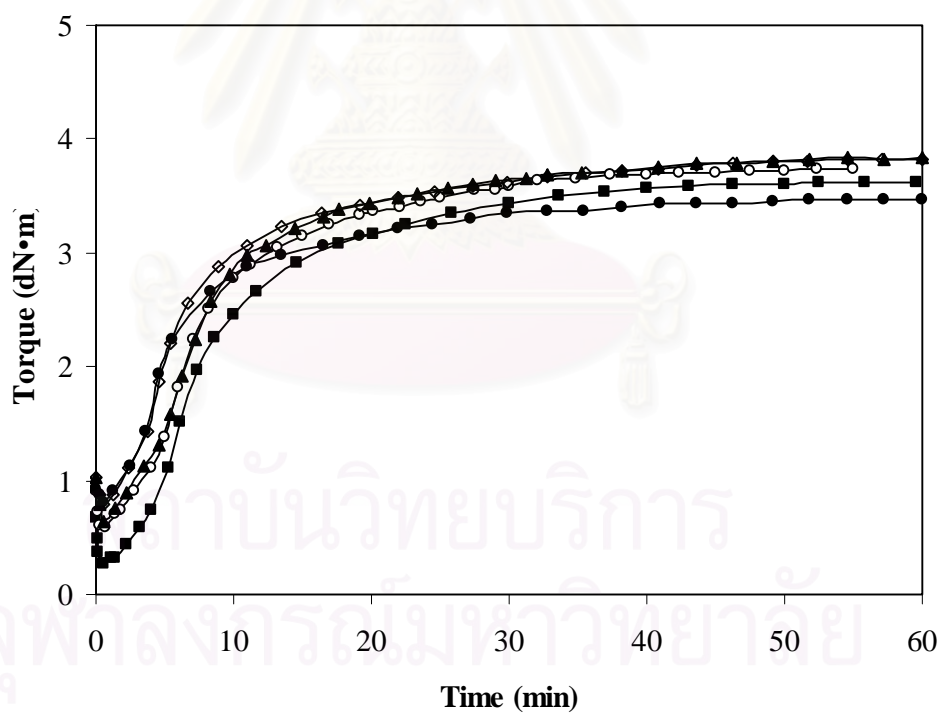


**Figure 4.21** Cure characteristics of vulcanized at various rubber blend ratios of HSNR/NR cured by EPV system with 2 phr of DCP; HSNR/NR = 0/100 (■), HSNR/NR = 25/75 (○), HSNR/NR = 50/50 (▲), HSNR/NR = 75/25 (◇) and HSNR/NR = 100/0 (●).

#### 4.9 Mechanical Properties of HSNR/NR Vulcanizates

Mechanical properties of vulcanized HSNR/NR blends using efficient peroxide cure (EPV) system were measured in terms of tensile strength, ultimate elongation and hardness. The thin rubber sheets from two-roll mill were pressed under pressure by compression molding at a temperature and time interval from the MDR study. The thickness vulcanizate was ca. 2 mm. and the sheet was cut into standard specimens according to the ASTM test method. The mechanical properties of vulcanized HSNR/NR blends are summarized in Table 4.5.

**Table 4.5** Effect of blend ratio on the thermal stability of HSNR/NR cured by EPV system with 2 phr of DCP.

Blends ratio (HSNR/NR)	Crosslink density (mmol/cm <sup>3</sup> )	Tensile strength (MPa)		Elongation at break (%)		Hardness	
		Before aging	%Retention <sup>1</sup>	Before aging	%Retention <sup>1</sup>	Before aging	%Retention <sup>1</sup>
0/100	0.096	9.26	59.9	575	67.6	32.5	103
25/75	0.040	6.43	92.7	620	93.2	34.8	101
50/50	0.062	7.45	96.0	666	93.0	36.0	101
75/25	0.035	4.14	87.2	524	97.2	37.7	101
100/0	0.031	2.65	98.5	503	97.9	36.3	102

$$^1\% \text{Retention} = (\text{Properties after aging} / \text{Properties before aging}) \times 100$$

The mechanical properties of vulcanizates at various contents of HSNR in the blends were investigated. From Table 4.5, the tensile strength of HSNR/NR vulcanizates decreased when the HSNR content increased. It is possible that HSNR is incompatible with NR due to the imbalance in the unsaturation level. The NR vulcanizate before heat aging had high value of mechanical properties due to the presence of proteins in the rubber structure [54]. The high tensile strength with lower ultimate elongation of NR vulcanizate was also due to the high crosslink density (0.096 mmol/cm<sup>3</sup>). From the morphology of the fracture surface of HSNR/NR vulcanizates at a 25/75 (Figure 4.22b), the small particles of HSNR were dispersed in

the NR phase. This could result in the reduction of tensile strength. However, the addition of peroxide as the co-curable with the sulfur donor in the efficient vulcanization can improve the mechanical properties of the blends consisting of two dissimilar rubbers by possibly reducing the effect of cure-rate mismatch. Therefore, the EPV system gave tensile strengths of the HSNR/NR vulcanizates as high as the vulcanizates containing bis(diisopropyl)thiophosphoryl disulfide (DIPDIS) as a coupling agent accelerator in the two-stage vulcanization of the rubber blends [55].

The HSNR/NR vulcanizates at blend ratio of 50/50 had a maximum elongation at break at ~666 %. It can be explained that the vulcanizates exhibited a synergistic effect due to the compatibility of the different morphology of HSNR and NR. This result was also confirmed by the SEM micrograph (Figure 4.22c), which shown the morphology of the continuous phase with homogeneity that resulted in the increment of the elongation at break. Hussien *et al.* [56] reported that a hydrogenated acrylonitrile-butadiene rubber (HNBR/NBR) blend at 50/50 wt ratio also exhibited the co-continuous morphology (smooth fracture surface) which resulted in an increase in stress at high strains. Moreover, HSNR/NR vulcanizates at 50/50 wt ratio with the high crosslink density ( $0.062 \text{ mmol/cm}^3$ ) had high mechanical properties (tensile strength and elongation at break). When HSNR loading in the blends was increased to 75 phr, the ultimate elongation decreased and leveled off at ~524% due to the higher incompatibility involving the phase separation. From Figure 4.22e, SEM micrographs of HSNR vulcanizate show the rough fracture surface due to the reduction in tensile strength and elongation at break of HSNR at 100% wt. Nang *et al.* [57] reported that the mechanical properties of vulcanizates of hydrogenated *cis*-1,4-polyisoprene (11.7-33.3% hydrogenation) produced by diimide reduction were lower than that of the starting material, owing to depolymerization during the hydrogenation.

The hardness of vulcanizates tends to increase with an increasing amount of HSNR in the rubber blending. Due to the more flexible NR replaced by the less flexible HSNR resulted in the higher hardness of rubber vulcanizates.

#### 4.10 Thermal Stability of HSNR/NR Vulcanizates

The thermal stability of HSNR/NR vulcanizates are presented in term of mechanical properties after aging and the retention after aging as shown in Table 4.5. For the potential to retain the mechanical properties of the blends after heat aging, the NR vulcanizates showed the lowest retention of tensile strength (59.9%) and elongation at break (67.6%). The tensile strength and elongation at break of HSNR/NR (blend ratio of 50/50) after thermal aging was also retained at 96.0% and 93.0%, respectively. It indicated that HSNR was more resistance to heat due to the low saturation level in the rubber structures [55]. In addition, it is possible that the addition of peroxide in efficient vulcanization may retard the reactivity of the sulfur donor, TMTD, for curing NR in the blends. Consequently, the cure-rate mismatch due to the imbalance in unsaturation levels of the HSNR and NR was reduced to give the better mechanical properties of blends. Moreover, the use of a TMTD sulfurless cure system in the presence of ZnO gives stable crosslinks and produces the zinc-dimethyldithiocarbamate (ZCMDC) which is also an efficient antioxidant [58]. The %retention in hardness of HSNR/NR blends after heat aging did not have a significant variation when the blend ratio was changed.

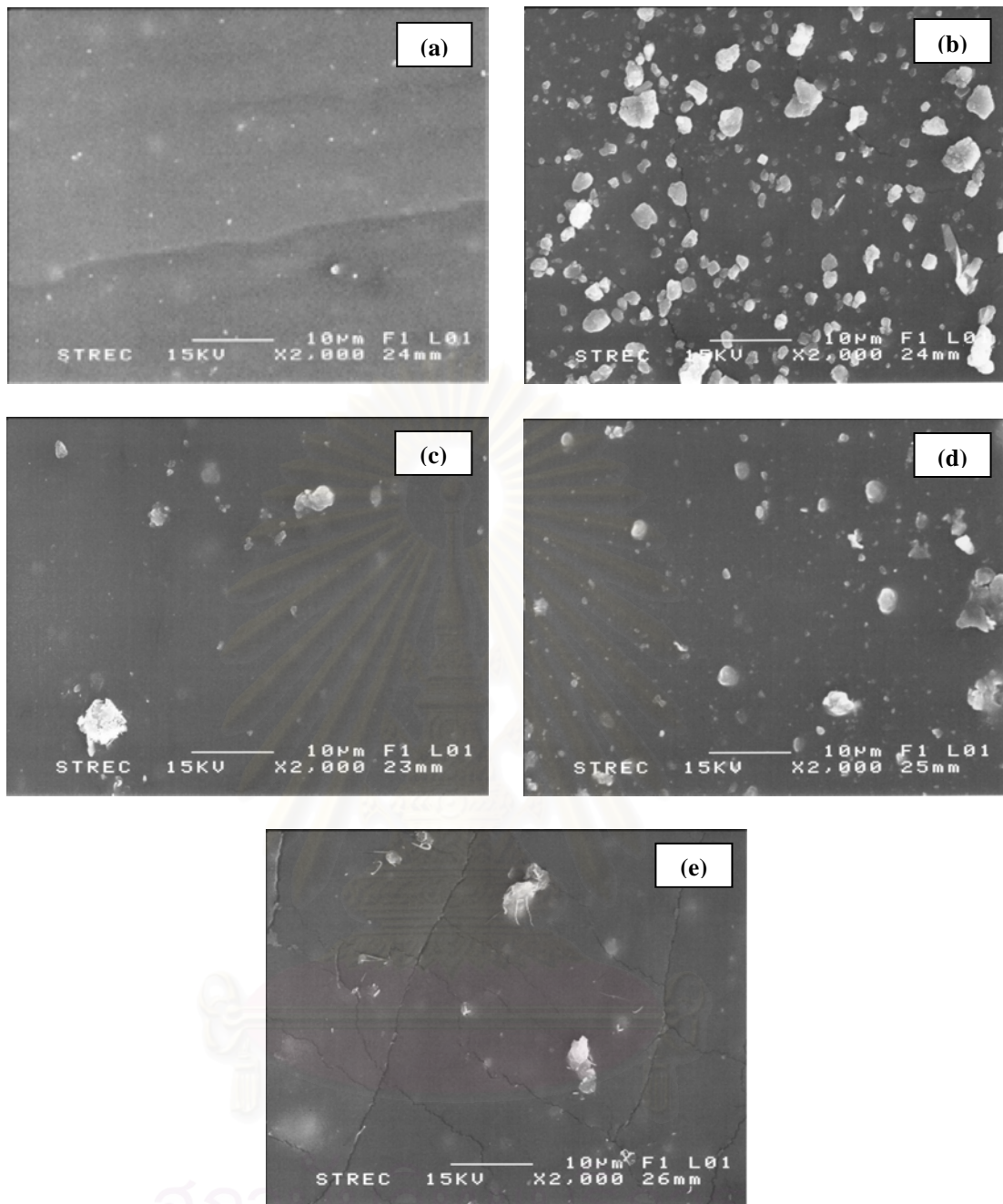


**Figure 4.22** Scanning electron micrograph of tensile fracture surface of vulcanized at various rubber blend ratios of HSNR/NR cured by EPV system: (a) HSNR/NR = 0/100; (b) HSNR/NR = 25/75; (c) HSNR/NR = 50/50; (d) HSNR/NR = 75/25; (e) HSNR/NR = 100/0 (magnification: 2000 $\times$ ).



#### 4.11 Ozone Resistance of Vulcanized Hydrogenated Skim Natural Rubber

Many unsaturated rubbers are susceptible to degradation by heat, humidity, light ozone and radiation etc. [59]. Nowadays ozone resistance of polymer products becomes of importance because the atmospheric ozone concentration has gradually increased: especially in industrialized areas [60]. Ozone presented in the atmosphere at a concentration up to 7 parts per hundred million (pphm) can severely attack on non-resistant rubbers. The series of crack on the rubber surface developed over time, which were perpendicular to applied stress [61].

The greater level of double bonds within unsaturated rubber, higher the susceptibility to ozonation. This can often be noted in natural rubber, but in contrast chloroprene rubber (CR) and ethylene-propylene diene rubber (EPDM) are less reactive to ozone. Ethylene-propylene rubber (EPM and EPDM) have a completely saturated hydrocarbon main chain, so they have excellent ozone resistance and very good resistance to heat and oxidation. The structure of SNR after hydrogenation is an alternating ethylene-propylene copolymer which believed to have better ozone resistance. The possible reaction mechanisms of ozone attack or ozonolysis on diene-containing polymer are shown in Figure 4.23. The reaction between the carbon-carbon double bonds and ozone leads to the formation of an unstable molozone. This unstable species can easily cleave to a stable carbonyl compound (aldehyde or ketone) and an unstable carbonyl oxide (zwitterions). The carbonyl oxides then undergo reaction reactions leading to final, stable products. These reactions may involve a number of steps and the preferred route may depend on the structure of the rubber:

1. The carbonyl oxide may recombine with the carbonyl compound to give an ozonide. Ozonides are relatively stable in neutral environments but will decompose readily under the influence of various reducing or oxidizing agents, or heat, to give scission products such as alcohols, carboxylic acids, aldehydes and ketones [62]. It was also suggested that the decomposition of an ozonide can take place via the attack of an ozone molecule on the ozonide [63].
2. The carbonyl oxide may polymerize to yield polymeric peroxides but these products are relatively unstable and will eventually decompose to give chain scission products [62].

3. The carbonyl oxide may form diperoxides by dimerization [64]. Similar to ozonides, diperoxides can be decomposed by suitable reducing or oxidizing agent to give scission products.
4. In the presence of molecules containing active hydrogen, such as alcohols and water, the carbonyl oxide may abstract a proton leading to the formation of a reactive hydroperoxide [62, 64].

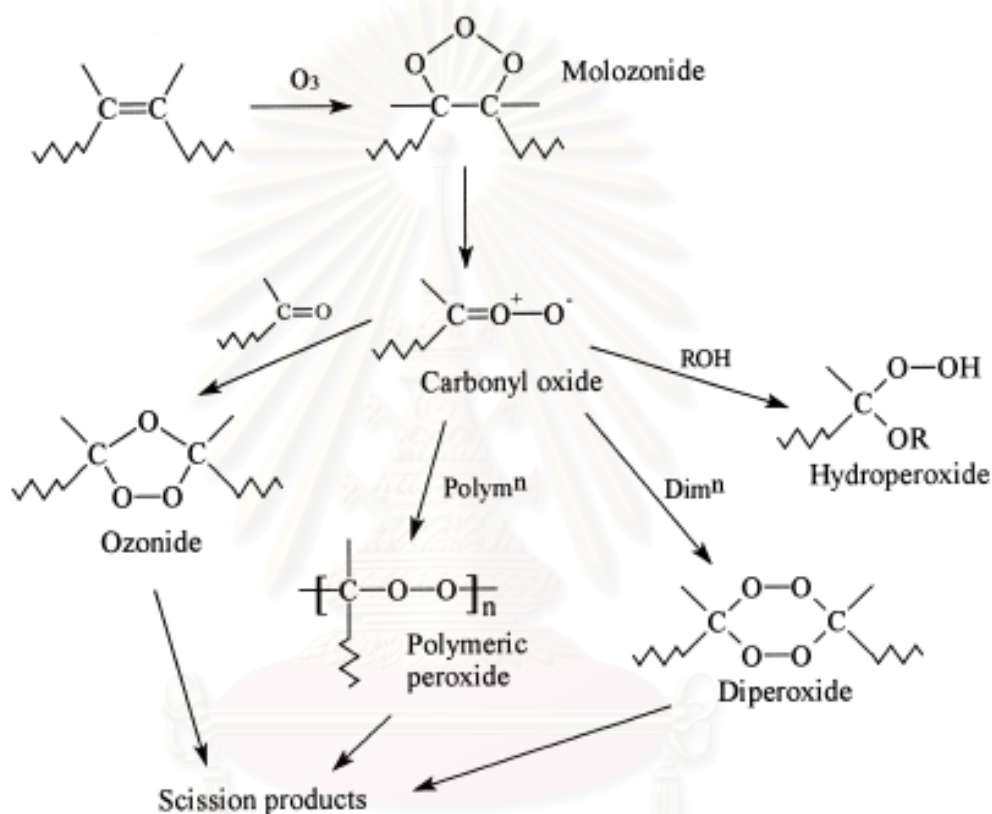


**Figure 4.23** Possible reactions following ozonolysis of diene-containing polymer [65].

The HSNR/NR vulcanizates were exposed in HAMPDEN ozone cabinet at  $40^\circ C$  in an atmosphere of 50 pphm by volume of ozone concentration for 3, 6, 24, 27 and 48 h. A type of ozone cracking on the rubber surface of each specimen was classified according to Table 3.2 (classification of cracking on rubber surface).

The ozone cracking of HSNR/NR vulcanizates at various blend ratios are presented in Table 4.6. The significant cracking (C-3) appeared on the surface of NR specimen after 24 h exposure. For HSNR/NR blends at ratio of 25/75, 50/50, 75/25 and 100/0, the cracking was not observed after 24 h exposure. It can be concluded that the corporation of HSNR could prevent the initiation and propagation of ozone

cracking on the surface, resulting in more ozone resistance of HSNR/NR blends. Inoue and Nishio [20] also reported that the surface cracking on 100% HNR was not observed.

**Table 4.6** Ozone cracking of vulcanized rubber.

HSNR/NR	Type of cracking				
	3 h	6 h	24 h	27 h	48 h
0/100	nc	nc	C-3	C-3	C-3
25/75	nc	nc	nc	nc	C-3
50/50	nc	nc	nc	nc	C-3
75/25	nc	nc	nc	nc	C-3
100/0	nc	nc	nc	nc	C-3

nc = The number of cracking appeared on the surface of rubber specimens.

The ozone resistance of vulcanizates with various content of HSNR at 24 h exposure is presented in Fig. 4.24a. The NR vulcanizate had more numerous ozone cracking traces on the surface of the specimens after 24 h exposure as shown in Fig. 4.24a. The possible reaction mechanism during ozonolysis of NR involves the formation of an intermediate carbonyl oxide which then further reacts to produce primary and secondary ozonides and various peroxidic species resulting in the scission products [65]. On the other hand, the increase in the HSNR content (Fig. 4.24b-4.24e) the results showed that the cracking traces from ozonolysis did not appear on the surface of vulcanizate. It can be concluded that the corporation of HSNR could prevent the initiation and propagation of ozone cracking on the surface, resulting in more ozone resistance of HSNR/NR blends. The ozone resistance of HSNR/NR at 48 h exposure is also presented in Fig. 4.25. HSNR/NR at all blend ratio had C-3 type of cracking. However, the HSNR/NR vulcanizates at blend ratios 25/75, 50/50, 75/25 and 100/0 exhibited less number of cracking than NR vulcanizate.

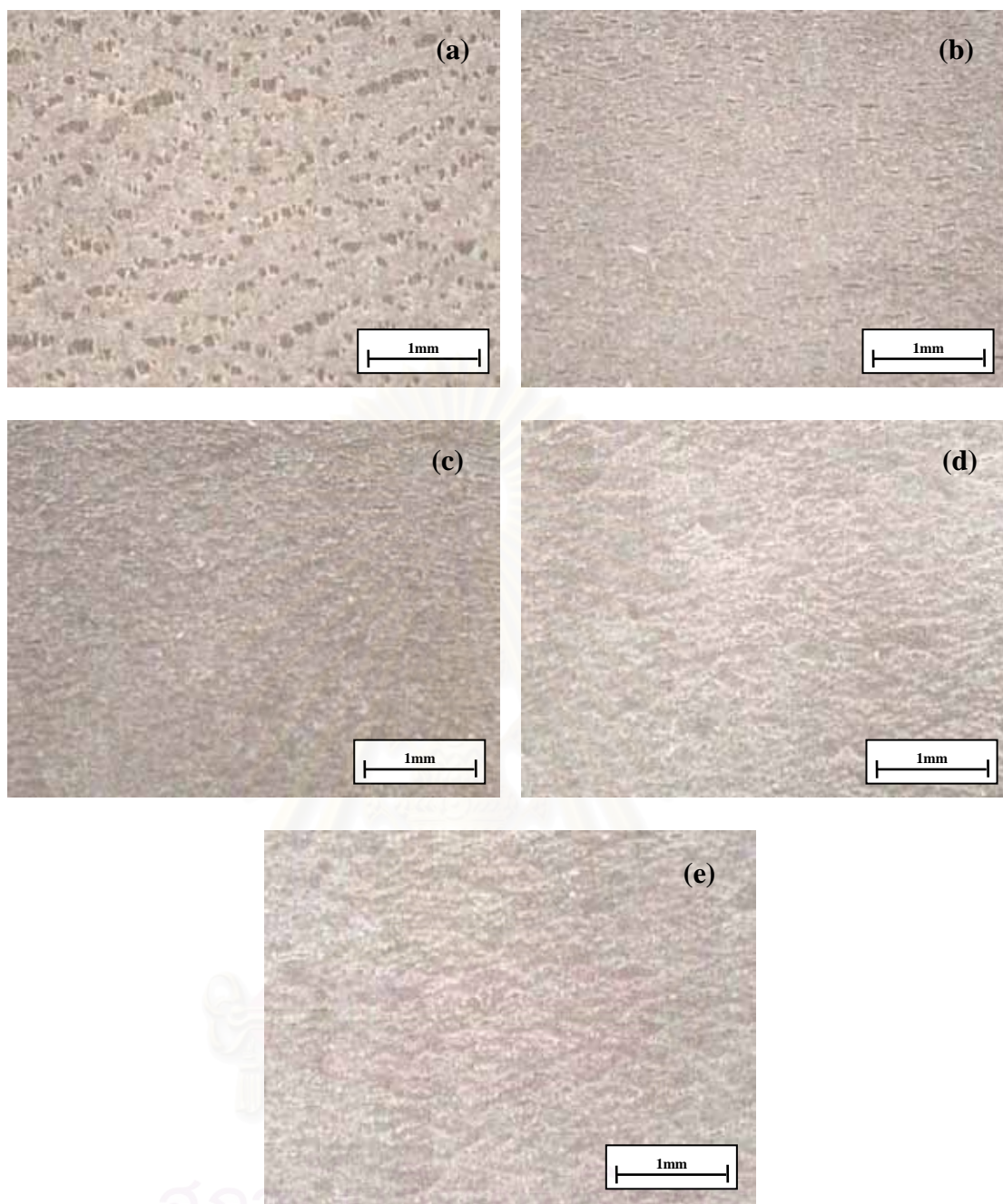


**Figure 4.24** Surface of HSNR/NR vulcanizates at various blend ratios after exposure to ozonised air of 50 ppm ozone concentration at 40°C for 24 h: (a) 0/100, (b) 25/75, (c) 50/50, (d) 75/25, (e) 100/0.

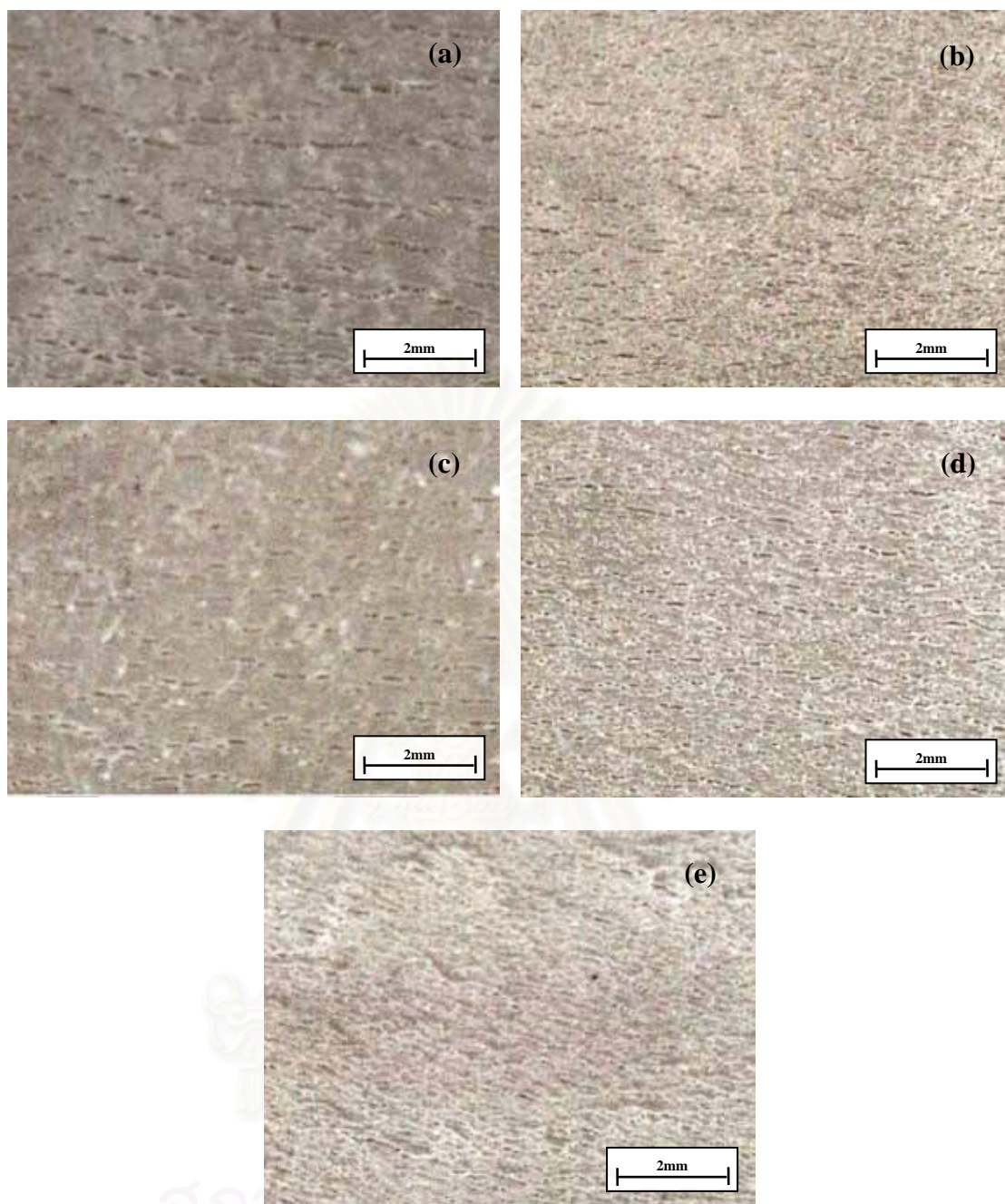


**Figure 4.25** Surface of HSNR/NR vulcanizates at various blend ratios after exposure to ozonised air of 50 ppm ozone concentration at 40°C for 48 h: (a) 0/100, (b) 25/75, (c) 50/50, (d) 75/25, (e) 100/0.

## CHAPTER V

### CONCLUSION AND SUGGESTION

#### 5.1 Conclusions

The major conclusions of this study can be highlight and further elaborated as follows:

1) The hydrogenated skim natural rubber latex was prepared by using diimide reduction technique. The optimum reaction condition was achieved at low temperature, long reaction time, high amount of hydrazine and less amount of hydrogen peroxide and copper sulfate. The increase in the amount of SDS, the degree of hydrogenation decreased. The degree of hydrogenation increased with increasing the amount of boric acid as catalyst and a maximum hydrogenation degree was achieved at 62 mM. When the amount of hydroquinone was increased, the degree of hydrogenation and the gel content decreased. Copper acetate was found to be the most effective catalyst for the diimide hydrogenation of SNRL.

2) The kinetic plot indicated that the hydrogenation reaction was apparently first-order with respect to C=C concentration. The apparent activation energy of the catalytic and non-catalytic hydrogenation of SNRL was calculated as 9.5 and 21.1 kJ/mol, respectively.

3) The hydrogenation level increased with successive treatment of hydrogenation. From TEM micrograph, the non-hydrogenated core and hydrogenated outer layer of HSNRL particle were observed according to the layer model.

4) The DSC thermogram of SNR and EPDM samples exhibited one step of base-line shift. In contrast, the HSNR samples showed two step of base-line shift which the first step and second step were at  $-63^{\circ}\text{C}$  and  $-50^{\circ}\text{C}$ , respectively. The TGA thermogram, the degradation temperature of HSNR increased with increasing hydrogenation degree.

5) The mechanical properties of HSNR/NR blends were did not all that different after heat aging at  $100^{\circ}\text{C}$  for  $22 \pm 2$  h. This implied that the hydrogenated rubbers were more resistant to heat than natural rubber due to the low saturation level in the backbone chain.

6) From the SEM micrograph, HSNR/NR blend at 50/50 wt ratio was shown the co-continuous morphology supported the maximum value of ultimate elongation. The HSNR/NR vulcanizates at various blend ratios had more resistance in surface cracking caused by ozone.

## 5.2 Suggestions for The Future Work

A future investigation of hydrogenation of skim nature rubber should be carried out with the following aspects:

1. Improvement of diimide hydrogenation

Diimide hydrogenation of other polymer such as the synthetic *cis*-1,4-polyisoprene latex with smaller particle size than skim natural rubber latex should be carried out. It is expected that the degree of hydrogenation should be improved.

2. Applications of hydrogenated skim natural rubber

The diimide hydrogenation of graft skim natural rubber latex should be investigated. The blends of hydrogenated skim natural rubber and other polymers should be further studied.

## REFERENCES

- [1] McManus, N. T. and Rempel, G. L. Chemical modification of polymers: catalytic hydrogenation and related reactions. Rev. Macromol. Chem. Phys. C35, 2 (1995): 239-285.
- [2] Kageyama, K. Application of natural rubber serum. Natural rubber current developments in product manufacture and application. Cetaktama Sdn Bhd: Rubber Research Institute of Malaysia, 1993.
- [3] Tanaka, Y. Structure characterization of natural polyisoprenes: solve the mystery rubber based on structure study. Rubber Chem. Tech. 74 (2001): 355-375.
- [4] Morton, M., ed. Rubber Technology. Dordrecht: Kluwer Academic Publishers, 1999.
- [5] Verhaar, G. Natural latex as a colloid system. Rubber Chem. Technol. 32 (1959): 1627-1659.
- [6] Subranium, A. Molecular weight and other properties of natural rubber: a study of clonal variations. Proc. Int. Rubb. Conf. Kuala Lumpur 4, 1975, 3.
- [7] Subranium, A. Molecular weight and molecular weight distribution of natural rubber. Rubb. Res. Inst. Malaysia Technol. Bull. No4, April 1980.
- [8] Allen, P. W. and Bristow, G. M. The gel phase in natural rubber. J. Appl. Polym. Sci. 7 (1963): 603-615.
- [9] Tangpakdee, J. and Tanaka, Y. Purification of natural rubber. J. Nat. Rubb. Res. 12 (1997): 112-119.
- [10] Sakdapanich, J. T., Suksujatporn, S. and Tanaka, Y. Structure characterization of the small rubber particle in fresh *Hevea* latex. J. Rubb. Res. 2(2) 1999: 160-168.
- [11] Blackley, D. C. Polymer lattice science and technology vol 2 type of lattices, 2<sup>nd</sup> ed., London: Chapman & Hall 1997, p 79
- [12] Bhowmick, A. K. and Stephens, H. L., eds. Handbook of elastomers. New York and Basel: Marcel Dekker, 1988.



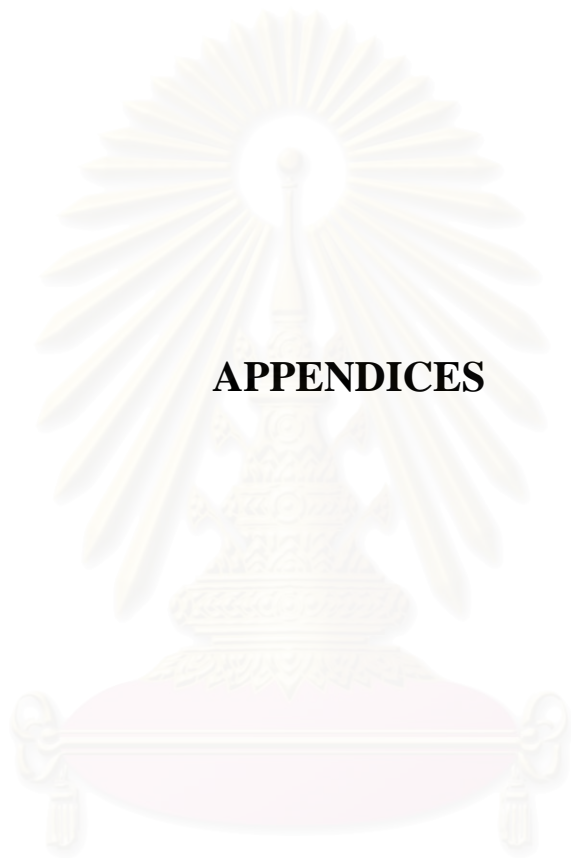
- [13] Schultz, D. N., Turner, S. R. and Golub, M. A. Recent advances in the chemical modification of unsaturated polymers. Rubber Chem. Tech. 55 (1982): 809-859.
- [14] Wideman, L. G. Process for hydrogenation of carbon-carbon double bonds in an unsaturated polymer in latex form. U.S. Patent 4,452,950 (1984).
- [15] Parker, D. K., Roberts R. F. and Schiessl H. W. A new process for the preparation of highly saturated nitrile rubber in latex form. Rubber Chem. Technol. 65 (1992): 245-257.
- [16] He, Y., Daniels, E.S., Klein, A. and El-Asser, M. S. Hydrogenation of styrene-butadiene rubber (SBR) latexes. J. Appl. Polym. Sci. 64 (1997): 2047-2056.
- [17] Belt, J. W., Vermeulen, J. A. A. and Kostermann, M. Process for hydrogenation of carbon-carbon double of unsaturated polymer. WO/09568, (2000).
- [18] Belt, J. W. and Driessen, M. M. Process for the properties of hydrogenated polymer composed of diene monomer unit containing a nitrile group. US 6,635,718 B2, (2003).
- [19] Xie, H. Q., Li, X. D. and Guo, J. S. Hydrogenation and neutralization of carboxylic styrene-butadiene latex to form thermoplastic elastomer with excellent thermooxidation resistance. J. Appl. Polym. Sci. 83 (2002): 1375-1384.
- [20] Xie, H. Q., Li, X. D. and Guo, J. S. Hydrogenation of nitrile-butadiene rubber latex to form thermoplastic elastomer with excellent thermooxidation resistance. J. Appl. Polym. Sci. 90 (2003): 1026-1031.
- [21] Zhou, S., Bai, H. and Wang, J. Hydrogenation of acrylonitrile-butadiene rubber latexes. J. Appl. Polym. Sci. 91 (2004): 2072-2078.
- [22] Lin, X. L., Pan, Q. and Rempel, G. L. Hydrogenation of nitrile-butadiene rubber latex with diimide. Appl. Cat. A: General 276 (2004): 123-128.
- [23] Lin, X. L., Pan, Q. and Rempel, G. L. Gel formation in diimide-hydrogenation polymers. J. Appl. Polym. Sci. 96 (2005): 1122-1125.
- [24] Lin, X. L., Pan, Q. and Rempel, G. L. Modeling and simulation of diimide hydrogenation of nitrile butadiene rubber latex. Ind. Eng. Chem. Res. 45 (2006): 1300-1306.

- [25] Mahittikul, A., Prasassarakich, P. and Rempel, G. L. Diimide hydrogenation of natural rubber latex. J. Appl. Polym. Sci. 105 (2007): 1188-1199.
- [26] Nishi, T. and Nagano, F. The physical testing standard of rubber. Rubber research centre. Document number 117 (1983): 114-121.
- [27] Sirqueira, A. S. and Soares, B. G. The effect of mercapto- and thioacetate-modified EPDM on the curing parameters and mechanical properties of natural rubber/EPDM blends. Eur. Polym. J. 39 (2003):2283-2290.
- [28] Sperling, L. H. Introduction to Physical Polymer Science. John Wiley & Sons: New Jersey, 2006.
- [29] Aik-Hwee, E., Tanaka, Y. and Seng-Neon, G. FTIR studies on amino groups in purities *Hevea* rubber. J. Nat. Rubber. Res. 7(2) (1992): 152-155.
- [30] Inoue, S. I., Nishio, T. Synthesis and Properties of Hydrogenated Natural Rubber. J. Appl. Polym. Sci. 103 (2007): 3957-3963.
- [31] Sarkar, M. D., De, P. P. and Browmick, A. K. Diimide reduction of carboxylated styrene-butadiene rubber in latex stage. Polymer 41 (2000): 907-915.
- [32] Sarkar, M. D., De, P. P. and Browmick, A. K. Thermoplastic elastomeric hydrogenated styrene-butadiene elastomer: optimization of reaction condition, thermodynamics, and kinetics. J. Appl. Polym. Sci. 66 (1997): 1151-1161.
- [33] Lin, X. Hydrogenation of unsaturated polymer in latex form. Doctoral dissertation, Department of Chemical Engineering, Faculty of Engineering, University of Waterloo, 2005.
- [34] Dafader, N. C., Haque, M. E., Akhtar, F., Ahmad, M. U. and Utama M. Evaluation of the properties of natural rubber latex concentrated by creaming method for gamma ray irradiation. J. Macromol. Sci. A33(2) (1996): 73-81.
- [35] Seong, H.S., Whang, H.S. and Ko, S.W. Synthesis of a quaternary ammonium derivative of chito-oligosaccharide as antimicrobial agent for cellulosic fibers J Appl. Polym. Sci. 76 (2000): 2009-2015.
- [36] Parker, D. K. and Ruthenvurg, D. M. Process for the preparation of hydrogenated rubber. US Patent 5,424,356 (1995).
- [37] Gangadhar, A., Chandrasekhara R. T., Subbarao R. and Lakshminarayana, G. Hydrogenation of unsaturated fatty acid methyl esters with diimide

- from hydroxylamine-ethyl acetate. J. of the Am. Oil Chem. Soc. 66 (1989): 1507-1508
- [38] Bhattachajee, S., Bhowmick, A. K. and Avasthi, B. N. High-pressure hydrogenation of nitrile rubber: Thermodynamics and kinetics. Ind. Eng. Chem. Res. 30 (1991): 1086-1092.
- [39] Cassano, G. A., Valles, E. M. and Quinzani, L. M. Structure of partially hydrogenated polybutadienes. Polymer 39 (1998): 5573-5577.
- [40] Singha N. K., P. P. and Sivaram S., Homogeneous catalytic hydrogenation of natural rubber using  $\text{RhCl}(\text{PPh}_3)_3$ . J. Appl. Polym. Sci. 66 (1997): 1647-1652.
- [41] Parker D. K., Roberts R. F. and Schiessl H. W. Preparation, properties and potential applications of diimide hydrogenated styrene-butadiene (HSBR) and polybutadiene (HBR) thermoplastic elastomers. Rubber Chem. Technol. 67 (1994): 288-298.
- [42] Kubo Y. Development and commerization of hydrogenated nitrile rubber produced by selective hydrogenation. International Chemical Engineering 33 (1993): 113-123.
- [43] Charmondusit, K. Hydrogenation of *cis*-1,4-polyisoprene and natural rubber catalyzed by  $\text{OsHCl}(\text{CO})(\text{O}_2)(\text{PCy}_3)_2$  and  $[\text{Ir}(\text{COD})\text{py}(\text{PCy}_3)]\text{PF}_6$ . Doctoral Dissertation, Department of Chemical Technology, Chulalongkorn University, Thailand, 2002.
- [44] Tangthongkul, R. Hydrogenation of synthetic rubber *cis*-1,4-polyisoprene and natural rubber catalyzed by ruthenium (II) complex. Doctoral Dissertation, Department of Chemical Technology, Chulalongkorn University, Thailand, 2003.
- [45] Hinchiranan, N. Hydrogenation of natural rubber catalyzed by  $\text{OsHCl}(\text{CO})(\text{O}_2)(\text{PCy}_3)_2$  and  $[\text{Ir}(\text{COD})\text{py}(\text{PCy}_3)]\text{PF}_6$ . Doctoral Dissertation, Department of Chemical Technology, Chulalongkorn University, Thailand, 2004.
- [46] Mahittikul, A. Structure and properties of hydrogenated natural rubber latex using  $\text{OsHCl}(\text{CO})(\text{O}_2)(\text{PCy}_3)_2$  and  $[\text{Ir}(\text{COD})\text{py}(\text{PCy}_3)]\text{PF}_6$  as a catalyst and dimide reduction. Doctoral Dissertation, Department of Chemical Technology, Chulalongkorn University, Thailand 2005.

- [47] Sandler, S. R., Karo, W., Bonesteel, J. A. and Pearce, E. Polymer synthesis and characterization. A laboratory manual. (San Diego: Academic Press, 1998), pp.108-130, 140-147.
- [48] Rosen, S. L. Fundamental principles of polymeric materials. 2<sup>nd</sup> ed. (New York: John Wiley and Sons, Inc., 1993), pp. 103-107.
- [49] Hinchiranan, N., Charmondusit, K., Prasassarakich, P. and Rempel, G. L., Hydrogenation of synthetic cis-1,4-polyisoprene and natural rubber catalyzed by [Ir(COD)py(PCy<sub>3</sub>)]PF<sub>6</sub>. J. Appl. Polym. Sci. 100 (2006): 4219-4233.
- [50] Mahittikul, A., Prasassarakich, P. and Rempel, G. L. Noncatalytic hydrogenation of natural rubber latex. J. Appl. Polym. Sci. 103 (2007): 2885-2895.
- [51] Nair, T. M., Kumran, M. G. and Unnikrishnan, G. Mechanical and aging properties of cross-linked ethylene propylene diene rubber/styrene butadiene rubber blends. J. Appl Polym Sci. 93 (2004): 2606-2621.
- [52] Das, C. K., Ghosh A. K. and Banerjee. S. Studies of vulcanization with tetramethylthiuram disulfide and sulphur vulcanization accelerated by tetramethylthiuram disulfide of styrene-butadiene rubber in presence and absence of dicumyl peroxide. J. Polym. Sci.: Polym. Chem. ed. 15 (1977): 2255-2268.
- [53] Hinchiranan, N., Lertweerasirikun, W., Poonsawad, W. Rempel, G. L. and Prasassarakich, P. Cure characteristics and mechanical properties of hydrogenated natural rubber/natural rubber blends. J. Appl. Polym. Sci. 111 (2009): 2813–2821.
- [54] Morton, M. Rubber Technology. New York: Van Nostrand Reinhold Company. 1987.
- [55] Ghosh, A. K., Depnath, S. C., Naskar, N. and Basu, D. K. NR-EPDM co-vulcanization: A novel approach. J. Appl. Poly. Sci. 81 (2001): 800-808.
- [56] Hussein, I. A., Chaudhry, R. A. and Abu Sharkh, B. F. Study of the miscibility and mechanical properties of NBR/HNBR blends. Polym. Eng. Sci. 44 (2004): 2346-2352.

- [57] Nang T. D., Katabe, Y. and Minoura, Y. Diimide reduction of *cis*-1,4-polyisoprene with *p*-toluenesulphynylhydrazide. Polymer 17 (1997): 2359-2365.
- [58] Morrell, S. H. Rubber Technology and Manufacture, Blow, C. M.; Hepburn, C., Ed.; Butterworth Scientific: London, 1982, Chap. 5.
- [59] Vinod, V. S., Varghese, S. and Kuriakose, B. Degradation behaviour of natural rubber-aluminum powder composites: effect of heats, ozone and high energy radiation. Polym. Degrad. Stab. 75 (2002): 405-412.
- [60] Allen, N. S., Edge, M., Mourelatou, D., Wilkinson, A., Liaw, C. M., Parellada, M. D., Barrio, J. A. and Quiteria, V. R. S. Influence of ozone on styrene-ethylene-butadiene-styrene (SEBS) copolymer. Polym. Degrad. Stab. 79 (2003): 297-307.
- [61] Findik, F., Yilmaz, R. and Koksall, T. Investigation of mechanical and physical properties of several industrial rubbers. Material and Design 25 (2004): 269-276.
- [62] Lattimer, R.P., Layer, R.W. and Rhee, C.K. Atmos. Oxid. Antioxid. 2 (1993): 363-384.
- [63] Ho, K.W. Ozonation of hydrocarbon diene elastomers: A mechanistic study. J. Polym. Sci., Part A 24 (1986): 2467-2484.
- [64] Criegee, R. Mechanism of Ozonolysis Angew. Chem. Internat. Edit. 14 (1975): 745-752.
- [65] Nor, H. M. and Ebdom, J. R. Ozonolysis of natural rubber in chloroform solution Part 1. A study by GPC and FTIR spectroscopy. Polymer 41 (2000): 2359-2365.



**APPENDICES**

สถาบันวิทยบริการ  
จุฬาลงกรณ์มหาวิทยาลัย

## Appendix A

### The Overall Composition of Rubber

**Table A-1** Properties of skim natural rubber latex

Properties	Test Results*
Total solid content (% wt.)	7.78
Dry rubber content (% wt.)	5.08
Non rubber solid (% wt.)	4.10
Ammonium content (on total weight) (% wt.)	0.44
Ammonium content (on water phase) (% wt.)	0.47
Mechanical stability time @ 55% TS (s)	Cannot test
Volatile fatty acid number (VFA number)	150.84
Potassium hydroxide number (KOH number)	Cannot test
Specific gravity at 25°C	1.0130
Coagulum content (% m/m)	0.0001
pH	11
Magnesium content on solids (ppm)	0.41
61% TSC, 25 C by Brookfield LVT; Spindle No. 1	
Speed 6 rpm (cPs)	Cannot test
Speed 6 rpm (cPs)	Cannot test
Speed 6 rpm (cPs)	Cannot test

\*From Rubber Technology Division, Rubber Research Institute of Thailand, Department of Agriculture.

**Table A-2** Properties of standard thai natural rubber 5L (STR-5L)

Properties	Limit	Test Result
Dirt (max, % wt.)	0.04	0.014
Ash (max, % wt.)	0.40	0.22
Nitrogen (max, % wt.)	0.60	0.35
Volatile matter (max, % wt.)	0.80	0.13
Initial Wallace plasticity range (P <sub>0</sub> )	35	35.4
Colour Lavibond Scale (PRI, min)	6.0	3.5
Plasticity Retention Index (PRI, min)	60	88.3
Mooney Viscosity ML (1+4) 100°C	-	59.2

**Table A-3** Properties of ethylene-propylene-diene copolymer (EPDM)

Properties	Values
Mooney viscosity ML (1+4) 125°C	65
Polymer composition (% mass)	
Ethylene	50
Propylene	42.5
Ethylidenenorbornene	7.5
Molecular weight distribution	Medium
Density (g/cc)	0.86
Residual transition metal (max, ppm)	10
Ash content (max, % mass)	0.1
Total volatiles (max, % mass)	0.4

\*EPDM has an ethylene/propylene ratio of 50/50 and diene content of 9.5%.



## Appendix B

### Determination of Total Solid Content (TSC) and Dry Rubber

#### Content (DSC)

Total Solid Content (TSC) and Dry Solid Content (DRC) are the general specification requirements for latex. The determination of TSC and DRC of skim natural rubber latex was analyzed following ASTM D1076.

#### Total Solid Content (TSC)

Skim natural rubber latex was weighted accurately with microbalance near  $2.5 \pm 0.5$  g to nearest 1 mg was in the covered weighing dish. The latex was distributed over the bottom of dish and dried in a vented air oven for 16 hours at  $70 \pm 2^\circ\text{C}$ . The dried rubber was cooled in a desiccator to room temperature and weigh. Drying and weighing was repeated until the mass is constant to 1 mg or less. The triplicate of sample was done for the average result. The percentage of total solid content was as follows Eq. B-1.

$$\%TSC = \frac{(C - A)}{(B + A)} \times 100 \quad \text{B-1}$$

Where:

A = the weight of the weighing dish (g)

B = the weight of the weighing dish plus the original sample (g)

C = the weight of the weighing dish plus the dried sample (g)

#### Dry Solid Content (DRC)

Skim natural rubber latex was weighted approximately 10 g to nearest 1 mg into a porcelain evaporation dish. For completely coagulum of skim natural rubber, sufficient 2% (w/v) of acetic acid was added while stirring constantly over a 5

minutes period. The dish was stand at room temperature until a clear serum appeared. A coagulum latex particle was picked up with the main body of the coagulum. The coagulum was washed with running water, passed between rolls to a thickness of 2 mm and dried at  $70\pm 2^{\circ}\text{C}$  in a vented air oven atmosphere. The dried rubber was cooled in a desiccator to room temperature and weight. Drying and weighing was repeated until the mass is constant to 1 mg or less. The percentage of dry solid content was as follows Eq. B-2.

$$\% \text{DRC} = \frac{\text{Weight of dry coagulum}}{\text{Weight of sample}} \times 100$$

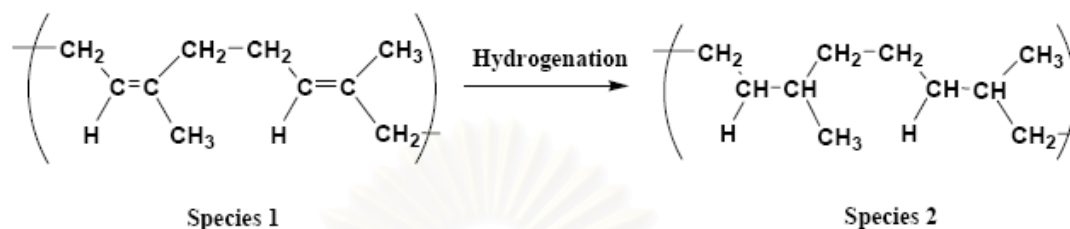
B-2



สถาบันวิทยบริการ  
จุฬาลงกรณ์มหาวิทยาลัย

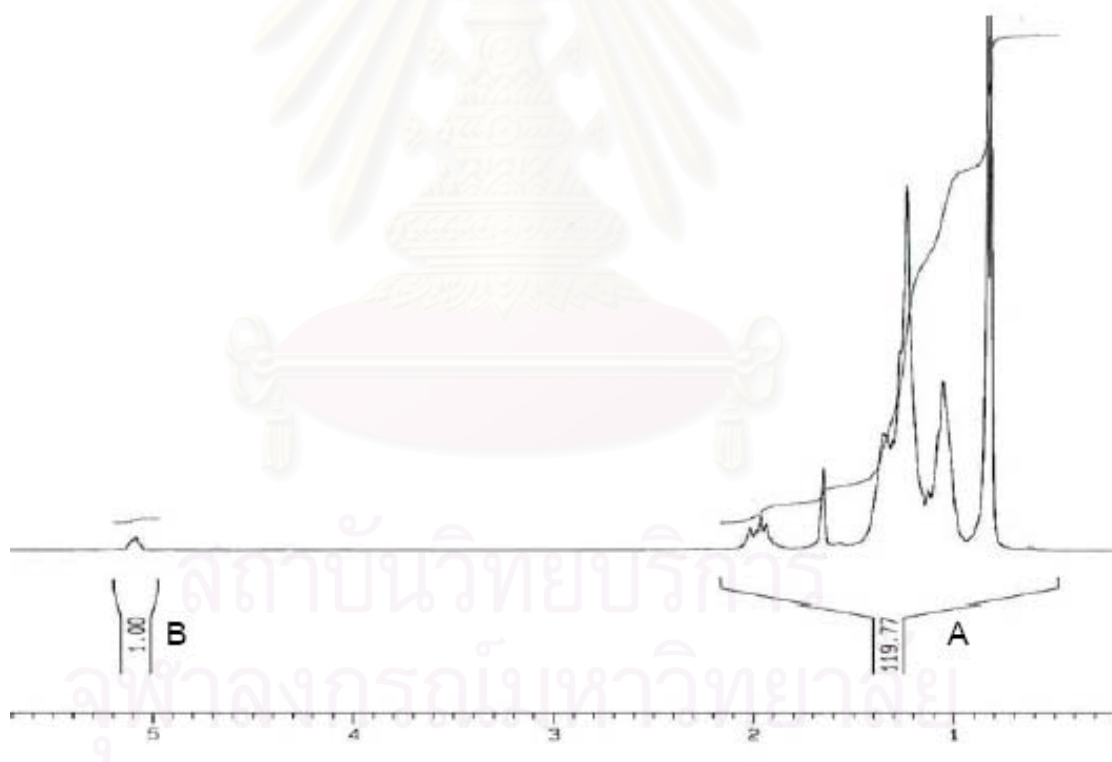
## Appendix C

### Calculation of Degree of Hydrogenation [48]



Proton of repeating unit except =CH in species 1 = 7 protons

Proton of repeating unit in species 2 = 10 protons



Where:

A = Peak area except at 5.2 ppm

B = Peak area at 5.2 ppm

C = Peak area of saturated -CH<sub>2</sub>- and -CH<sub>3</sub>

$$A = 10C + 7B$$

$$C = \frac{A - 7B}{10}$$

Total peak area = Peak area of saturated  $-\text{CH}_2-$  and  $-\text{CH}_3$  + Peak area at 5.2 ppm

$$= \frac{A - 7B}{10} + B$$

$$= \frac{A - 3B}{10}$$

%Hydrogenation = [(Peak area of saturated  $-\text{CH}_2$  and  $-\text{CH}_3$ )/(Total peak area)]  $\times 100$

$$\% \text{Hydrogenation} = \frac{(A - 7B)/10}{(A + 3B)/10} \times 100$$

$$\% \text{Hydrogenation} = \frac{A - 7B}{A + 3B} \times 100$$

For example: A = 138.56 and B = 1.00

$$\begin{aligned} \% \text{Hydrogenation} &= \frac{138.56 - 7(1.00)}{138.56 + 3(1.00)} \times 100 \\ &= 92.94\% \end{aligned}$$

สถาบันวิทยบริการ  
จุฬาลงกรณ์มหาวิทยาลัย

**Table C-1** FTIR assignments for SNR

Wave number (cm <sup>-1</sup> )	Assignments Reference
Isoprene	
3033	=CH stretching
2962	C-H stretching of CH <sub>3</sub>
2927	C-H stretching of CH <sub>2</sub>
2855	C-H stretching of CH <sub>2</sub> and CH <sub>3</sub>
1664	C=C stretching
1450	C-H bending of CH <sub>2</sub>
1375	C-H bending of CH <sub>3</sub>
1127	C-H bending
836	C=CH bending
Protein/Phospholipid	
3440	-OH stretching
3280	N-H stretching
1732	C=O stretching
1530	N-H bending
1140	C-O
1014	-O-O-

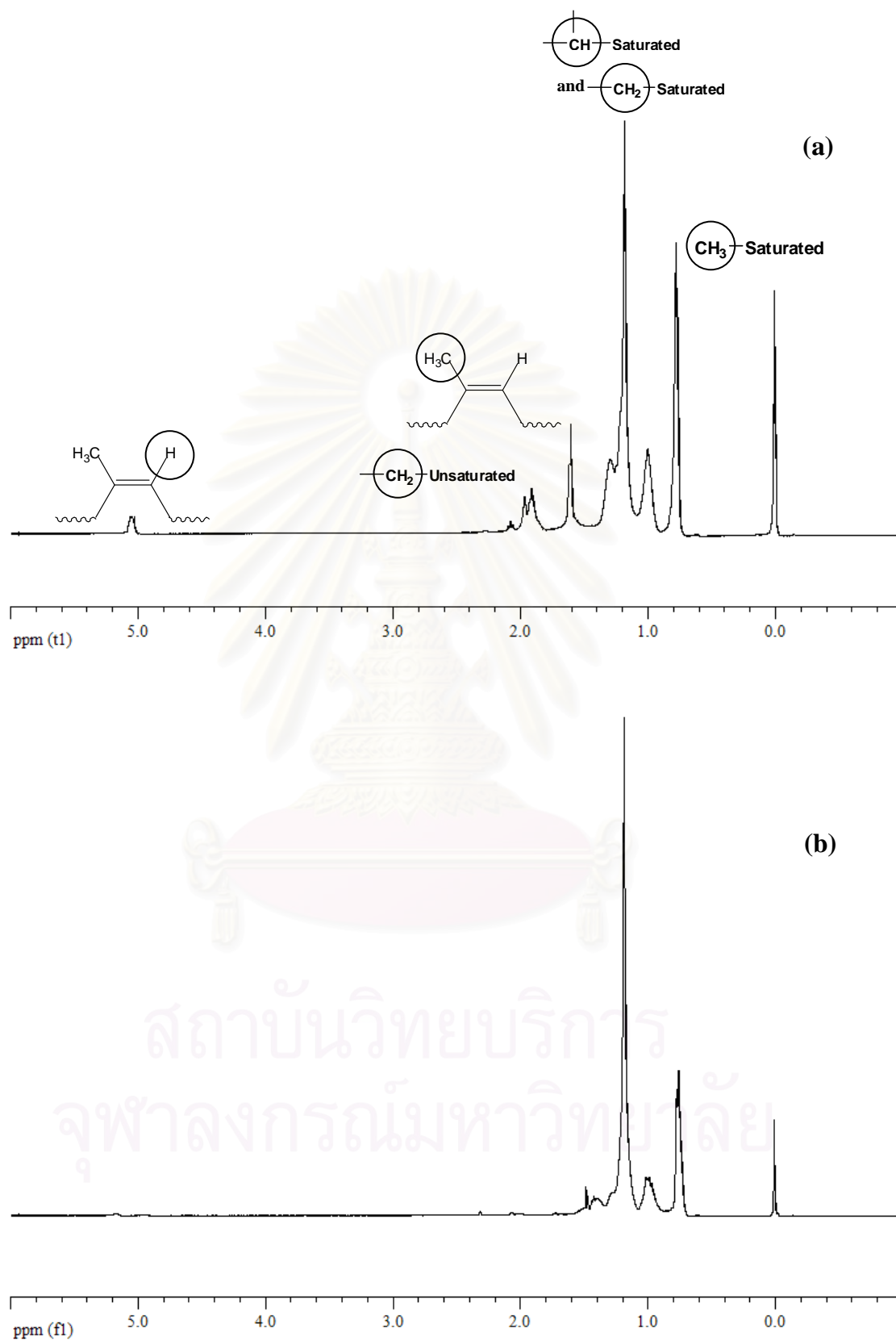
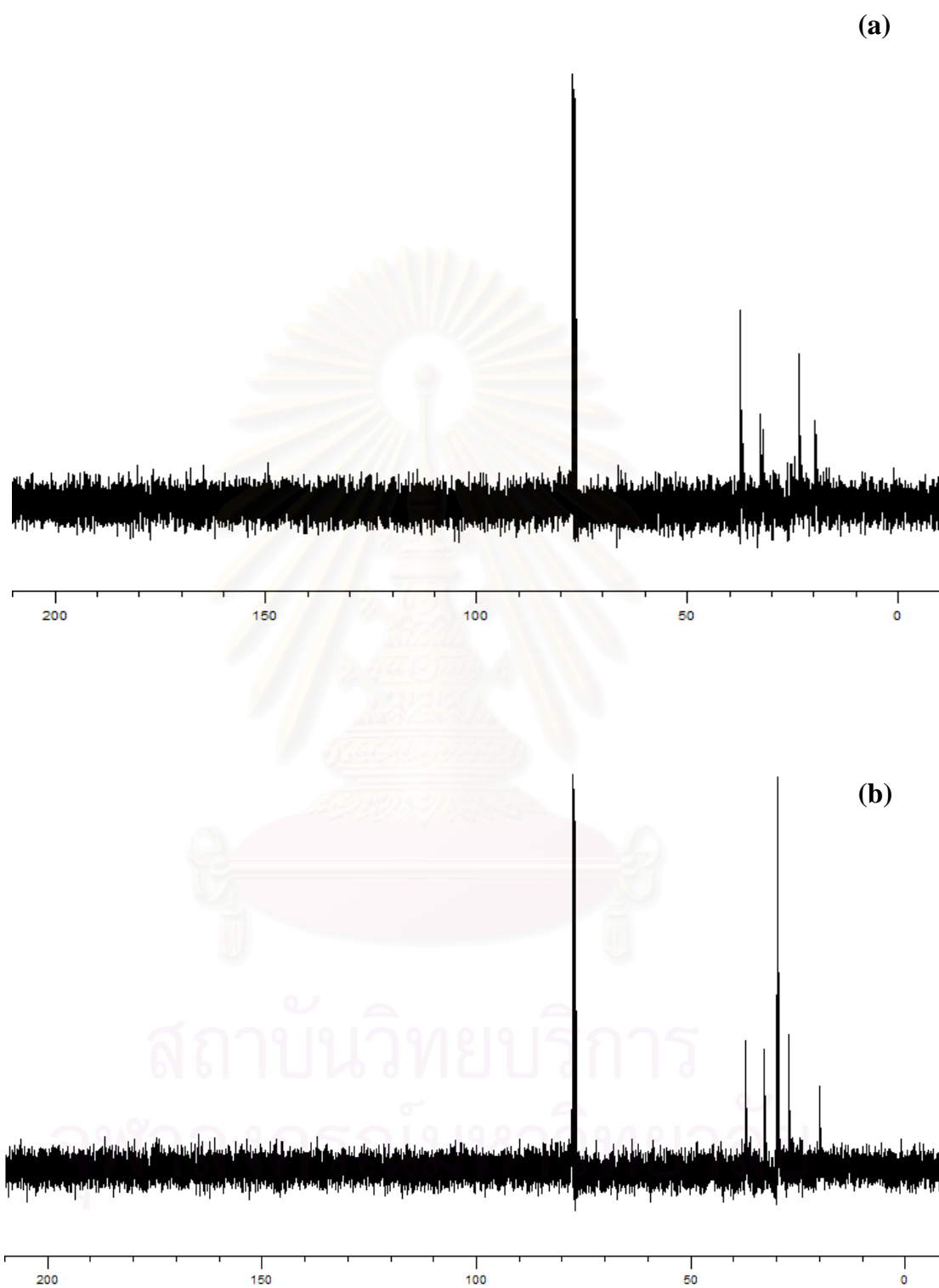


Figure C-1  $^1\text{H-NMR}$  spectra of (a) HSNR, (b) EPDM.



**Figure C-2**  $^{13}\text{C}$ -NMR spectra of (a) HSNR, (b) EPDM.

**Table C-2**  $^{13}\text{C}$ -NMR assignments for SNR and HSNR

Chemical shift (ppm)	Carbon type
SNR	
23.5	C-1
26.4	C-2
32.3	C-5
124.9	C-4
135.1	C-3
HSNR	
19.6	-CH <sub>3</sub>
23.5	C <sub>ββ</sub>
32.6	-CH-
37.2	C <sub>αγ</sub>

สถาบันวิทยบริการ  
จุฬาลงกรณ์มหาวิทยาลัย



## Appendix D

### Data of Hydrogenation Degree

**Table D-1** Results of SNRL by diimide hydrogenation in presence of copper sulfate as catalyst

Exp	CuSO <sub>4</sub> ( $\mu$ M)	N <sub>2</sub> H <sub>4</sub> (mM)	H <sub>2</sub> O <sub>2</sub> (mM)	C=C (M)	Temp (°C)	Total Volume (ml)	Degree of Hydrogenation (%)
1 <sup>a</sup>	0	2.20	3.53	0.55	60	162.0	42.7
2	24.7	2.20	3.53	0.55	60	162.0	57.5
3	49.4	2.20	3.53	0.55	60	162.0	64.5
4	74.0	2.20	3.53	0.55	60	162.0	56.7
5	98.8	2.20	3.53	0.55	60	162.0	53.6
6	246.9	2.20	3.53	0.55	60	162.0	49.7
7 <sup>b</sup>	49.4	0.60	3.53	0.55	60	149.3	43.1
8	49.4	1.65	3.53	0.55	60	153.6	49.3
9	49.4	1.70	3.53	0.55	60	158.0	58.0
10	49.4	2.20	3.53	0.55	60	162.3	64.5
11	49.4	2.68	3.53	0.55	60	166.7	64.7
12	49.4	3.14	3.53	0.55	60	171.0	61.8
13	49.4	3.57	3.53	0.55	60	175.4	54.7
14 <sup>c</sup>	49.4	2.20	1.23	0.55	60	144.8	37.8
15	49.4	2.20	2.34	0.55	60	152.6	50.1
16	49.4	2.20	2.76	0.55	60	155.8	55.7
17	49.4	2.20	3.15	0.55	60	158.9	60.2

Exp	CuSO <sub>4</sub> ( $\mu$ M)	N <sub>2</sub> H <sub>4</sub> (mM)	H <sub>2</sub> O <sub>2</sub> (mM)	C=C (M)	Temp ( $^{\circ}$ C)	Total Volume (ml)	Degree of Hydrogenation (%)
18	49.4	2.20	3.53	0.55	60	162.0	64.5
19	49.4	2.20	3.90	0.55	60	165.2	60.6
20	49.4	2.20	4.25	0.55	60	168.3	56.6
21	49.4	2.20	5.08	0.55	60	176.2	53.4
22 <sup>d</sup>	49.4	2.20	3.53	0.49	60	121.9	52.4
23	49.4	2.20	3.53	0.52	60	138.5	58.8
24	49.4	2.20	3.53	0.55	60	161.9	64.5
25	49.4	2.20	3.53	0.58	60	185.3	55.9
26	49.4	2.20	3.53	0.59	60	195.2	52.5
27	49.4	2.20	3.53	0.60	60	208.7	47.9
28	49.4	2.20	3.53	0.63	60	281.8	28.1
29 <sup>e</sup>	49.4	2.20	3.53	0.55	40	162.0	38.9
30	49.4	2.20	3.53	0.55	50	162.0	43.1
31	49.4	2.20	3.53	0.55	55	162.0	49.0
32	49.4	2.20	3.53	0.55	60	162.0	64.5
33	49.4	2.20	3.53	0.55	65	162.0	68.1
34	49.4	2.20	3.53	0.55	70	162.0	70.7
35	49.4	2.20	3.53	0.55	80	162.0	72.3
36	49.4	2.20	3.53	0.55	90	162.0	56.7

<sup>a</sup>Effect of copper sulfate catalyst concentration

<sup>b</sup>Effect of hydrazine concentration

<sup>c</sup>Effect of hydrogen peroxide concentration

<sup>d</sup>Effect of rubber concentration

<sup>e</sup>Effect of reaction temperature

**Table D-2** Effect of SDS concentration on SNRL hydrogenation

Exp	CuSO <sub>4</sub> ( $\mu$ M)	N <sub>2</sub> H <sub>4</sub> (mM)	H <sub>2</sub> O <sub>2</sub> (mM)	C=C (M)	SDS ( $\mu$ M)	Temp (°C)	Total Volume (ml)	Degree of Hydrogenation (%)
37	49.4	2.20	3.53	0.55	0	60	162.0	64.5
38	49.4	2.20	3.53	0.55	24.7	60	162.0	55.2
39	49.4	2.20	3.53	0.55	49.4	60	162.0	52.8
40	49.4	2.20	3.53	0.55	74.0	60	162.0	52.2
41	49.4	2.20	3.53	0.55	246.9	60	162.0	51.4
42	49.4	2.20	3.53	0.55	493.8	60	162.0	49.1

**Table D-3** Effect of hydroquinone concentration on SNRL hydrogenation

Exp	CuSO <sub>4</sub> ( $\mu$ M)	N <sub>2</sub> H <sub>4</sub> (mM)	H <sub>2</sub> O <sub>2</sub> (mM)	C=C (M)	Hydroquinone (mM)	Temp (°C)	Gel Content (%)	Degree of Hydrogenation (%)
43	49.4	2.20	3.53	0.55	0	60	45.3	64.5
44	49.4	2.20	3.53	0.55	0.06	60	40.5	55.2
45	49.4	2.20	3.53	0.55	0.30	60	31.2	52.8
46	49.4	2.20	3.53	0.55	0.61	60	23.1	52.2
47	49.4	2.20	3.53	0.55	1.23	60	16.0	51.4
48	49.4	2.20	3.53	0.55	3.08	60	11.3	49.1

สถาบันวิทยบริการ  
จุฬาลงกรณ์มหาวิทยาลัย

**Table D-4** Effect of boric acid concentration on SNRL hydrogenation

Exp	H <sub>3</sub> BO <sub>3</sub> (mM)	N <sub>2</sub> H <sub>4</sub> (mM)	H <sub>2</sub> O <sub>2</sub> (mM)	C=C (M)	Temp (°C)	Total Volume (ml)	Degree of Hydrogenation (%)
49	0	2.20	3.53	0.55	60	162.0	42.7
50	3.08	2.20	3.53	0.55	60	162.0	46.6
51	6.17	2.20	3.53	0.55	60	162.0	49.8
52	30.86	2.20	3.53	0.55	60	162.0	59.1
53	61.72	2.20	3.53	0.55	60	162.0	62.3
54	92.59	2.20	3.53	0.55	60	162.0	60.5
55	123.45	2.20	3.53	0.55	60	162.0	55.2
56	185.18	2.20	3.53	0.55	60	162.0	44.3

**Table D-5** Effect of number of treatment on SNRL hydrogenation

Exp	No. of treat	CuSO <sub>4</sub> (μmol)	N <sub>2</sub> H <sub>4</sub> (mol)	H <sub>2</sub> O <sub>2</sub> (mol)	C=C (mmol)	Temp (°C)	Total Volume (ml)	Degree of Hydrogenation (%)
57	1 <sup>st</sup>	8	0.35	0.57	89.6	60	162.0	64.5
58	2 <sup>nd</sup>	8	0.35	0.57	-	60	204.0	75.7
59	3 <sup>rd</sup>	8	0.35	0.57	-	60	246.0	81.4
60	4 <sup>th</sup>	8	0.35	0.57	-	60	288.0	83.5

**Table D-6** Results for kinetic study of SNRL by diimide hydrogenation

Exp	Time (h)	Degree of Hydrogenation (%)			ln(1-x)		
		60°C	70°C	80°C	60°C	70°C	80°C
61 <sup>a</sup>	0	0	0	0	0	0	0
62	1	12.6	14.7	15.8	-0.135	-0.159	-0.172
63	2	19.5	23.9	26.1	-0.217	-0.273	-0.302
64	3	27.3	32.8	34.8	-0.319	-0.397	-0.428
65	4	35.7	40.3	46.1	-0.442	-0.516	-0.618
66	5	39.6	45.7	50.8	-0.504	-0.611	-0.709
67	6	42.7	52.7	58.8	-0.557	-0.749	-0.887
68	7	42.7	52.7	58.8	-0.557	-0.749	-0.887
69	8	42.7	52.7	58.8	-0.557	-0.749	-0.887
80	9	42.7	52.7	58.8	-0.557	-0.749	-0.887
81	10	42.7	52.7	58.8	-0.557	-0.749	-0.887
82	11	42.7	52.7	58.8	-0.557	-0.749	-0.887
83	12	42.7	52.7	58.8	-0.557	-0.749	-0.887
84 <sup>b</sup>	0	0	0	0	0	0	0
85	1	16.7	19.3	22.6	-0.183	-0.214	-0.256
86	2	26.8	31	35.2	-0.312	-0.371	-0.434
87	3	38.3	42.8	48.2	-0.483	-0.559	-0.658
88	4	50.2	56.1	59.4	-0.697	-0.823	-0.901
89	5	59.6	63.7	66.7	-0.906	-1.013	-1.099
90	6	64.6	69.7	72.3	-1.038	-1.194	-1.284
91	7	64.7	69.7	71.7	-1.041	-1.194	-1.262
92	8	64.7	69.4	71.7	-1.041	-1.184	-1.262
93	9	65.1	69.3	71.7	-1.053	-1.181	-1.262
94	10	65.3	69.3	71.6	-1.058	-1.181	-1.259
95	11	65.7	69.2	71.8	-1.070	-1.178	-1.266
96	12	65.7	69.2	71.7	-1.070	-1.178	-1.262

<sup>a</sup>Results for kinetic study of SNRL by diimide hydrogenation (Without Catalyst);  
 $[\text{N}_2\text{H}_4] = 2.20 \text{ mM}$ ,  $[\text{H}_2\text{O}_2] = 3.53 \text{ mM}$ ,  $[\text{C}=\text{C}] = 0.55 \text{ M}$ ,  $t = 0\text{-}12 \text{ h}$  and  $T = 60\text{-}80^\circ\text{C}$ .

<sup>b</sup>Results for kinetic study of SNRL by diimide hydrogenation (With Catalyst);  
 $[\text{CuSO}_4] = 49.38 \text{ }\mu\text{M}$ ,  $[\text{N}_2\text{H}_4] = 2.20 \text{ mM}$ ,  $[\text{H}_2\text{O}_2] = 3.53 \text{ mM}$ ,  $[\text{C}=\text{C}] = 0.55 \text{ M}$ ,  $t = 0\text{-}12 \text{ h}$  and  $T = 60\text{-}80^\circ\text{C}$ .

## Appendix E

### Data of Cure Characteristics of Vulcanized Rubber Using Moving

#### Die Rheometer (MDR)

**Table E-1** The cure characteristics of various for HSNR/NR blends using moving die rheometer

HSNR/NR	Minimum Torque (ML, dN·m)	Maximum Torque (MH, dN·m)	Scorch time (ts <sub>2</sub> , min)	Optimum cure time (tc <sub>90</sub> , min)
0/100	0.27	3.69	10.29	25.21
	0.25	3.59	10.40	25.87
25/75	0.64	3.82	11.64	24.80
	0.56	3.84	10.41	24.17
50/50	0.81	3.89	11.13	22.42
	0.61	3.86	9.84	22.21
75/25	0.61	3.86	9.84	22.21
	0.77	3.82	10.11	10.11
100/0	0.97	3.56	18.69	21.88
	0.82	3.52	16.34	16.34

สถาบันวิทยบริการ  
จุฬาลงกรณ์มหาวิทยาลัย

## Appendix F

### Data of Mechanical Properties of Vulcanized Rubber

**Table F-1** Data of tensile strength of vulcanized rubber samples

	HSNR/NR	No. of Experiment			Mean	S.D.
		1	2	3		
Before aging	0/100	9.58	9.29	8.91	9.26	0.33
	25/75	6.21	6.65	6.44	6.43	0.22
	50/50	6.91	7.77	7.69	7.45	0.47
	75/25	4.61	4.19	3.62	4.14	0.49
	100/0	2.68	2.68	2.59	2.65	0.05
After aging <sup>a</sup>	0/100	5.45	5.55	5.63	5.54	0.09
	25/75	6.07	5.96	5.84	5.95	0.11
	50/50	7.81	7.18	6.43	7.14	0.69
	75/25	3.71	3.37	3.74	3.60	0.20
	100/0	2.87	2.31	2.64	2.60	0.28

<sup>a</sup>Thermal ageing was done at 100°C for 22 ± 2 h.

**Table F-2** Data of elongation at break (%) of vulcanized rubber samples

	HSNR/NR	No. of Experiment			Mean	S.D.
		1	2	3		
Before aging	0/100	558.81	593.70	573.12	575.21	17.54
	25/75	622.20	625.33	614.09	620.54	5.80
	50/50	654.27	672.54	671.25	666.02	10.20
	75/25	621.60	388.92	563.15	524.56	121.05
	100/0	492.07	513.72	504.83	503.54	10.88
After aging <sup>a</sup>	0/100	389.8	388.22	382.61	386.87	3.77
	25/75	570.58	563.56	600.12	578.09	19.39
	50/50	625.46	604.85	627.68	619.33	12.58
	75/25	518.72	512.45	498.12	509.76	10.55
	100/0	499.16	490.06	488.92	492.71	5.61

<sup>a</sup>Thermal ageing was done at 100°C for 22 ± 2 h.

**Table F-3** Data of hardness of vulcanized rubber samples

	HSNR/NR	No. of Experiment					Mean	S.D.
		1	2	3	4	5		
Before aging	0/100	32.0	32.5	32.5	33.0	32.5	32.5	0.35
	25/75	35.5	35.0	35.0	34.5	35.5	35.1	0.41
	50/50	36.0	36.5	36.0	35.5	36.0	36.0	0.35
	75/25	38.0	37.5	37.5	37.5	38.0	37.7	0.27
	100/0	37.5	36.0	36.0	36.0	36.0	36.3	0.67
After aging <sup>a</sup>	0/100	34.0	33.0	33.0	33.0	34.5	33.5	0.70
	25/75	35.0	35.0	34.0	35.0	35.0	34.8	0.44
	50/50	36.5	36.0	36.5	36.0	36.5	36.3	0.27
	75/25	38.5	37.5	37.5	38.0	38.5	38.0	0.50
	100/0	37.5	37.0	36.5	36.5	37.5	37.0	0.50

<sup>a</sup>Thermal ageing was done at 100°C for 22 ± 2 h.

สถาบันวิทยบริการ  
จุฬาลงกรณ์มหาวิทยาลัย



## VITA

Mr. Khosit Simma was born on December 19, 1983 in Prachinburi, Thailand. He graduated with a Bachelor's Degree of Science in Industrial Chemistry from Department of Chemistry, Faculty of Science, King Mongkut's Institute of Technology Ladkrabang in 2006. He has continued his study in Master Degree in the Program of Petrochemistry and Polymer Science, Faculty of Science, Chulalongkorn University since 2006 and finished his study in 2008.



สถาบันวิทยบริการ  
จุฬาลงกรณ์มหาวิทยาลัย